TWO-DIMENSIONAL NUMERICAL ANALYSIS OF
TUNNEL COLLAPSE DRIVEN IN
POOR GROUND CONDITIONS

A THESIS SUBMITTED TO
THE GRADUATE SCHOOL OF NATURAL AND APPLIED SCIENCES
OF
MIDDLE EAST TECHNICAL UNIVERSITY

BY

MELİH TÜRKOĞLU

IN PARTIAL FULFILLMENT OF THE REQUIREMENTS
FOR
THE DEGREE OF THE MASTER OF SCIENCE
IN
CIVIL ENGINEERING

JANUARY 2013

Approval of the thesis:

**TWO-DIMENSIONAL NUMERICAL ANALYSIS OF
TUNNEL COLLAPSE DRIVEN IN
POOR GROUND CONDITIONS**

submitted by **MELİH TÜRKOĞLU** in partial fulfillment of the requirements for the degree of **Master of Science in Civil Engineering Department, Middle East Technical University** by,

Prof. Dr. Canan Özgen   _____
Dean, Graduate School of **Natural and Applied Science**

Prof. Dr. Ahmet Cevdet Yalçıner   _____
Head of Department, **Civil Engineering**

Prof. Dr. Bahadır Sadık Bakır   _____
Supervisor, **Civil Engineering**

Examining Committee Members:

Prof. Dr. Erdal Çokça   _____
Civil Engineering Dept., METU

Prof. Dr. Bahadır Sadık Bakır   _____
Civil Engineering Dept., METU

Prof. Dr. Tamer Topal   _____
Geology Engineering Dept., METU

Dr. Onur Pekcan   _____
Civil Engineering Dept., METU

Dr. Serkan Üçer   _____
Geopro Consulting Construction Engineering LLC.

                                          Date: _____

I hereby declare that all information in this document has been obtained and presented in accordance with academic rules and ethical conduct. I also declare that, as required by these rules and conduct, I have fully cited and referenced all material and results that are not original to this work.

Name, Last name : Melih Türkoğlu

Signature :

ABSTRACT

TWO-DIMENSIONAL NUMERICAL ANALYSIS OF TUNNEL COLLAPSE DRIVEN IN POOR GROUND CONDITIONS

Türkoğlu, Melih
M.Sc., Department of Civil Engineering
Supervisor: Prof. Dr. Bahadır Sadık Bakır

January 2013, 98 pages

Insufficient information on the host medium can cause serious problems, even collapse, during construction in a tunnel. This study focuses on understanding the reasons behind the collapse of the Tunnel BT24 to be opened within the framework of Ankara-İstanbul High Speed Railway Project. The tunnel is located near Bozüyük in the Bilecik Province. The collapsed section of the tunnel was driven into a highly weathered, weak to medium rock mass. Unanticipated geological/geotechnical circumstances caused excessive deformations at the section on which the primary support system was applied, leading eventually to collapse. To understand the response of the tunnel and the collapse mechanism, the construction sequence is simulated using two-dimensional plane-strain and axisymmetric finite element models. The analyses were carried out for the section with and without invert closure of the shotcrete liner. To implement the effects of likely unfavorable ground conditions on the tunnel response, a number of fault scenarios and possible creep effects were also considered with those two alternatives. Displacements in the tunnel periphery, forces and moments in the primary liner as well as the plastic deformation zones in the surrounding ground were determined for each case and comprasions were made accordingly. İt is concluded that the unforseen ground circumstances might have substantially aggravated the deformations in the section and that the lack of ring closure of the primary liner at invert played the key role in the collapse.

Keywords: Tunnel, NATM, Collapse

ÖZ

OLUMSUZ ZEMİN KOŞULLARINDA AÇILMIŞ
TÜNEL GÖÇÜĞÜNÜN
İKİ BOYUTLU SAYISAL ANALİZİ

Türkoğlu, Melih
Yüksek Lisans, İnşaat Mühendisliği Bölümü
Tez Yöneticisi: Prof. Dr. Bahadır Sadık Bakır

Ocak 2013, 98 sayfa

Tünel inşaatı sırasında zemin hakkındaki yetersiz bilgi ciddi problemlere hatta çökmeye sebep olabilir. Bu çalışma, Ankara-İstanbul Hızlı Tren Projesi kapsamında açılan BT24 Tüneli'nin çökmesinin arkasındaki sebepleri anlamaya odaklanmaktadır. Tünel, Bilecik ili içerisinde Bozüyük yakınında yer almaktadır. Tünelin çöken kısmı çok ayrışmış ve zayıf – orta dayanımlı kaya kütlesi içerisinde açılmıştır. Öngörülmeyen jeolojik ve geoteknik zemin koşulları, birincil destek sisteminin uygulandığı kısımda sonuçta yıkılmaya yol açan aşırı deformasyonlara sebebiyet vermiştir. Tünel davranışını ve çökme mekanizmasını anlamak için, inşaat aşamaları yapım sırası iki boyutlu düzlemsel birim deformasyon ve aksisimetrik sonlu eleman modelleri kullanılarak modellenmiştir. Analizler, püskürtme beton kaplamalı invert kapanmalı ve kapanmasız durumlar için gerçekleştirilmiştir. Olası olumsuz zemin koşullarının tünel davranışı üzerindeki etkisini modelleyebilmek amacıyla, bu iki alternatifle birlikte bir dizi fay senaryoları ve sünme etkileri ayrıca dikkate alınmıştır. Tünel çeperindeki deplasmanlar, birincil kaplamadaki kuvvet ve momentler, ayrıca çevreleyen zemindeki plastik deformasyon bölgeleri herbir vaka için belirlenmiş ve bu doğrultuda kıyaslamalar yapılmıştır. Öngörülmeyen zemin koşullarının deformasyonları büyük oranda artırmış olabileceği ve invertteki birincil kaplamada halka kapanması uygulanmamış olmasının çökmede anahtar rol oynadığı sonucuna varılmıştır.

Anahtar Kelimeler: Tünel, YATM, Çökme

To My Family

ACKNOWLEDGEMENTS

TABLE OF CONTENTS

LIST OF TABLES

TABLES

LIST OF FIGURES

FIGURES

CHAPTER 1

INTRODUCTION

Construction of tunnels in recent years all over the world is increasing due to transportation needs and environmental considerations. Excavation for an underground structure, such as tunnel or cavern, causes a local redistribution in the vicinity of the excavation such that the forces previously carried by the excavated rock must now be transmitted or arched around the opening. In many cases the strength of the medium around the periphery may be insufficient to withstand these changes, and excessive deformation or collapse of the walls may ensue.

Where unacceptable levels of deformations are likely, some form of support must be installed to carry a proportion of the forces so that the final rock deformations remain within tolerable limits and collapse is avoided. It is in this sense that the purpose of the support is said to be to help the medium to support itself, or to ensure that the effective arching action of the forces occurs around the tunnel. At the face of the excavation, where the arching of forces occurs onto the rock ahead of the face as well as on to the walls, it is sometimes referred to as dome action.

As with other engineered structures, design of an excavation support must consider the forces imposed on the support and the deformations induced by these forces. However, the uncertainties involved with respect to both the imposed forces and the ability of the medium to withstand them are of a higher order than is typical of design involving fabricated materials only. As a consequence of these constraints, the design of supports for excavations is not only less precise than for many engineered structures, but must also follow different strategy – sometimes referred to as "design as you go," or "the observational approach" (Peck, 1969).

Excessive deformations often result in collapse mechanisms in soil or rock formations such as: burst mechanisms, blow-out failure, chimney caving, rock fall, failure of lining before or after ring closure and squeezing or swelling ground behavior. Therefore, tunnel design and construction involves: geological and geotechnical aspects, safety, economy and serviceability considerations.

Earthquakes, groundwater regime, disadvantageous ground conditions are examples of factors that may induce collapse in tunneling. In addition, the failure of a tunnel also can occur as the result of poor engineering or construction process. Consequences of tunnel collapse are huge economic loss and delay of crucial projects besides, endangering of human safety.

1.1   Problem Statement

The Ankara – İstanbul High-Speed Railway Project aims to provide a fast, comfortable and safe transportation system as the second phase of this project, which is located between Köseköy and İnönü and started in September 2008. Within this phase, 33 tunnels will be built. All of these tunnels will be placed within a total distance of 55 kilometres in a topographically difficult region. One of those tunnels, which is coded as BT24, is located between Bilecik and Bozüyük stations. The construction of the tunnel was initiated in June -

July 2010 using New Austrian Tunneling Method (NATM). During construction of the tunnel, excessive deformations occurred at some sections. As a result, tunnel shotcrete lining and steel supports were extremely deformed at several locations. Finally, deformations could not be stabilized and the section between KM: 215+409 and KM: 215+468 collapsed.

1.2   Objective and Scope

The primary objective of the thesis is to enlighten the reasons behind the collapse of the tunnel. Accordingly, the response of the tunnel is aimed to be simulated using numerical modeling.

Following the introduction, general approach in tunnel design and principles of NATM construction will be reviewed in Chapter 2. Chapter 3 presents the background information on the BT24 Tunnel including the geology of project area, monitoring and geotechnical mapping details, basic design criteria and the history of collapsed section of the tunnel. Chapter 4 consists of the fundamental issues of the study which include two-dimensional (2D) finite element modeling, assessment of the material properties used in analyses and implementation of the excavation stages. Also the generation of axisymmetric and plane-strain models in Phase^2 is described in detail and the analyses are evaluated. Results of the study and discussion are given in Chapter 5.

CHAPTER 2

LITERATURE REVIEW

2.1 General Approach in Tunnel Design

In general terms the process of engineering design inherently consists of selecting material and member sections which will not fail and will satisfactorily provide the required functional response of the proposed structure. The final displacements and the forces developing in the element members should not exceed the allowable limits which will hamper the proper functioning of the structure as a whole. Two essential steps can be identified in the design of underground structures:

- Conceptual modeling of the boundary value problem, which is, stating the problem in terms of geometry, rock mass characterization and boundary conditions including in-situ stresses.

- Selecting an approach for analysis of the problem in terms of stress concentrations, deformations, failure mechanism and support system.

2.2 Empirical Design Methods

Empirical design methods are related to the anticipated conditions of the proposed site and to the experience which is gained from former projects. The empirical methods usually result in overdesigned structures but they are simple to use and do not require elaborate calculations. The principle of the empirical design method is based on the rock mass classifications which are broadly used in rock engineering. As a matter of fact, the classification method is used at least for preliminary design approach for complex underground structures, in general.

2.2.1 Conventional Analysis (Tezaghi)

The conventional analysis method is introduced by Terzaghi (1946). In this method, the magnitude of load is represented by the height of rock mass assumed to be supported by the steel rib section. It is supposed that the rock mass tends to fail in the form of a wedge or inclined block. Terzaghi's rock load concept consists of nine classes of rock classified according to qualitative properties of rocks, based on the width and height of the opening (Table 2.1).

Table 2.1 Terzaghi's rock load classification (Terzaghi, 1946)

Rock Class	Definition	Rock Load Factor Hp (feet) (B and H_t)	Remark
I. Hard and intact	Hard and intact rock contains no joints and fractures. After excavation the rock may have popping and spalling at excavated face.	0	Light lining required only if spalling or popping occurs.
II. Hard stratified and schistose	Hard rock consists of thick strata and layers. Interface between strata is cemented. Popping and spalling at excavated face is common.	0 to 0.5 B	Light support for protection against spalling. Load may change between layers.
III. Massive, moderately jointed	Massive rock contains widely spaced joints and fractures. Block size is large. Joints are interlocked. Vertical walls do not require support. Spalling may occur.	0 to 0.25 B	Light support for protection against spalling.
IV. Moderately blocky and seamy	Rock contains moderately spaced joints. Rock is not chemically weathered and altered. Joints are not well interlocked and have small apertures. Vertical walls do not require support. Spalling may occur.	0.25 B to 0.35 (B + H_t)	No side pressure.
V. Very blocky and seamy	Rock is not chemically weathered, and contains closely spaced joints. Joints have large apertures and appear separated. Vertical walls need support.	(0.35 to 1.1) (B + H_t)	Little or no side pressure.
VI. Completely crushed but chemically intact	Rock is not chemically weathered, and highly fractured with small fragments. The fragments are loose and not interlocked. Excavation face in this material needs considerable support.	1.1 (B + H_t)	Considerable side pressure. Softening effects by water at tunnel base. Use circular ribs or support rib lower end.
VII. Squeezing rock at moderate depth	Rock slowly advances into the tunnel without perceptible increase in volume. Moderate depth is considered as 150 ~ 1000 m.	(1.1 to 2.1) (B + H_t)	Heavy side pressure. Invert struts required. Circular ribs recommended.
VIII. Squeezing rock at great depth	Rock slowly advances into the tunnel without perceptible increase in volume. Great depth is considered as more than 1000 m.	(2.1 to 4.5) (B + H_t)	
IX. Swelling rock	Rock volume expands (and advances into the tunnel) due to swelling of clay minerals in the rock at the presence of moisture.	up to 250 feet, irrespective of B and H_t	Circular ribs required. In extreme cases use yielding support.

Notes: The tunnel is assumed to be below groundwater table.   For tunnel above water tunnel, H_p for Classes IV to VI reduces 50%.

The tunnel is assumed excavated by blasting.   For tunnel boring machine and roadheader excavated tunnel, H_p for Classes II to VI reduces 20-25%.

The approach assumes that the ribs are firmly connected to the rock surface at the blocking points and sufficient friction develops between the blocking and rock as radial reaction. Also, no outward and inward deflections are presumed to occur in the rib, because the rock and blocking are rigid. By the blocking points, loads are radially transmitted to the support and radial passive resistance develops between the support and the rock. It is assumed that the direction and location of the thrust at each blocking point is known. Then, thrust values acting in the steel rib can be determined graphically by means of trial solutions. After obtaining the extreme thrust and its corresponding point, the stress in steel rib can be determined.

2.2.2 Geomechanics Classification (RMR System)

A rock mass rating concept was originally introduced by Bieniawski (1974). Table 2.2 presents the Geomechanics Classification, which is divided into two sections. Five parameters are clustered into five value spectrums in section A of the table. These parameters are strength of intact rock material, rock quality designation (RQD), spacing of joints, condition of joints and ground water conditions.

Table 2.2 Geomechanics Classification of rock mass (After Bieniawski, 1979)

A. CLASSIFICATION PARAMETERS AND THEIR RATINGS								
Parameter		Range of values						
1	Strength of intact rock material	Point-load strength index	>10 MPa	4 - 10 MPa	2 - 4 MPa	1 - 2 MPa	For this low range - uniaxial compressive test is preferred		
		Uniaxial comp. srength	>250 MPa	100 - 250 MPa	50 - 100 MPa	25 - 50 MPa	5 - 25 MPa	1 - 5 MPa	< 1 MPa
	Rating		15	12	7	4	2	1	0
2	Drill core Quality RQD		90% - 100%	75% - 90%	50% - 75%	25% - 50%	< 25%		
	Rating		20	17	13	8	3		
3	Spacing of discontinuities		> 2 m	0.6 - 2 m	200 - 600 mm	60 - 200 mm	< 60 mm		
	Rating		20	15	10	8	5		
4	Condition of discontinuities (See E)		Very rough surfaces Not continuous No separation Unweathered wall rock	Slightly rough surfaces Separation < 1 mm Slightly weathered walls	Slightly rough surfaces Separation < 1 mm Highly weathered walls	Slickensided surfaces or Gouge < 5 mm thick or Separation 1-5 mm	Soft gouge >5 mm thick or Separation > 5 mm Continuous		
	Rating		30	25	20	10	0		
5	Groundwater	Inflow per 10 m tunnel length (l/m)	None	< 10	10 - 25	25 - 125	> 125		
		(Joint water press)/ (Major principal cr)	0	< 0.1	0.1, - 0.2	0.2 - 0.5	> 0.5		
		General conditions	Completely	Damp	Wet	Dripping	Flowing		
	Rating		15	10	7	4	0		

B. RATING ADJUSTMENT FOR DISCONTINUITY ORIENTATIONS (See F)						
Strike and dip orientation		Very favourable	Favourable	Fair	Unfavourable	Very Unfavourable
Ratings	Tunnels & mines	0	-2	-5	-10	-12
	Foundations	0	-2	-7	-15	-25
	Slop	0	-5	-25	-50	

C. ROCK MASS CLASSES DETERMINED FROM TOTAL RATINGS					
Rating	100 ♦81	80 ♦61	60 ♦41	40 ♦21	< 21
Class number	I	II	III	IV	V
Description	Very good rock	Good rock	Fair rock	Poor rock	Very poor rock

D. MEANING OF ROCK CLASSES					
Class number	I	II	III	IV	V
Average stand-up time	20 yrs for 15 m span	1 year for 10 m span	1 week for 5 m span	10 hrs for 2.5 m span	30 min for 1 m span
Cohesion of rock mass (kPa)	> 400	300 - 400	200 - 300	100 - 200	< 100
Friction angle of rock mass (deg)	> 45	35 - 45	25 - 35	15 - 25	<15

Table 2.2 Geomechanics Classification of rock mass (continued)

E. GUIDELINES FOR CLASSIFICATION OF DISCONTINUITY conditions					
Discontinuity length (persistence)	< 1 m	1 - 3 m	3 - 10 m	10 - 20 m	> 20 m
Rating	6	4	2	1	0
Separation (aperture)	None	< 0.1 mm	0.1 - 1.0 mm	1 - 5 mm	> 5 mm
Rating	6	5	4	1	0
Roughness	Very rough	Rough	Slightly rough	Smooth	Slickensided
Rating	6	5	3	1	0
Infilling (gouge)	None	Hard filling < 5 mm	Hard filling > 5 mm	Soft filling < 5 mm	Soft filling > 5 mm
Rating	6	4	2	2	0
Weathering	Unweathered	Slightly weathered	Moderately weathered	Highly weathered	Decomposed
Ratings	6	5	3	1	0

F. EFFECT OF DISCONTINUITY STRIKE AND DIP ORIENTATION IN TUNNELLING**			
Strike perpendicular to tunnel axis		Strike parallel to tunnel axis	
Drive with dip - Dip 45 - 90°	Drive with dip - Dip 20 - 45°	Dip 45 - 90°	Dip 20 - 45°
Very favourable	Favourable	Very unfavourable	Fair
Drive against dip - Dip 45-90°	Drive against dip - Dip 20-45°	Dip 0-20 - Irrespective of strike°	
Fair	Unfavourable	Fair	

* Some conditions are mutually exclusive. For example, if infilling is present, the roughness of the surface will be overshadowed by the influence of the gouge. In such cases use A.4 directly.

** Modified after Wickham et al (1972).

The uniaxial compressive strength is used as the strength criterion of intact rock material. The point load index may be preferred as a measure of intact rock strength for very low strength rocks. RQD, which was set forth by Deere in 1964, is assumed to measure the drill core quality. The term joint refers to all discontinuities such as joints, faults, bedding planes, etc. The concept considers the presence of infilling materials in the joints, the wall condition, the surface roughness, continuity and the separation of joints. The observed rate of flow into excavation per 10 m tunnel length and the ratio of joint water pressure to major principal stress or general qualitative description of ground water conditions are utilized as a criterion for determining the influence of ground water flow on the stability of opening. A rating is assigned to each spectrum of values for each parameter and these ratings for each of the parameter are added in order to reach a comprehensive rating for the rock mass.

Section B takes the influence of joint orientation into account. The comprehensive rating is accorded for joint strike and dip orientation. Adjustment ratings for joint orientation are given in Table 2.2. The adjusted rating, which is called rock mass rating (RMR), ranges from 20 to 100. Based on the RMR values, it is possible to predict internal friction angle, cohesion and stand-up time of intact rock material and to determine the suggested support systems depending on such factors as the tunnel size and shape, and the method of excavation (Sinha and Schoeman, 1983).

2.2.3 Q System

Barton et al (1974) introduced a design concept based on an index derived from six parameters. These parameters are joint alteration number (J_a), rock quality designation (RQD), joint water reduction factor (J_w), joint set number (J_n), stress reduction factor (SRF) and joint roughness number (J_r). The index Q proposed for determining the tunneling quality of a rock mass is composed of three quotients which are described as (RQD/J_n), (RQD/J_a) and (RQD/SRF), and is obtained by directly multiplying these three quotients with each other.

After estimating the rock mass quality (Q), the excavation diameter or span is divided by the excavation support ratio in order to get the equivalent dimension (D_e), which is required for making the rock mass quality pertaining to the support requirements of the opening. Based on rock mass quality and equivalent dimension, 38 typical ground categories and their required support systems are proposed to be included in any kind of rock mass as presented in Figure 2.1.
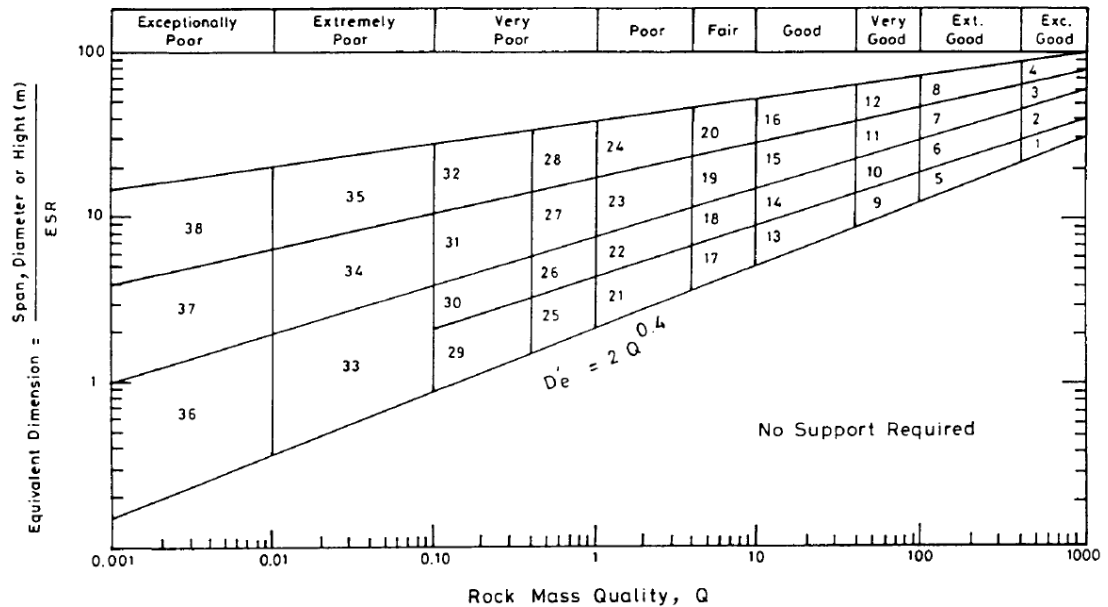
Figure 2.1 Excavation support chart showing the box numbering for 38 categories of supports (After Barton et al., 1974)

An empirical formula has been developed which relates permanent support pressure to rock mass quality in the Q-System. The value obtained for the roof of the tunnel is multiplied by wall factor for determining the wall support pressure. Practical estimation of the permanent radial support pressure, apparently required to stabilize the roof and the wall of opening, is graphically illustrated in Figure 2.2.
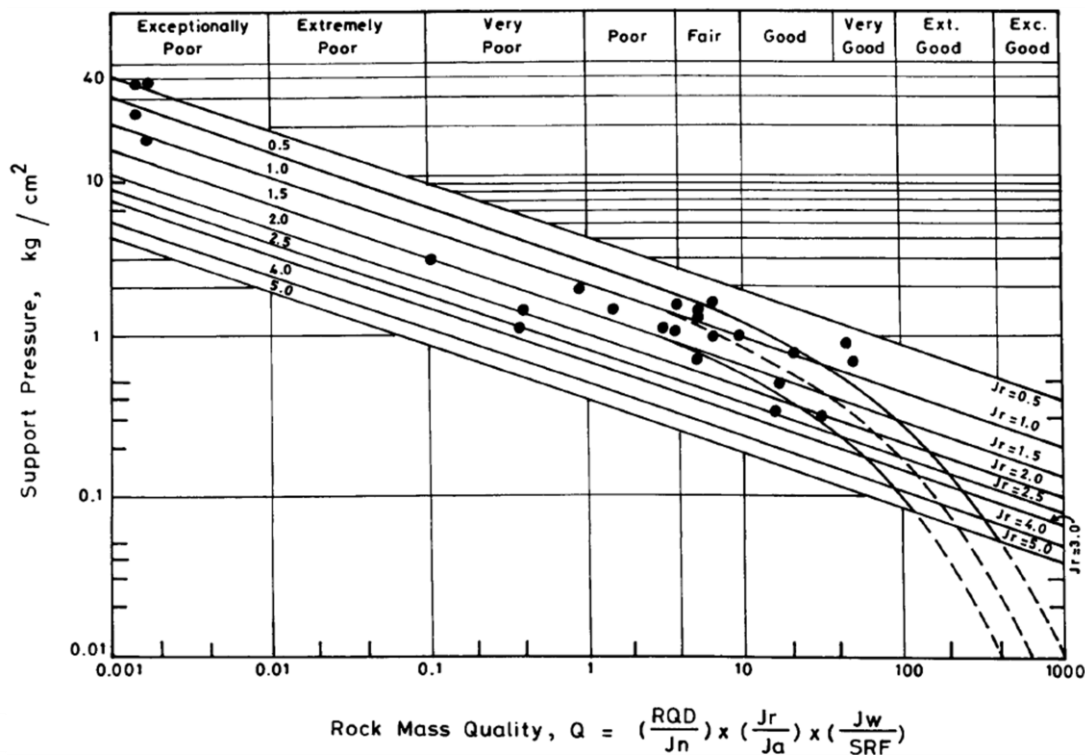
Figure 2.2 Excavation correlation between support pressure and rock mass quality Q (Barton et al., 1974)

2.3 Convergence Confinement Method

The Convergence – Confinement method introduced by Ladanyi (1974), and Hoek and Brown (1980) recognizes the behavior of the rock mass as tending to close the excavation. The excavation of tunnel disturbs the original stresses and equilibrium conditions prevailing in the rock mass. The stress changes require displacements to occur and the excavated ground tries to converge toward the opening. The amount of convergence depends on the host ground characteristics, method of construction and the size of opening used.

While a change in the original stress distribution is occurring, the supports are installed. The movement of rock mass is resisted by the installed support system during the progress of excavation. The redistribution of stresses and the displacements are influenced by the interaction of the support with rock. This phenomenon from the initial conditions to the final interaction of ground with support is considered by the convergence-confinement method.

The method recognizes the temporal behavior of rock mass loading during construction. A curve is constructed to characterize the convergence behavior of rock mass (Figure 2.3). Its construction depends on the strength criterion such as uniaxial compressive strength, primary stress condition, elastic modulus, etc. The support characteristics curve together with the complementary ground characteristics curve provides excellent tools for illustrating the support and ground behavior. At point A on the G curve, the ground stress equals that existing prior to excavation σ_0 and the convergence is equal to zero. As σ_0 reduces due to creation of opening, the ground converges elastically up to point B on the curve G. The further reduction of σ_b to σ_c will bring more radial convergence into existence. The

8

determination of the value of U_f, i.e. the radial displacement of inelastic zone requires nonlinear analysis preferably using numerical methods such as the finite element method with realistic ground parameters (which are usually difficult to assess). Beyond the point C, the material starts to loosen and it is important to provide confinement before the material reaches the point C. The confinement provided by a support system has its own characteristics curves shown as graphs s, s1 and s2 on Figure 2.3. These curves are easier to determine than curve G. this is because the constitutive relationship of support material is easily determinable (Sinha, 1989).
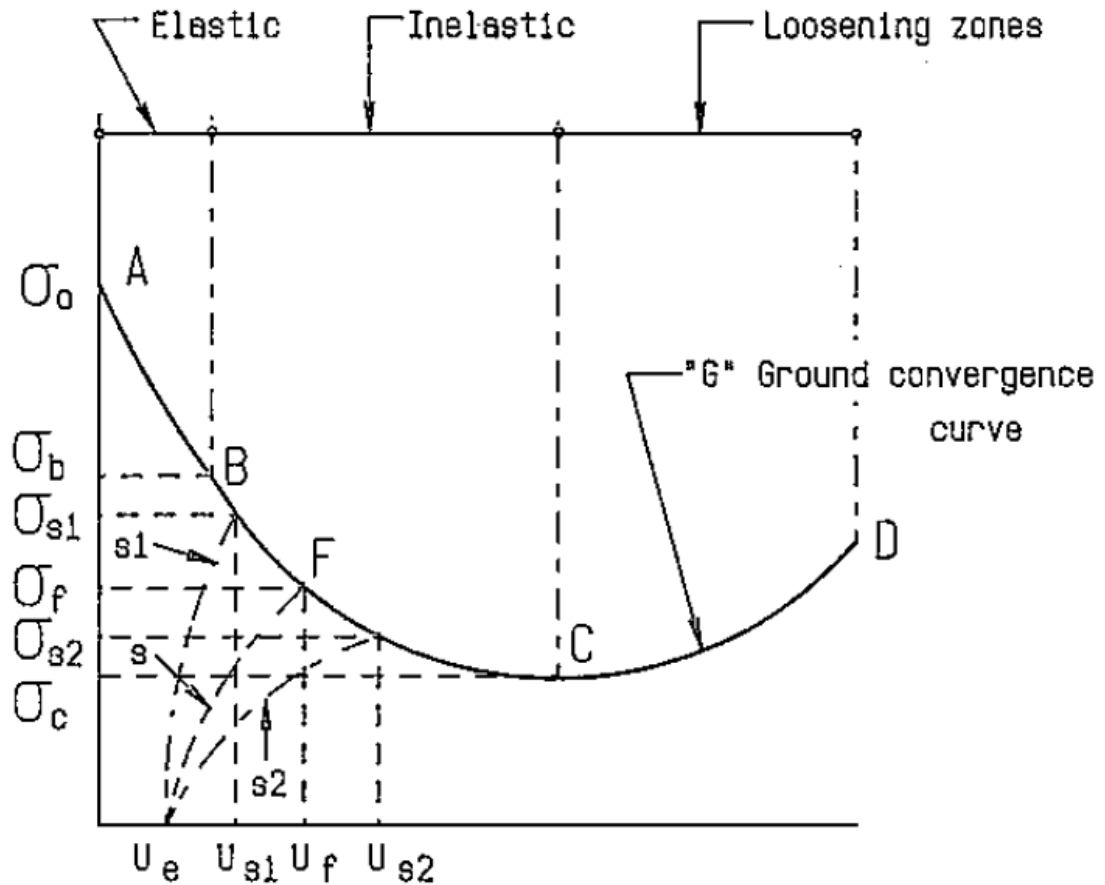
Figure 2.3 Ground characteristics and support confinement curves

2.4   New Austrian Tunneling Method (NATM)

The NATM is based on the philosophy of "Build as you go" approach with the following caution "not too stiff, nor too flexible; not too early, nor too late" (Figure 2.4).

9
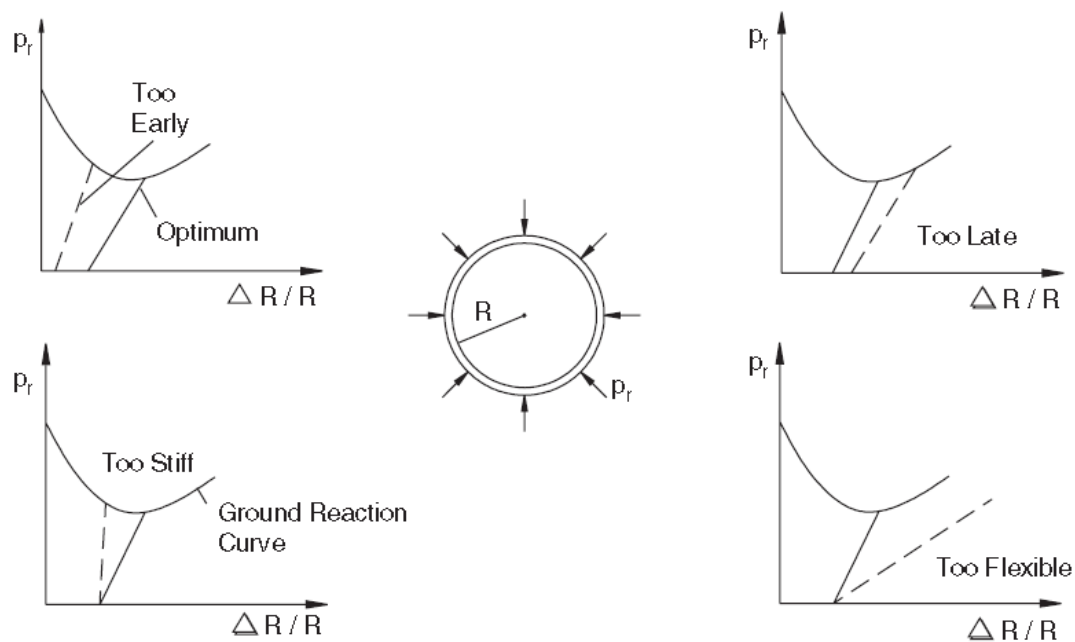
Figure 2.4 Philosophy of NATM: Support (external lining) not too early, not too late, not too stiff, not too flexible

The NATM implies a particular design and construction philosophy (Rabcewicz, 1964; Müller, 1978; Brown, 1981), introducing a new design and construction concept which was characterized by technical, operational and contractual improvements. It is based on the principle that it is desirable to minimize the support requirements by mobilization of the ground resistance to the optimum extent without causing instability.

In NATM, the host ground surrounding an excavation is made into an integral part of the support structure for underground openings. The host ground and the external support structure (i.e.shotcrete, bolts, steel sets and wire mesh) together take the full load. The host ground takes a major share of the load and the support takes a relatively smaller share of the ground load. This results in saving costs of external support and increase in the speed of construction (Sinha, 1989).

The NATM suggests typically two support systems consisting of outer and inner arch. The outer arch called protective support is a flexible shell to stabilize surrounding rock. The supports recommended for the outer arch are typically shotcrete combined with bolts and reinforcement mesh (welded wire fabric) and in unfavorable conditions combined with light steel sets and possibly forepoling sheets. The inner arch consisting of concrete lining is not installed prior to the outer arch has reached equilibrium. It serves to increase the safety as necessary (Rabcewicz and Golser, 1973). Moreover, the ring closure around the tunnel periphery including an invert lining establishes continuity of tangential force resistance in the lining. This is particularly essential for most unfavorable ground conditions and it positively contributes to the stability of the opening.

Observations of support and ground behavior provide the most important criteria for the NATM. For this reason, it is defined as a most advanced observational method that integrates technical and contractual aspects (Einstein et al, 1980). The excavation causes a stress redistribution during which a sophisticated measuring system controls the behavior of surrounding rock and protective support. The deformations at the sections where support is fully applied are continuously monitored until they completely stop. If the observed convergence exceeds the acceptable limits, then, additional means of support is provided until satisfactory results are reached. Once the stability is attained, a final lining is applied to provide a smooth inner surface.

The tunnel advance can be achieved using blasting, a partial face boring machine or simply using an excavator, depending on the ground conditions. Full or step face excavation and fully rounded cross-section shapes are preferred. Generally, the advancement is spatially and timely staggered in the crown heading, bench heading and invert heading (Chapman, Metje, Stark, 2010) (Figure 2.5).
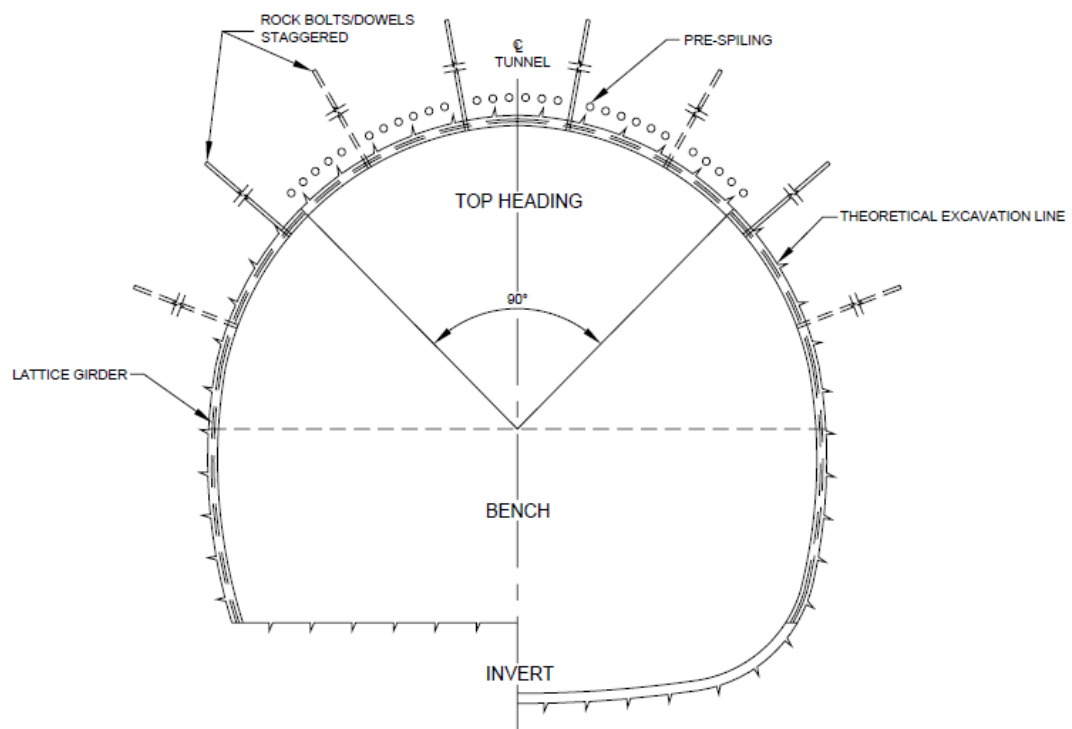
Figure 2.5 Example cross section through a tunnel constructed using NATM

2.5   Finite Element Method

Finite Element Method (FEM) is widely utilized as a design tool to analyze stresses and deformations around an underground structure. It can be used to provide analysis in which the rock is modeled with appropriate boundary conditions and support systems. Besides design analysis of an underground structure, it can provide wise and logical solutions to the problems which can develop in evaluating existing structures and post failure analysis, in monitoring and control of construction, in location of instrumentation and in the analysis of laboratory test specimens.

In the finite element method, the body to be analyzed is divided into a number of discrete homogeneous elements. A wide variety of such elements can be used. In 2D models, triangles and quadrilaterals are the most common types of elements and are connected to each other only at the nodes or nodal points. The finite element mesh is composed of the collection of elements and nodes. Stresses and strains within each element can be determined by the constitutive equations relating stress to strain. FEM mathematically is a numerical technique used to solve the differential equations by means of computers, and physically is a method to determine the element stiffness.

Analytical design procedures, FEM in particular, can handle intractable problems exerted by the complex geometry of an underground opening and the nonhomogeneous, discontinuous and nonlinear nature of geological materials. The finite element methods introduce two- or three-dimensional models that analyze a number of alternatives of loading and geometries. A finite element program used for analysis of an underground structure can consider the influence of sequential excavation and construction procedure that can be best represented by three dimensional models.

FEM is not used alone to design an underground opening. But if used discriminately, it can assist the tunnel designer in many decisions. It substantiates design procedure by other methods (Kripakov, 1983).

The simulation of three-dimensional stress state by a two-dimensional model requires experience and understanding of the relationship between these two models. The proper two-dimensional simulation of the three-dimensional load transfer in the proximity of tunnel face is particularly critical (Figure 2.6).
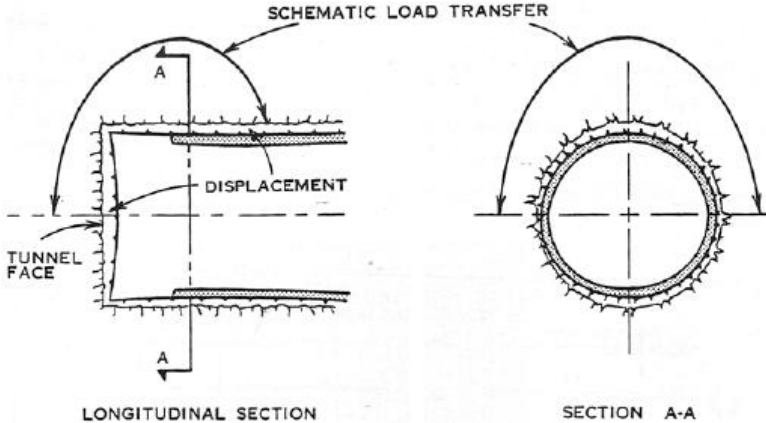
Figure 2.6 Three dimensionality of load and displacement at the tunnel interface (Gnilsen, 1989)

Three-dimensional stress distribution at the face of a tunnel can be simulated in two-dimensions through material softening. In order to model the three-dimensional stress distribution at the face, the behavior of the rock mass at the section during excavation is to be examined. When the section is at such a distance from the advancing tunnel face that its stress state is undisturbed, the unexcavated material within the section is undeformed and can be considered as having in-situ deformation modulus. As the face advances the material begins to soften. At the time support is installed at the excavated section, it would have experienced deformations that can be modeled in two dimensions by reducing the deformation modulus of the excavated material by a relaxation ratio.

CHAPTER 3

CONSIDERATIONS IN THE CASE STUDY OF BT24 TUNNEL

The Ankara-İstanbul High Speed Railway Project will connect İstanbul and Ankara in an approximate 3 hours travel time. Thereby, safe, economic, comfortable and fast transportation system will be provided with a maximum speed of 250 km/h. The passenger transportation share through railway is calculated to increase from 10% to 78% when the project is completed.

The project has two stages: Ankara-Eskişehir and Eskişehir-Köseköy. The first stage of the project is already taken into service. Length of the second stage is 158 km (Figures 3.1 and 3.2). 32 viaducts, 30 bored tunnels and 3 cut-cover tunnels are planned to be constructed in the second stage.

One of the planned tunnels is the BT24 Tunnel which is located between KM: 213+969.20 and KM: 216+167.00, near Bozüyük. The collapsed section between KM: 215+370 and KM: 215+470 of the BT24 Tunnel is modeled and analyzed in this study.
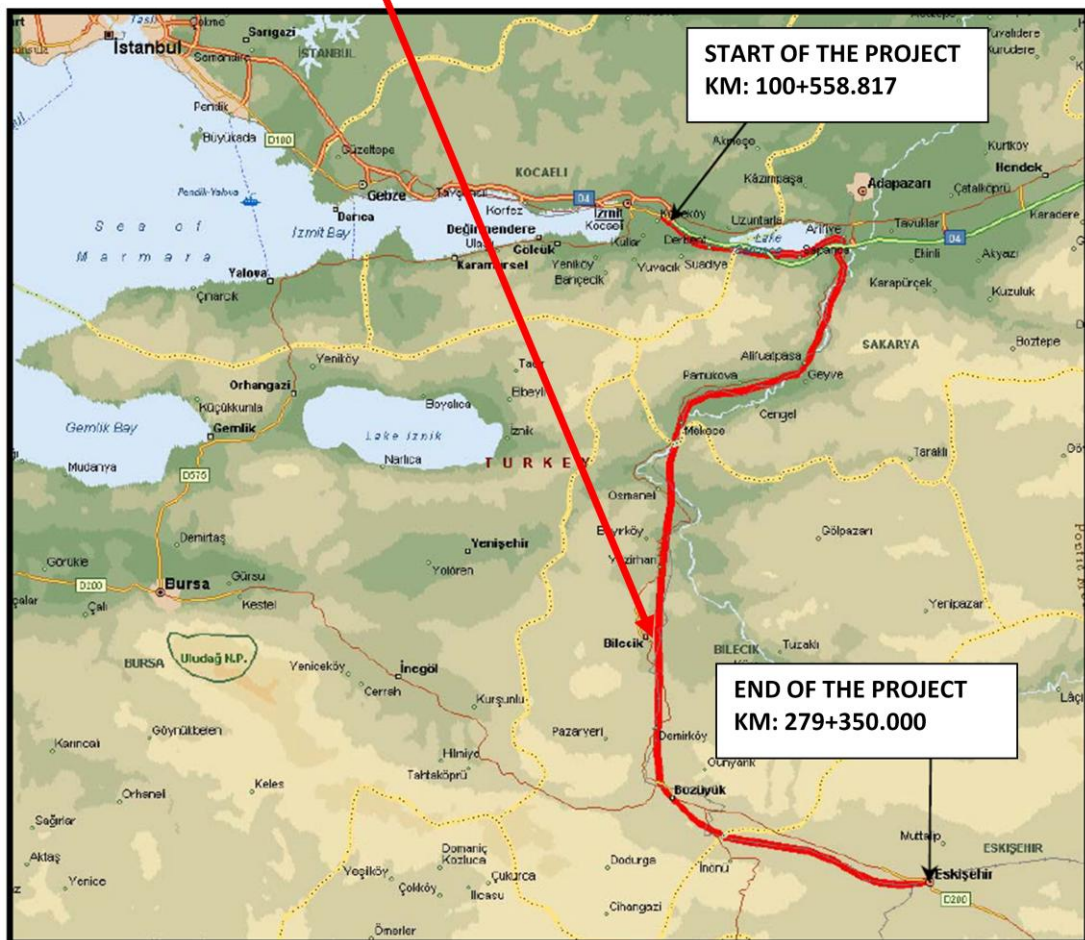
Figure 3.1 The location of the 2nd stage Ankara-İstanbul High Speed Railway Project
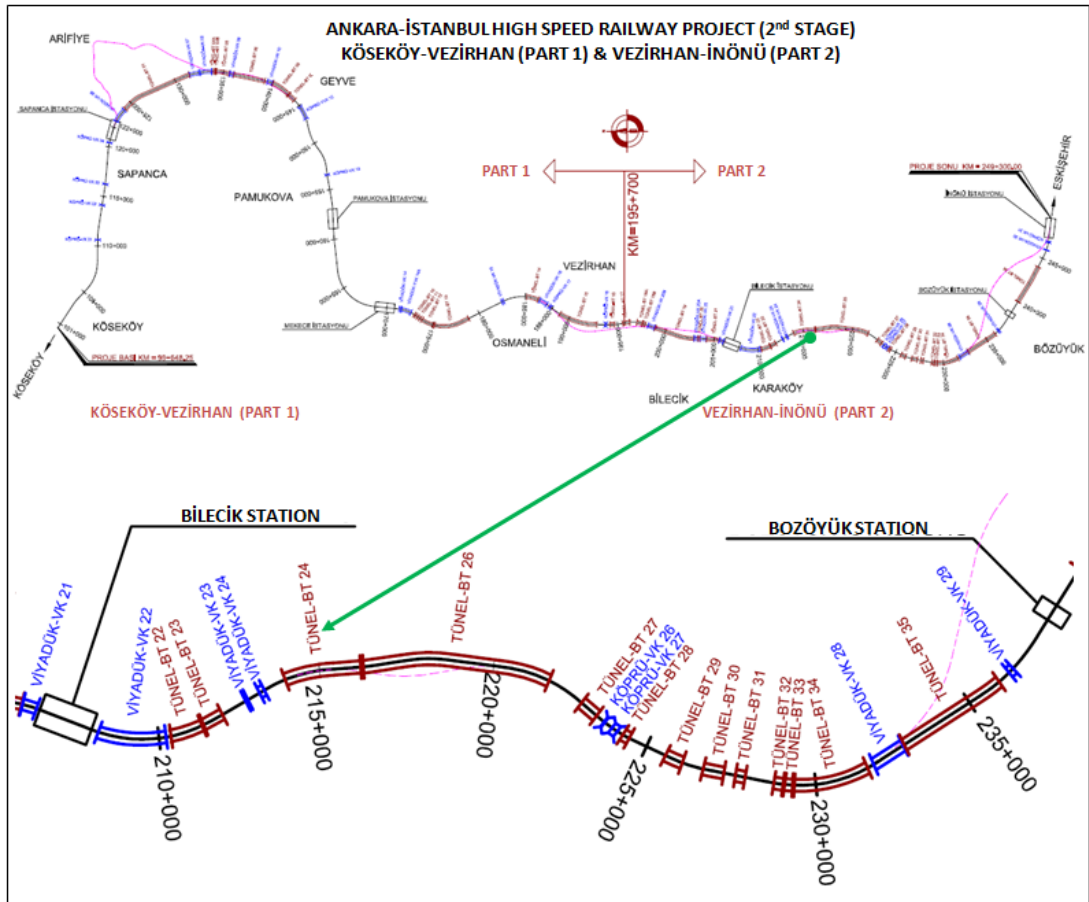
Figure 3.2 Details of the Ankara-İstanbul High Speed Railway Project with tunnels and viaducts

3.1 Collapsed Section of the Tunnel

BT24 Tunnel is located between KM: 213+969.20 and KM: 216+167.00. Design length of the tunnel is 2206.8 m. Tunnel support construction was completely finished except invert and final lining before the collapse incident. Figure 3.3 has been prepared to explain several milestones related with collapse. Final lining of the tunnel was under construction at the time of the collapse. Tunnel invert concrete construction was finished between KM: 213+969.20 and KM: 215+384 with a length of 1414.8 m. 1142.6 m final lining construction was completed till KM: 215+111.80. While workers were pouring invert concrete for the final lining, they heard cracking noises on 17.05.2011. According to the observations just before collapse for the section between KM: 215+409 and KM: 215+468, tunnel shotcrete lining and supports were severely deformed at some locations. Tunnel deformations had increased and as a result, the aforementioned section finally collapsed on 23.05.2011. Only the primary support system (shotcrete, rock bolts, wire mesh and steel sets) was implemented in the collapsed section of the tunnel.
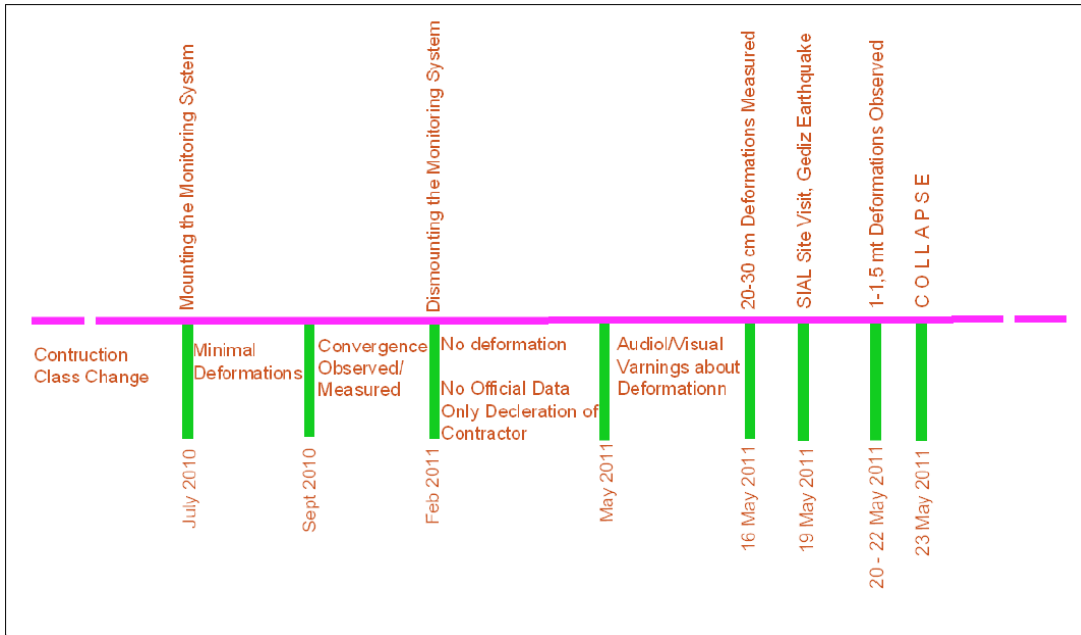
Figure 3.3 Milestones of Tunnel BT24 collapse

In addition, Simav Earthquake (ML=5.9) occurred on 19.05.2011 at local time 20.15. The epicenter of the Simav Earthquake was approximately 100 km away from the tunnel site. The peak ground acceleration (PGA) was around 0.14 m/s^2 at the epicenter. The nearest station to the tunnel site was Bozuyuk Station. Recorded PGA at that station was approximately the same with the epicenter, which is around 0.14-0.15 m/s^2.

Views of the section before collapse are illustrated in Figures 3.4 and 3.5. These pictures, taken on 19.05.2011, show the deformations in the primary support system.

Figure 3.4 Cracks on the upper bench KM: 215+415 (source: SIAL Report, 2010)

Figure 3.5 Deformations in shotcrete lining and steel supports at bench level (source: SIAL Report, 2010)

According to the Report prepared by Yüksel Proje (2008), problematic schists exist in the collapsed section with low rock mass classes. The classes assessed for Q, RMR and NATM classifications are given in Table 3.1. Based on the assessments, two support classes were defined by the contractor. The supports were then slightly modified during excavation based on the observed geological conditions on the face.

Table 3.1 Rock mass classes assessed for the collapsed section of BT24 Tunnel

ROCK TYPE	ROCK MASS CLASSES		
	Q	RMR	NATM
Chlorite schist	4.16 (fair rock)	50 (fair rock)	B2
Graphitic schist	-	-	B3
Graphitic/Chlorite schist	0.55 (extremely poor rock)	36 (poor rock)	-

During tunnel construction, the anticipated B2 class rock was modified as C3 and C2 (Figure 3.6) around the collapsed section. This means that the observed ground conditions during tunnel construction were worse compared to those anticipated previously. As it can be seen from Figure 3.7, the collapsed section of the tunnel belongs mostly to C2 rock class. In addition, the tunnel sections having C3 rock class were partially affected from the collapse.

Figure 3.6 Rock class type modified during tunneling

According to the design report on the tunnel support systems prepared by Sial (2011), 300 mm shotcrete, wire mesh (2 rows), systematic bolting (6 m long, 2x2 m spacing-SN type) and steel rib (1 m spacing with I-160 type) are recommended for C2 class rock mass. It is indicated that up to 15 cm of deformation may be seen in C2 type rock class.

The deformation was described by excessive, continuous movements, which could only be prevented or at least minimized, after ring closure. However tunnel invert concrete was not constructed at the collapsed section; hence, the ring closure was not provided.

3.2   Geology of the Project Area

Inönü-Köseköy section of the project is about 100 km long and crosses the E-W trending mountain range. Region is tectonically active and the ground conditions are generally quite adverse for tunneling. Swelling and squeezing rock conditions dominated along the planned route of the tunnel.

The tunnel alignment passes from the 250 m east of Ahmetpınar Village of Bilecik Province. At about 1 km westside of the railroad alignment and parallel to the highway, there is Karasu Creek. The topography along the route presents various relieves, and the thickness of overvurden above the tunnel varies between 50-160 m.

Along the tunnel alignment the so called Pazarcık Complex which is of Paleozoic age has been observed. The unit outcrops between Bilecik and Bozüyük, and various overlapping rock structures were encountered. The unit presents erosional contact relation with the Triassic aged Karakaya Group on top, and eroded, as well as the partly faulted Bayırköy formation. The unit on the whole, has gone through metamorphism under green schist facieses conditions and made up of structurally embedded rock of various thicknesses. Within the widespread outcropping schists, sandstones, marbles, migmatite-gneiss, and granodiorite were found in the form of mega blocks. The unit is cut by the quartz and aplite dykes of the Bozüyük granitoide.

The main unit which was observed between KM: 213+969 and KM: 216+167 is graphitic schist. Graphitic schists are black – dark grey – greenish dark grey coloured, with apparent schistosity, fragmented, medium to highly weathered and weak to medium strong (ISRM, 1981).

Within the graphite schists which can easily be separated along the schistosity planes, a few marble block with a length of 10 m, quartz seams of up to 2.00 m thickness, as well as mica schists in the form of mega blocks were observed.

Geological-geotechnical investigation report prepared by Yüksel Proje in 2010 before the tunneling indicated that graphitic/chlorite schist (Pzp) belonging to Paleozoic Pazarcık Complex with B2 (NATM) class was expected for the collapsed zone (Figure 3.7). The chlorite schist which is green-greenish gray colored was defined as slightly to moderately weathered, very weak to strong with some calcite and quartz veins. The discontinuities are slightly rough to smooth. However, during the investigation, no borehole was drilled within the collapsed zone. Additionally, no faults and/or shear zones were detected during the investigations. No information was presented in the investigation report about the groundwater inflow. According to classification provided by the Earthquake Design Code of Turkey, BT24 Tunnel was located within the second degree earthquake zone and no active faults were anticipated along the BT24 Tunnel.
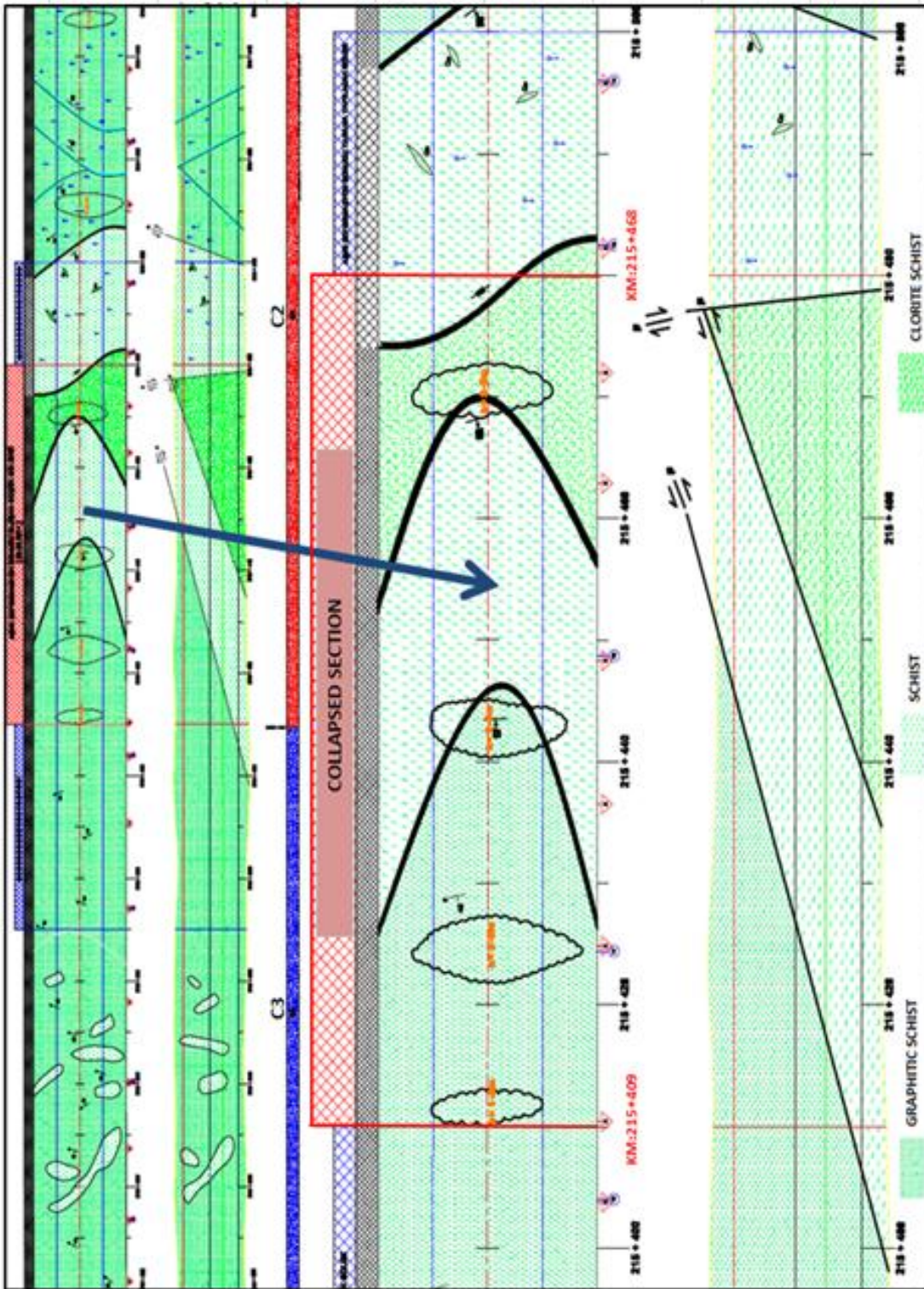
Figure 3.7 Geological map and cross-section of the BT24 Tunnel with observed NATM Classes

3.3 Monitoring and Geotechnical Mapping of BT24 Tunnel

3.3.1 Monitoring of BT24 Tunnel

The prediction of rock mass behavior, in particular when tunneling under high overburden, is a challenging task during design as well as during construction. Heterogeneous rock mass conditions significantly increase the difficulties in prediction of the tunnel performance. Although the general geological situation may be known, changes of rock mass stiffness or structure ahead of the face, influencing stresses to a great extent in the vicinity of the tunnel and thus deformations generally cannot be determined with sufficient accuracy.

Many tunneling problems are caused by unexpected changes in the strength or deformability of the host ground in which the tunnel is constructed. For safe and economical tunneling under difficult conditions a continuous adaptation of excavation and support design is required. Therefore, instrumentation and monitoring play a vital role in verifying design assumptions and calibrating numerical models for tunnel construction. Furthermore, monitoring serves as an alert if the initial support or lining is not performing as intended or if the tunnel is in danger of collapse. Deformation monitoring is the main factor in controlling the performance and cost-effectiveness of underground excavation. As such, in the last two decades deformation monitoring has become a fundamental requirement for assessing the stability of underground openings and for quantifying the acceptable risk of rock response. (Kontogianni and Stiros, 2003).

The monitoring program within the tunnel of BT24 is implemented by using the standard convergence and deformation measurements. Convergence measurement is a reliable, quick and economical indication of rock or soil mass stability and of support system effectiveness which can be obtained by simple surveying of wall-wall and roof-floor convergence. Deformation readings are obtained by measuring the coordinates of target plates installed on shotcrete shell. That information is then utilized in making decision on strengthening support elements to limit the deformations within the target tolerances.

Early prediction of tunnel convergence is crucial in tunnel construction with the NATM because it can help in timely adjustments of the design and consequently deadly hazards can be avoided. Moreover, in NATM, tunnel deformations are monitored both, during the construction period to modify the support system if deemed necessary, as well as following the installation of the main support for the assessment of performance previous to the placement of the final lining. Before the placement of the final lining, tunnel deformations are waited to converge fully and become stabilized. This procedure was also followed in BT24 Tunnel. Based on the deformation data relating to the tunnel periphery, it was concluded that the deformations were stabilized, and final lining construction was started. An example of deformation data record can be seen from Figure 3.8. It can be observed in that figure that the deformations were fully converged for a period of at least three months. However, records of the convergence measurements showed that stable conditions were only reached 3 months after the commencement of the top heading excavation with an excess convergence of over 150 mm.

Figure 3.8 Deformation data of KM: 215+410 (after SIAL Report, 2011)

3.3.2 Geotechnical Mapping of BT24 Tunnel

Before the excavation of a tunnel, only surface observations and very few boreholes in general are available to assess the ground attributes. Because of the considerable uncertainties involved in assessing the ground conditions, mapping of the temporary tunnel face during tunnel construction is extremely important. Face mapping, instrumentation and interpretation of monitoring results form the basis for the verification of the selected excavation and support class and the need to make any adjustments at frequent intervals as the tunnel advances. Face mapping of each excavated round provided opportunity required to observe the ground and its behavior during and after excavation. The data collected for each round of excavation include detailed rock mass behavior observations (interface boundaries between materials, discontinuity, joints and shear zones) and groundwater conditions.

For the BT24 Tunnel, face mapping was performed at almost every 10 m during tunnel construction. The prepared face maps clearly show that the collapsed section of the tunnel is within graphitic / chlorite schist (Figure 3.9). Other face maps are shown in Appendix A.

Moreover, the tunnel face maps between KM: 215+400 and KM: 215+480 indicate existence of various faults by means of appearance, extent and orientation. The fault mechanism clearly indicates highly complicated ground conditions in general along the alignment of the tunnel as the low angle faults are cut by a steeply inclined another fault at KM: 215+480.

Based on the tunnel face mapping, C3 class rock mass is observed between KM: 215+300 and KM: 215+409. Nevertheless, C2 class rock mass is encountered after KM: 215+409 where the collapsed section commences.

As stated in the tunnel face maps, although no significant groundwater inflow was noted, the tunnel faces were generally damp.

Figure 3.9 A typical tunnel face map showing highly fractured, highly-to completely weathered, faulted graphitic schist at Km: 215+412 of the tunnel

23

3.4   Basic Design Principles and Criteria

BT24 Tunnel was excavated according to the NATM using conventional excavation equipment. Due to the overwhelming success of the NATM, there has been a trend towards evaluation of the rock mass quality according to the criteria cited in the Austrian Standard ÖNORM B 2203. The ground is grouped into several classes each being given a specific type and the corresponding temporary support descriptions, in addition to the specific excavation steps. The project specific support types corresponding to the rock classes after ÖNORM B2203 usually cover a wide range of potential tunnel behavior and constitute the frame for the application phase of the NATM design. Such design is recently called the frame-design of NATM. Therefore, the design is based on the observational method with numerical analysis serving as a background to the development of the design framework. Final support criteria are determined from the observations during construction and the assessment of monitoring results together with the geological face mapping.

In the NATM applications, the type and extent of the support system to be used are prescribed initially in accordance with the rock class, which is identified utilizing the available ground information. This initially envisaged support system, which can be referred to as "pre-design," however, is subject to redefinition (or modification) based on the current conditions encountered on the tunnel face during the excavation.

For characteristic combinations of support measures and construction sequences the tunneling classes are determined according to the ÖNORM B 2203. NATM fundamentals based on ÖNORM B 2203 with some alterations, to surpass the sectional problems, are applied in the design. In the interest of rock, C2 support classes were considered. As stated in the Standard, C rock type is defined as squeezing rock and tends to collapse with prominent swelling behavior.

CHAPTER 4

NUMERICAL ANALYSES OF COLLAPSED SECTION

4.1 Finite element program Phase^2

Phase^2 is an implicit, elasto-plastic, 2D finite element program which is used to calculate stresses and displacements of a broad range of geotechnical problems including underground openings. Phase^2 program is suitable for plane-strain and axisymmetric idealizations. The "in plane" stresses and displacements can be calculated under plane-strain conditions and "out of plane" stresses and displacements can be found under axisymmetric conditions.

As in the other commercially available finite element programs, the domain is discretized into set of elements and corresponding nodes are assigned to each element. Displacements within these elements are calculated based on shape functions tied to the nodes of the elements. An implicit method is often used for solving the equations in which, every element communicates with nearby elements during a solution step and several iterations are necessary before compatibility and equilibrium can be reached.

A wide range of material models are provided in Phase^2 as shown in Table 4.1. The program also offers an extensive range of support modeling options for geotechnical applications under two basic types as; (i) liner and (ii) bolt. Liners can be simulated using beam elements. Bolts can be modeled with 5 different types of options as: (i) end anchored, (ii) fully bonded, (iii) plain strand cable, (iv) swellex/split-sets and (v) tieback.

Table 4.1 Constitutive models in Phase^2

Constitutive Models in Phase^2	
Elastic models	**Plastic Models**
1) Isotropic	1) Mohr-Coulomb
2) Transversely Isotropic	2) Hoek-Brown
3) Orthotropic	3) Drucker-Prager
4) Duncan-Chang Hyperbolic	4) Generalized Hoek-Brown
	5) Cam-Clay
	6) Modified Cam-Clay
	7) Discrete Function

The program generates the mesh automatically. 3, 6 node triangular elements and 4, 8 node quadrilateral elements are available in the program. Phase^2 allows multi-stage finite element analysis of excavation in up to 300 separate stages. Two options are available to define the initial field stresses in Phase^2: (i) constant, or (ii) gravity field stress option. Constant field stress option is used to define a constant stress field prior to excavation which does vary neither with position nor with depth. On the other hand, gravity field stress option is used to define an in-situ stress field which varies only with depth.

4.2   Fundamental Criteria

The computations of collapsed section are performed using the finite element program Phase^2 with Mohr-Coulomb elasto-plastic material model for the simulation of the behavior of rock mass. The Mohr-Coulomb model is a conventional model which is widely used to represent shear failure in soil and rock media.

Both axisymmetric and plane-strain finite element models are utilized in this study. Axisymmetric analyses are performed for the decision of initial relaxation factor necessary for the plane-strain analyses. The plane-strain analyses are used for the purpose of modeling stresses and deformations around the tunnel periphery. The 2D plane-strain analysis is used to model the tunnel excavation as the "out of plane" length of the tunnel is too large with respect to the tunnel cross section. The material softening method (Swoboda, 1979 and Swoboda et al., 1994) is used to define the amount of deformation before installation of rock support in the numerical model.

Tunnel excavation is simulated by the removal of elements within an excavation boundary. The top heading, bench and invert construction sequences are implemented in the plane-strain analysis. The support system of the tunnel consists of: (i) the outer lining (shotcrete), (ii) the inner lining (final) and (iii) the rock anchors (bolt). Application of shotcrete is implemented by the beam elements in 2D numerical analyses. The final lining is applied basically for esthetic purposes in NATM approach. Since the aim of this study is to evaluate the structural stability during construction of the tunnel, final lining is omitted in the models. Bolts are simulated using fully bonded elements in the analyses. The bolt length, "in plane" spacing and cross-sectional area are specified together with the "out of plane" spacing in the analyses. Tension failure occurs in a bolt element when the axial force on the bolt element exceeds the peak axial capacity. When the peak capacity of the bolt is exceeded, it reduces to the residual capacity.

The coefficient of earth pressure at rest (K_0) is a fundamental parameter in the analysis. Within the scope of this work, the value of K_0 is taken as 1.0, considering the available geological information on the project area.

The height of the overburden on the tunnel crown is taken as 160 m, which is the largest value along the tunnel. The ground is modeled only up to 56 m over the crown and the rest of the overburden is applied as additional uniformly distributed load over the upper boundary of mesh.

4.3   Material Parameters Used in the Analyses

The collapsed section of the BT24 Tunnel remains within the graphite schist formation according to the geological mapping. The geological mapping during construction of the tunnel clearly revealed that the geological conditions are very heterogeneous and therefore definition of reference cross sections with reasonably well-defined behavior proves to be very difficult. Geotechnical parameters of this material are of concern, since the numerical models are employed in this study to investigate the tunnel performance driven in rock mass.

26

In order to obtain relevant strength and elasticity parameters for this investigation, Roclab, Rocscience software (2007) was used. Roclab is to conduct rock mass strength analysis using the Hoek-Brown failure criteria in order to obtain Mohr-Coulomb parameters that can be used as input for numerical models. The use of the Roclab software allows for a simple and intuitive implementation of the Hoek-Brown failure criterion, allowing the user to easily obtain reliable estimates of rock mass properties. Material properties of the rock formation are obtained using the Hoek-Brown Criterion and converted into Mohr-Coulomb equivalent material properties. Geotechnical parameters used in the analyses for the rock mass are shown in Table 4.2.

The primary support system consists of shotcrete, steel rib, wire mesh and bolt. Shotcrete, steel rib and wire mesh are modeled as composite liner in the performed analyses. Strength, rigidity and section properties of the support systems used in analyses are shown in Table 4.3. The section properties of support systems are: (i) 30 cm width of the shotcrete, (ii) I-160 type of the steel rib with 1 m round length, (iii) Q221/221 type of the double layered wire mesh (iv) SN type, 6 m length, 28 cm diameter bolts with 1 m out plane and in plane spacing. The cross-section of the tunnel showing the primary support systems and excavation steps is presented in Figure 4.1.

Table 4.2 Geotechnical parameters for rock mass

PROPERTY	GRAPHITIC SCHIST
γ	26 kN/m^3
Φ	29.85°
c	206 kN/m^2
E	400,000 kN/m^2
ν	0.3

Table 4.3 Material properties of support elements (SİAL report, 2010)

PARAMETER	SHOTCRETE	BOLT (Φ28)	STEEL RIB (I160)	WIRE MESH (Q221/221)
Modulus of Elasticity (MPa)	15,000	210,000	210,000	210,000
Compressive Strength (MPa)	20	-	-	-
Cross-sectional Area (cm^2)	-	6,157	22,80	1,31
Tensile Strength (MPa)	1,6	-	400	400
Tensile Capacity (MN)	-	0,25	-	-
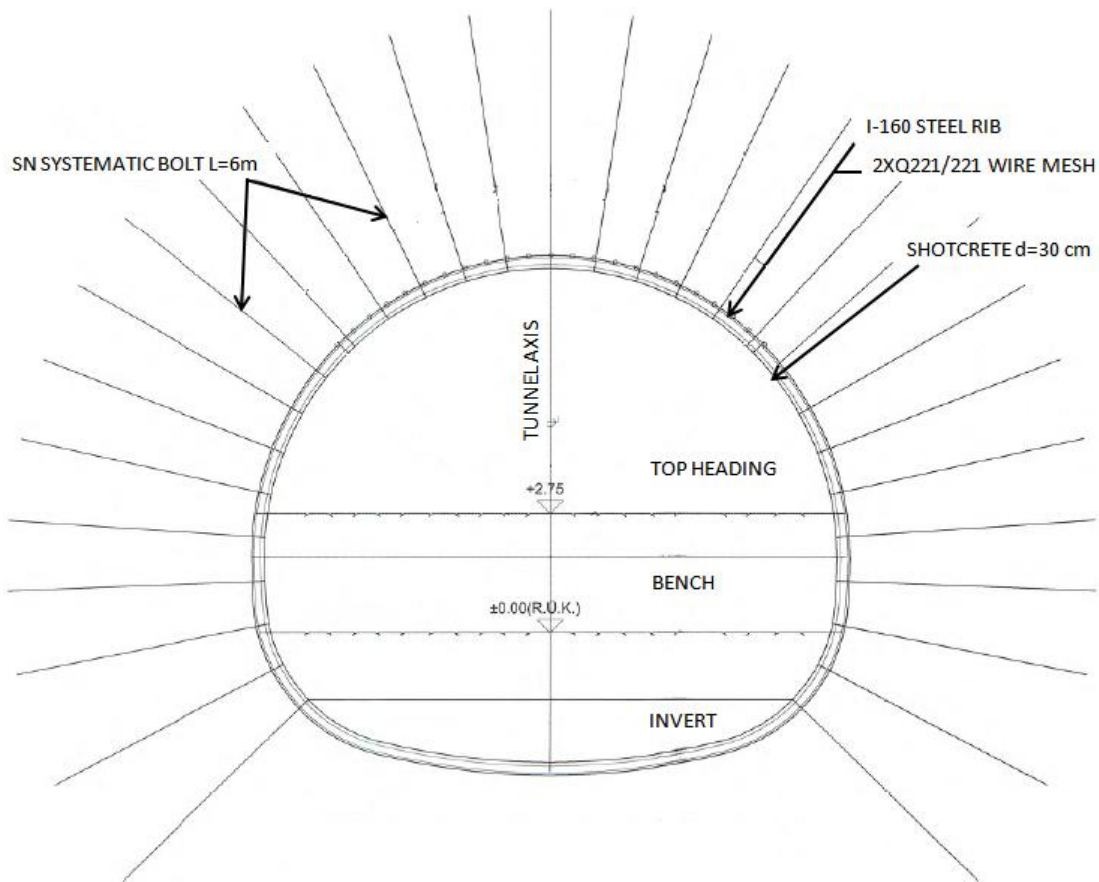
Figure 4.1 Typical tunnel section for C2 rock class

4.4 Determination of Initial Relaxation Factor

The initial relaxation factor is required for the 2D plane-strain analyses. To determine this parameter, two different models were utilized in a parallel manner. In the first, the radial deformation in the vicinity of the face is determined from the axisymmetric analysis with constant field stress option. In the second one, material softening method is used under plane-strain conditions with constant field stress option. The relaxation factor will be determined approximately when the radial movement in the plane-strain model is equivalent with the radial movement in the vicinity of the face in the axisymmetric model.

The axisymmetric simulation is shown in Figure 4.2. The tunnel radius is 6 m and 0.3 m thick shotcrete is implemented as the supporting element. The elastic modulus of the shotcrete is increased gradually at 2 m round lengths behind the face of the tunnel in order to model the hardening behavior of shotcrete with time. Excavation is simulated with consecutive removal of the portions inside the tunnel section.
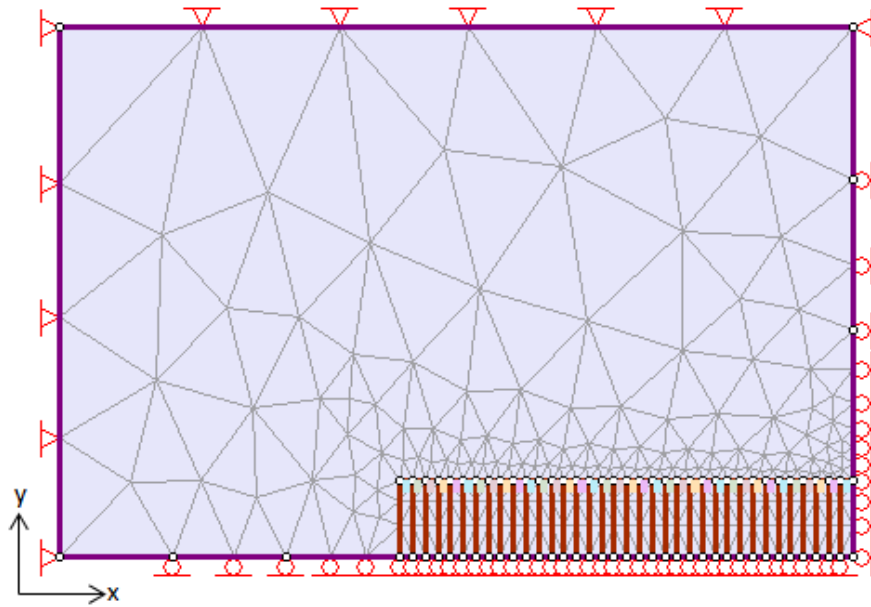
Figure 4.2 Axisymmetric model used for determination of initial relaxation factor

In plane-strain analysis (Figure 4.3), material softening technique is used. This technique can be explained as the incremental reduction of the stiffness of the ground material. The rock mass inside the tunnel is sequentially replaced with a more compressible rock mass than the proceeding stage by reduction of the elastic modulus. This reduction allows the periphery of the tunnel to deform progressively. The radial deformations corresponding to each stage are recorded as shown in Figure 4.4.
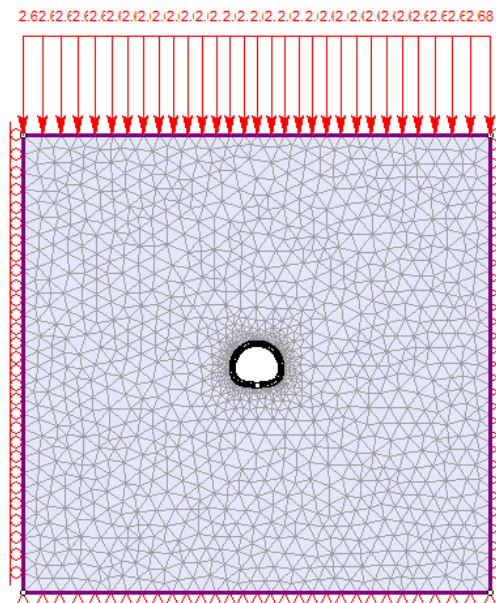
Figure 4.3 Plain strain model used for determination of initial relaxation factor

In the axisymmetric analysis, the radial deformation in the vicinity of the face is calculated as 12 cm (Figure 4.5). In plane strain analysis, 70% reduction in the stiffness of the rock material corresponds to the face radial deformation in the axisymmetric analysis. As a result, in 2D plane-strain analyses of the collapsed tunnel section, the initial relaxation factor is employed as 70%.
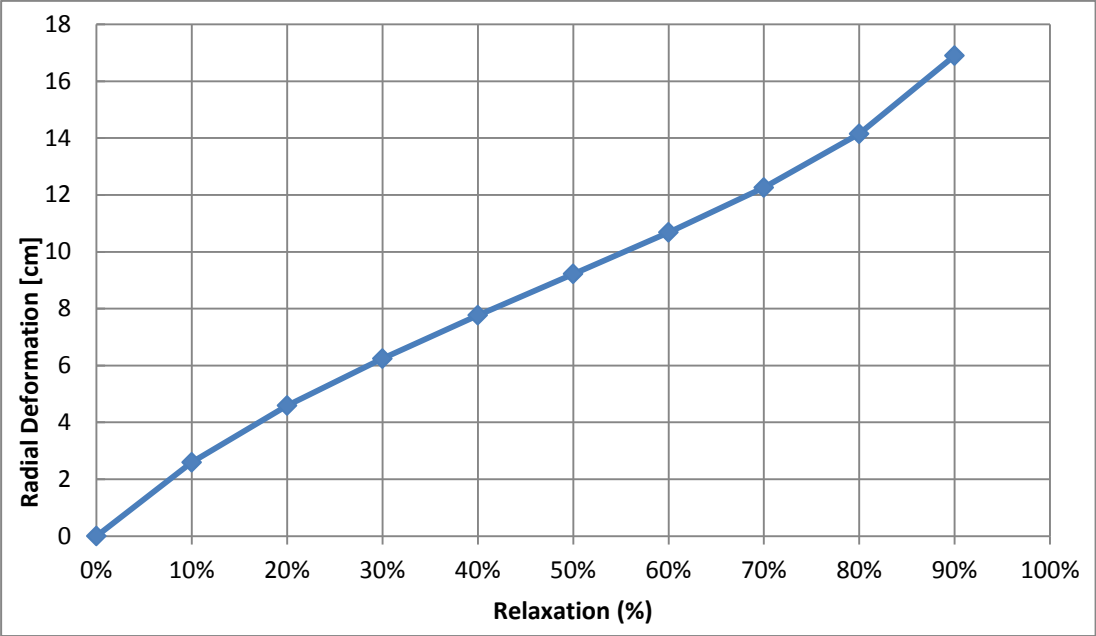
Figure 4.4 Radial deformations obtained from plane-strain model
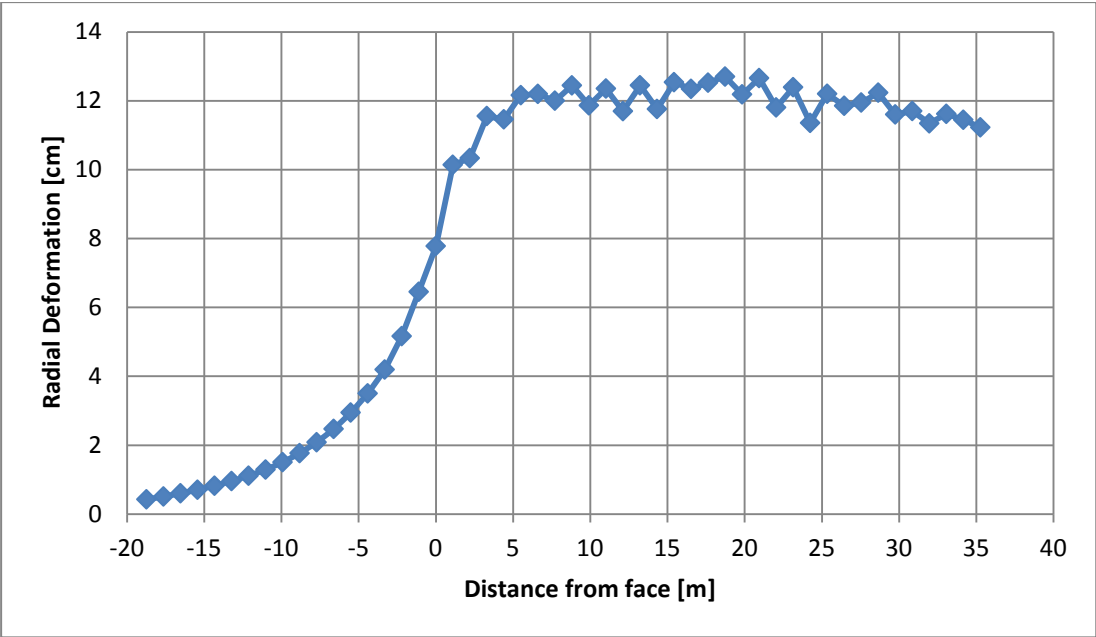
Figure 4.5 Radial deformations obtained from axisymmetric model

4.5   Plane-strain Analyses of BT24 Tunnel

In competent rock formations the tunnel invert may be flat, whereas in weak rock and soft ground tunnels the invert should be rounded to facilitate closure and stability. Since the aim of this study is to enlighten the reasons behind the collapse, analyses are performed in two alternatives: (A) section without a closed invert and (B) the ring closure of invert using invert shotcrete. The same ground material properties and support system with the exception of invert closing in case B were defined for the two alternatives in order to compare the tunnel behavior regarding closure of the invert. The faults of various alignments are known to exist in the rock mass along the route of the tunnel based on the information regarding geological mapping of the tunnel face. However, the exact positions and alignments of these faults are unknown. Accordingly, different scenarios were created by placing hypothetical faults in the model sections, to investigate their likely effects on the tunnel performance. Five different cases are analyzed for these two alternatives, namely: (I) Case 1 (no fault), (II) Case 2 (horizontal fault), (III) Case 3 (diagonal fault), (IV) Case 4 (intersecting faults), (V) Case 5 (combination of all faults). The 2D models used in the analyses for all cases are shown in Figures 4.6 through 4.10. Strength parameters may vary with time especially in weak rock mass commonly due to creep. In order to model creep effects, the strength parameters of the surrounding mass are reduced incrementally following the end of construction for all analyzed cases.

Numerical analyses are performed in stages simulating the driving sequence as top heading, bench and invert excavations of the tunnel. Construction of Alternative A, which represents the collapsed section without a closed invert, is modeled in 15 stages. Difference between Alternative A and Alternative B is the existence of closed invert. As a consequence, an additional stage (construction stage 11) is implemented in the analysis to model invert closure for Alternative B. Construction stages of Alternative B are presented in Table 4.4 and Figure 4.11.
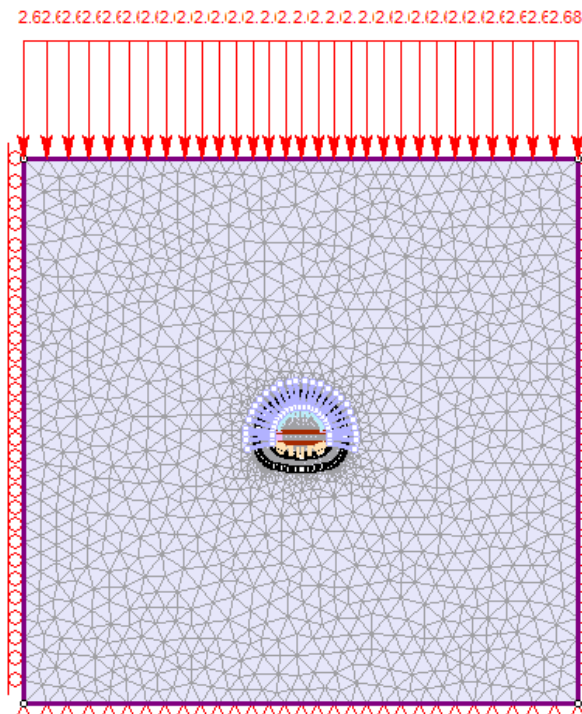
Figure 4.6 Plane-strain model for Case I
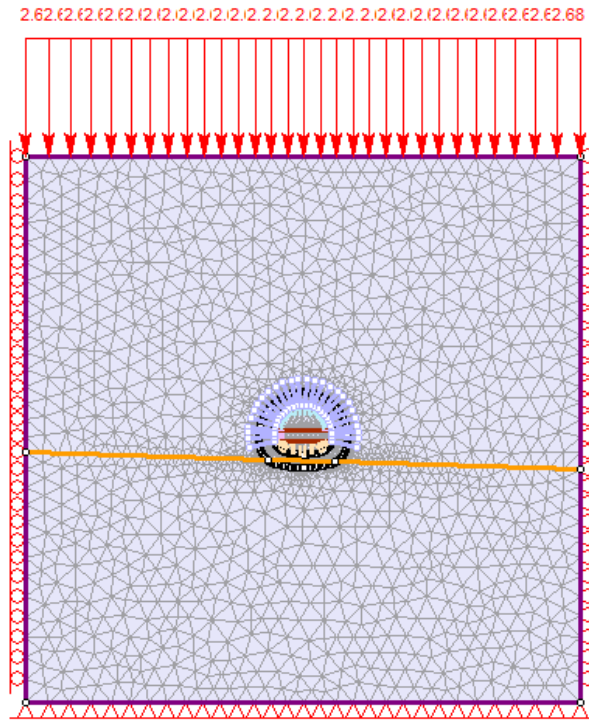
Figure 4.7 Plane-strain model for Case II (horizontal fault scenario)
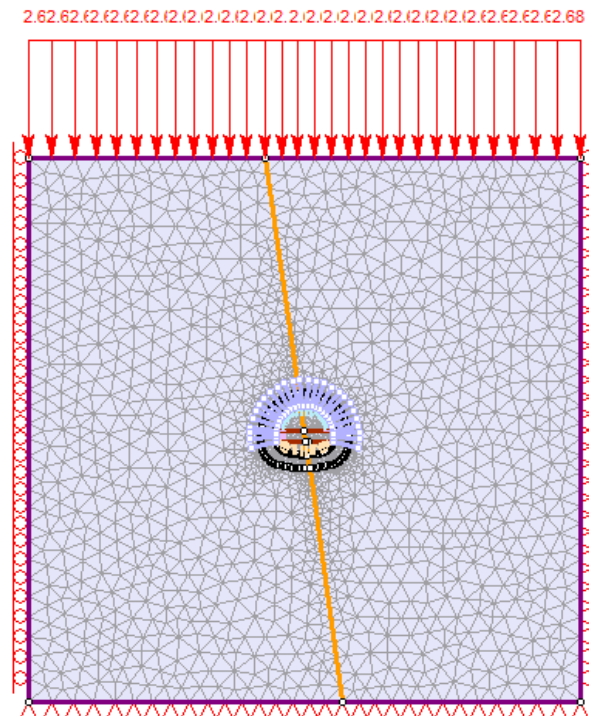
Figure 4.8 Plane-strain model for Case III (diagonal fault scenario)
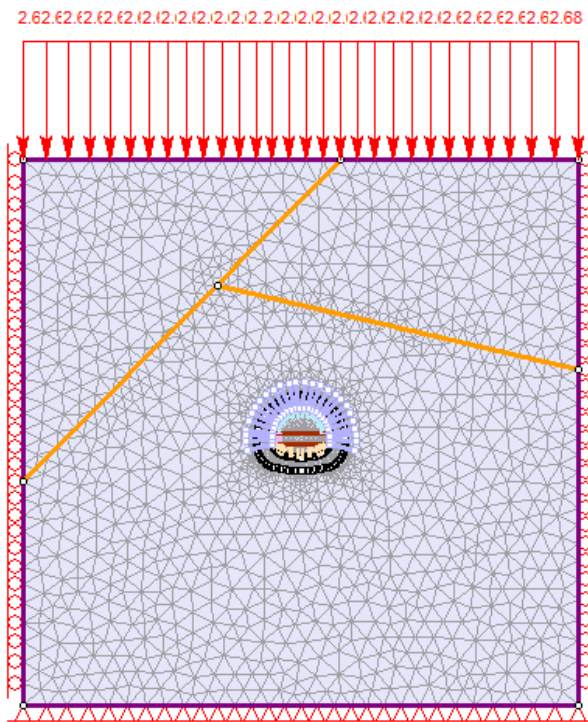
Figure 4.9 Plane-strain model for Case IV (intersecting fault scenario)
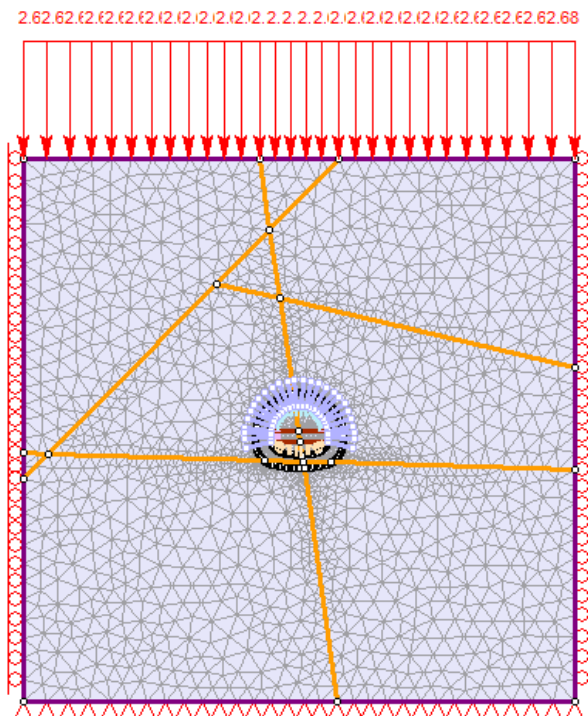
Figure 4.10 Plane-strain model for Case V (combination of all faults scenario)
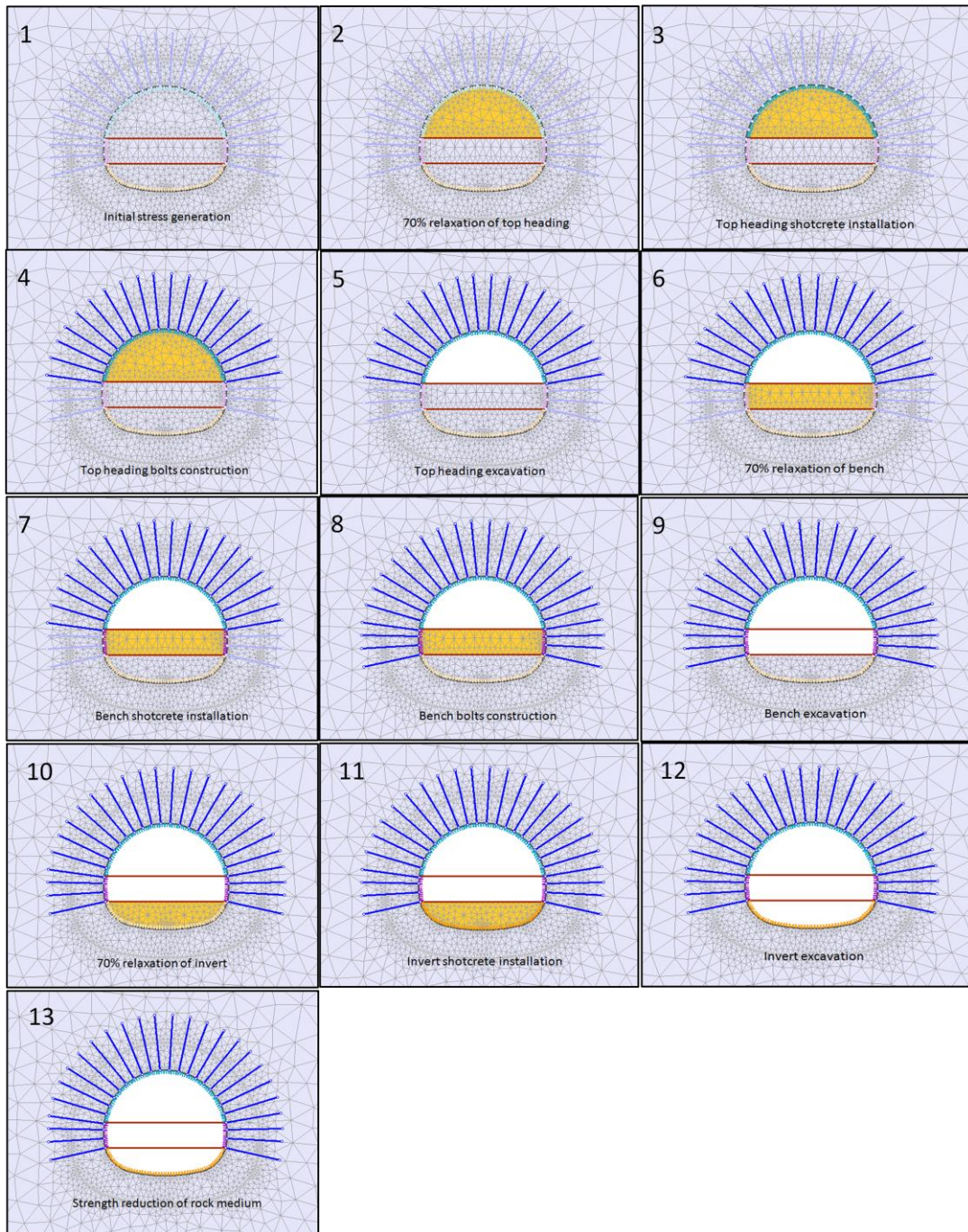
Figure 4.11 Construction stages for Alternative B

Table 4.4 Construction stages for Alternative B

Phase	Description
1	Initial stress (gravity) generation of the media
2	70% relaxation of the top heading
3	Top heading liner construction
4	Top heading bolts construction
5	Top heading excavation
6	70% relaxation of the bench
7	Bench liner construction
8	Bench bolts construction
9	Bench excavation
10	70% relaxation of the invert
11	Invert liner construction
12	Invert excavation
13	Strength reduction of rock media surrounding the tunnel periphery with a factor of 1.4

CHAPTER 5

RESULTS AND DISCUSSION

In this chapter the results obtained from the analyses of alternatives A and B, each with five different cases are presented. The results including displacements, distribution of internal effects (moment, axial and shear forces) throughout the liners at the periphery, as well as the occurrence of the plastic failure zones surrounding the tunnel are presented for Case I for the alternatives A and B, in the form of computer outputs of the section in Figures 5.1 through 5.14. The figures relating to the remaining cases for the two alternatives are presented in Appendix B. The results presented in the figures are summarized in Table 5.1 for an overall evaluation.

In all five cases, the deformations around the tunnel periphery both after completion of excavation and following the strength reduction for Alternative A (with no invert closure) are noted to be higher than for Alternative B (ring closure with closed invert). It is also noted that following the strength reduction, the deformations considerably increase for Alternative A in all cases. Whereas the ring closure in Alternative B helps to prevent excessive increasing of deformations almost in all cases. In Case IV, in which the fault is located way above the tunnel crown, the presence of fault does not influence the deformations. However, the deformations are affected widely when the fault is located just below the tunnel invert (Case II).

The invert deformations for alternatives A and B with no fault (Case I) are 34 cm and 25 cm, respectively just after the completion of all excavation stages. In order to investigate the long term creep effects on the tunnel performance, strength parameters of the rock mass (c,Φ) are reduced gradually. During strength reduction, radial deformations tend to increase and reach at 73 cm for Alternative A and at 27 cm for Alternative B for the case with no fault existing in the section (Case I).

The width of plastic zone around the tunnel periphery remains approximately the same (11-13 m) in two alternatives and in all cases following the completion of excavation. After the strength reduction, however, while the plastic zone does not increase to a great extent for Alternative B in any of the cases, it increases severely in all cases for Alternative A.

The bending moments obtained from the analyses of Alternative A are observed to be higher than those obtained from the analyses of Alternative B in all cases. On the other hand, the shear forces are quite close for both alternatives in all cases. However, the distribution of maximum values are observed to occur close to the crown for Alternative A, whereas at the invert for Alternative B. Invert closure in Alternative B is considered to be the reason for the location shift of shear forces. As would be expected, the axial forces for Alternative B are significantly higher compared to these of Alternative A in all cases. This can be attributed to the ring closure at the invert, which provides good confinement for the installed support system. Moreover, the axial force distribution is observed to be fairly uniform along the entire section of tunnel in Alternative B. In Alternative A, decrease in axial force and increase in moment values along the liner due to the lack of ring closure leads to collapse.

Table 5.1 Summary of the results of analyses

	Case 1		Case 2		Case 3		Case 4		Case 5	
Alternative	A	B	A	B	A	B	A	B	A	B
Radial Deformation at Invert after Completion of Excavation (cm)	34	25	79	64	50	43	33	25	102	79
Radial Deformation at Invert after Strength Reduction (cm)	73	27	129	65	96	68	76	27	170	101
Plastic Zone Radius after Completion of Excavation (m)	13.2	11.7	13.9	12.1	13.8	12.2	12.9	10.8	14.2	11.5
Plastic Zone Radius after Strength Reduction (m)	20.2	13.3	21	14.2	21.1	15.6	21.2	13.3	22.2	15.3
Maximum Axial Forces after Completion of Excavation (MN/m)	4.83	9.07	5.38	9.98	3.62	4.88	4.83	8.98	3.66	5.86
Maximum Axial Forces after Strength Reduction (MN/m)	4.06	10.43	4.07	11.06	3.36	6.15	4.25	10.46	3.76	7.33
Maximum Bending Moments after Completion of Excavation (MNm/m)	0.55	0.46	1.16	0.55	0.66	0.60	0.68	0.46	1.24	0.69
Maximum Bending Moments after Strength Reduction (MNm/m)	1.39	0.44	1.95	0.60	1.34	1.04	1.67	0.44	2.05	1.14
Maximum Shear Forces after Completion of Excavation (MN/m)	0.16	0.41	0.36	0.54	0.25	0.49	0.24	0.36	0.44	0.46
Maximum Shear Forces after Strength Reduction (MN/m)	0.40	0.30	0.47	0.42	0.45	0.69	0.37	0.31	0.62	0.64
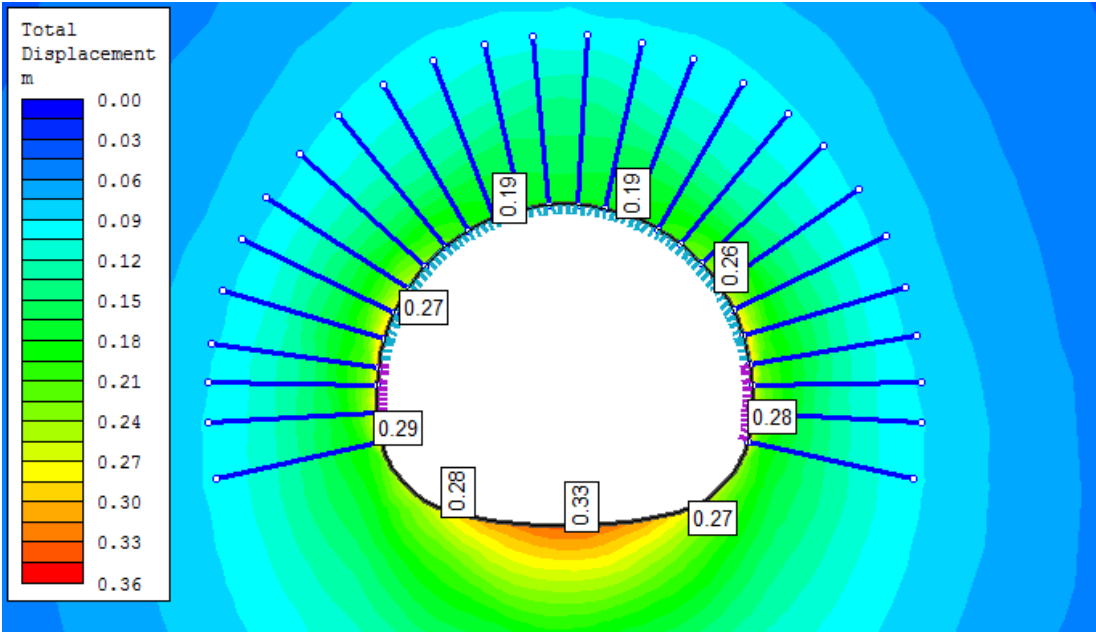
Figure 5.1 Radial deformations after the completion of excavation for Case I, Alternative A
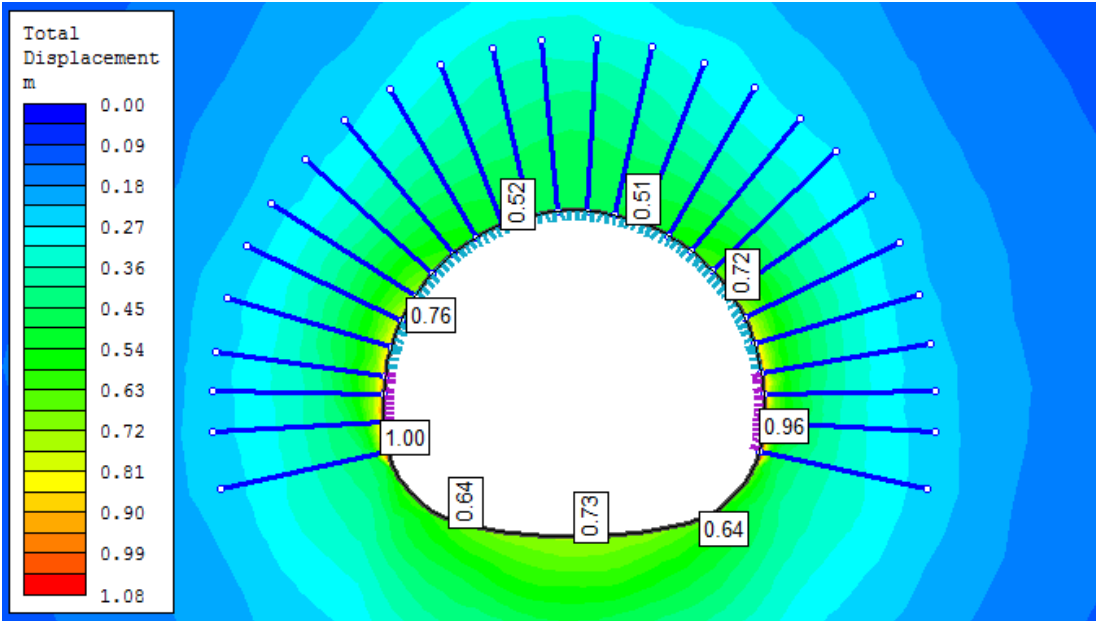
Figure 5.2 Radial deformations after strength reduction for Case I, Alternative A
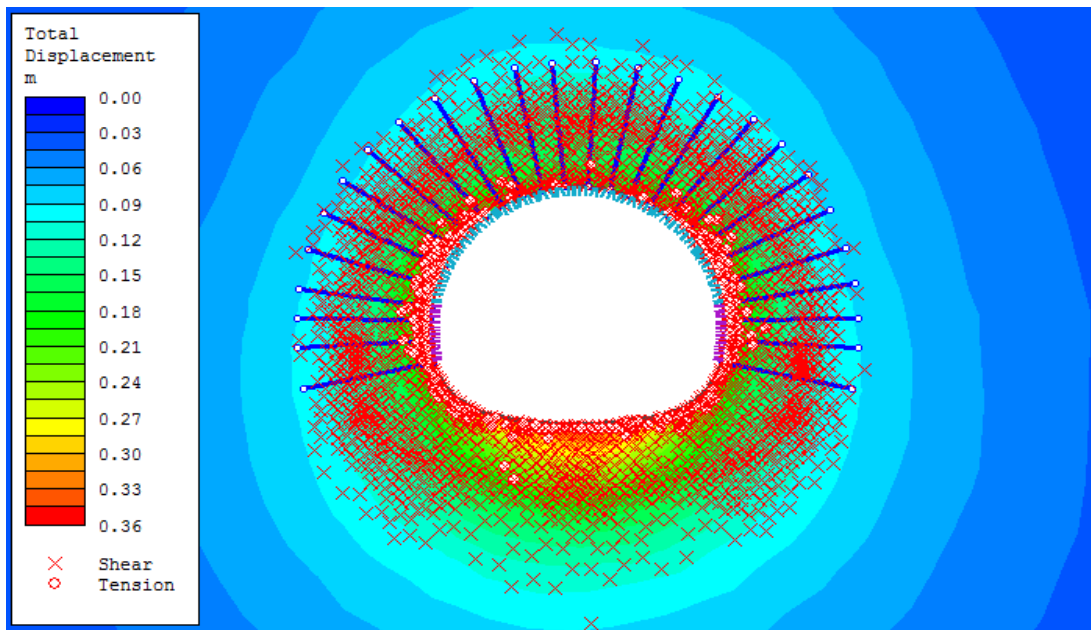
Figure 5.3 Plastic zone radius after the completion of excavation for Case I, Alternative A
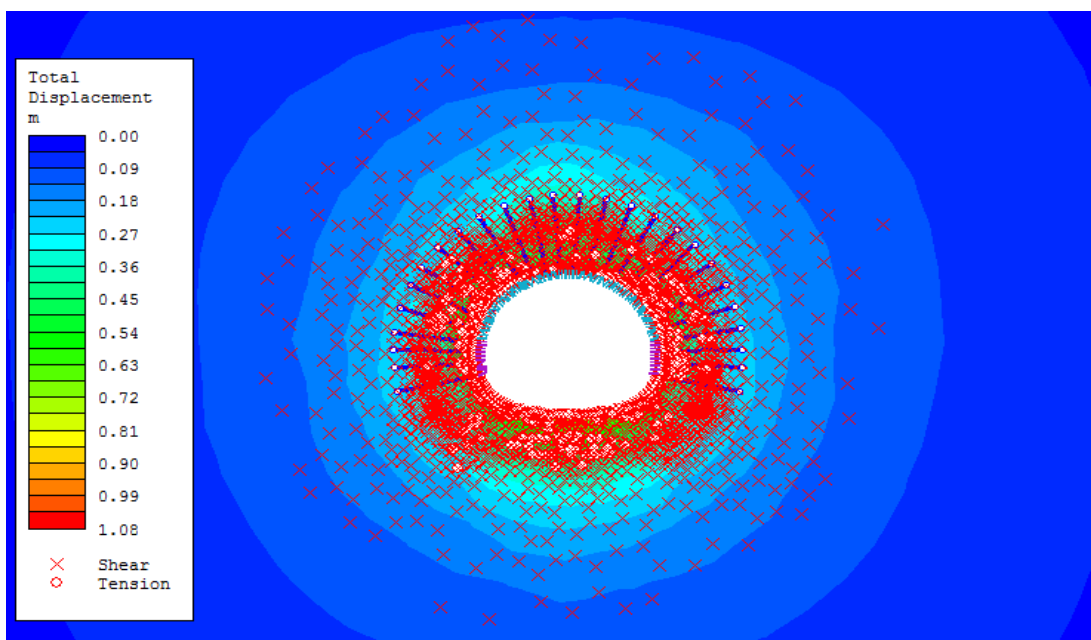
Figure 5.4 Plastic zone radius after the strength reduction for Case I, Alternative A
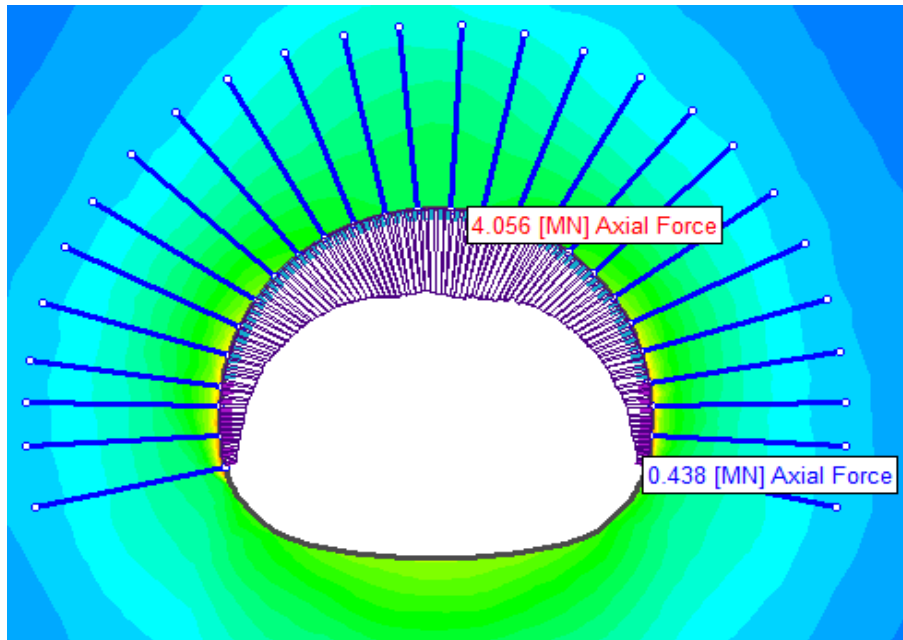
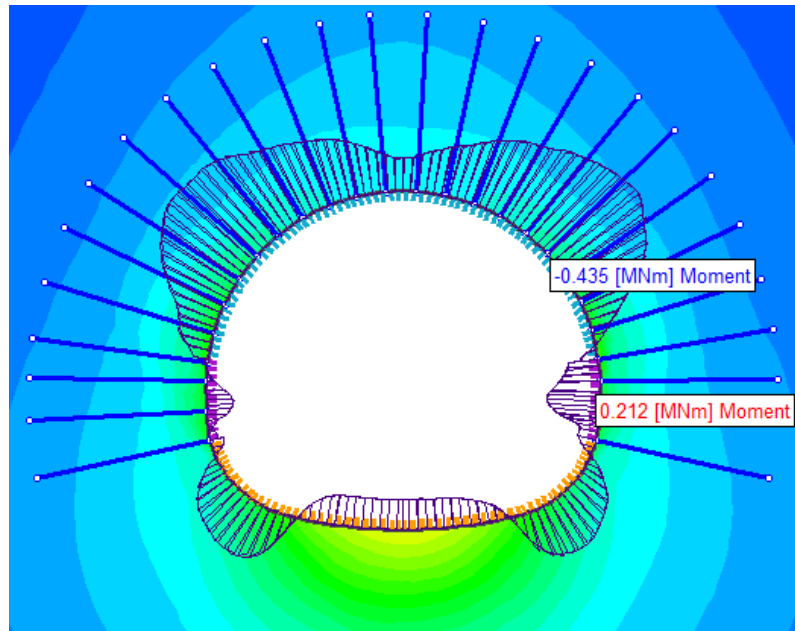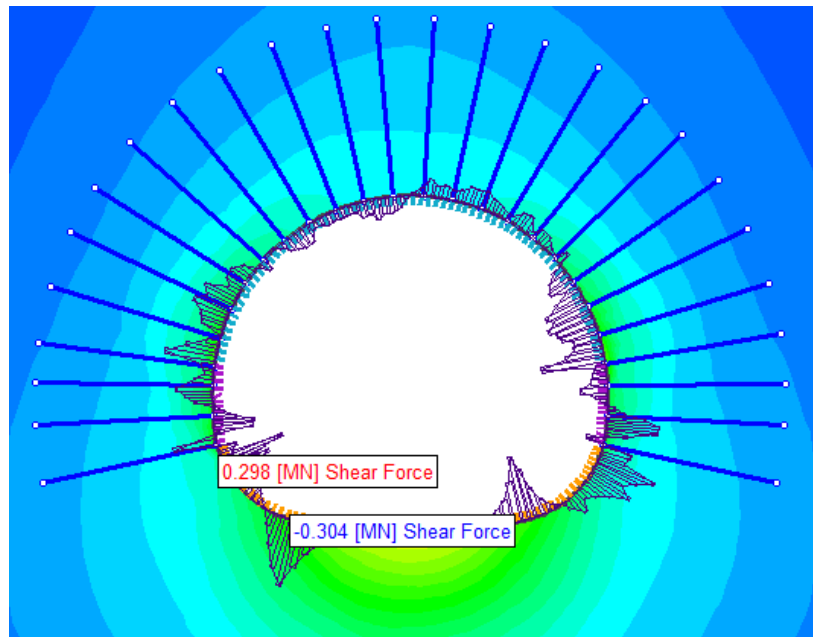Figure 5.5 Axial forces after the strength reduction for Case I, Alternative A
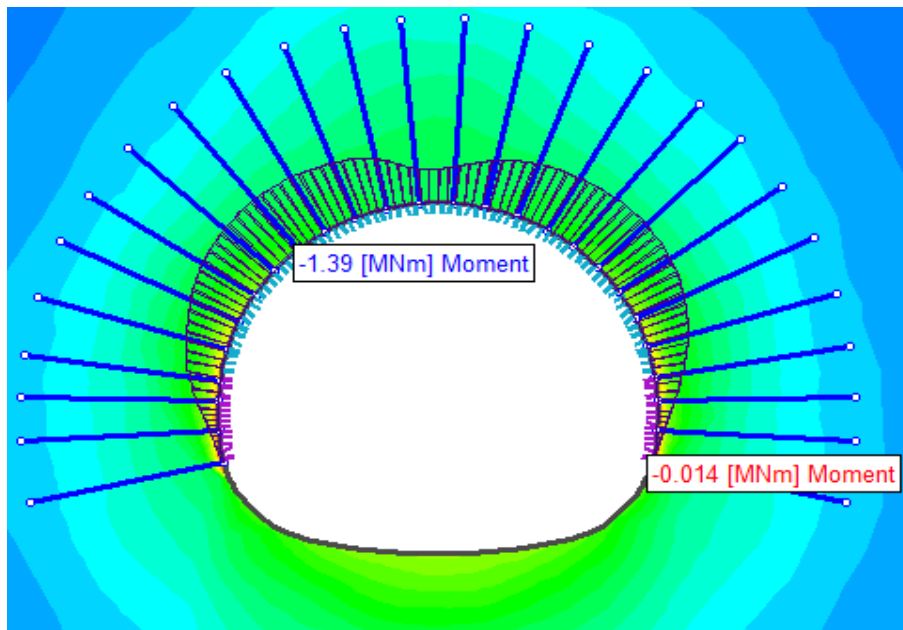
Figure 5.6 Bending moments after the strength reduction for Case I, Alternative A
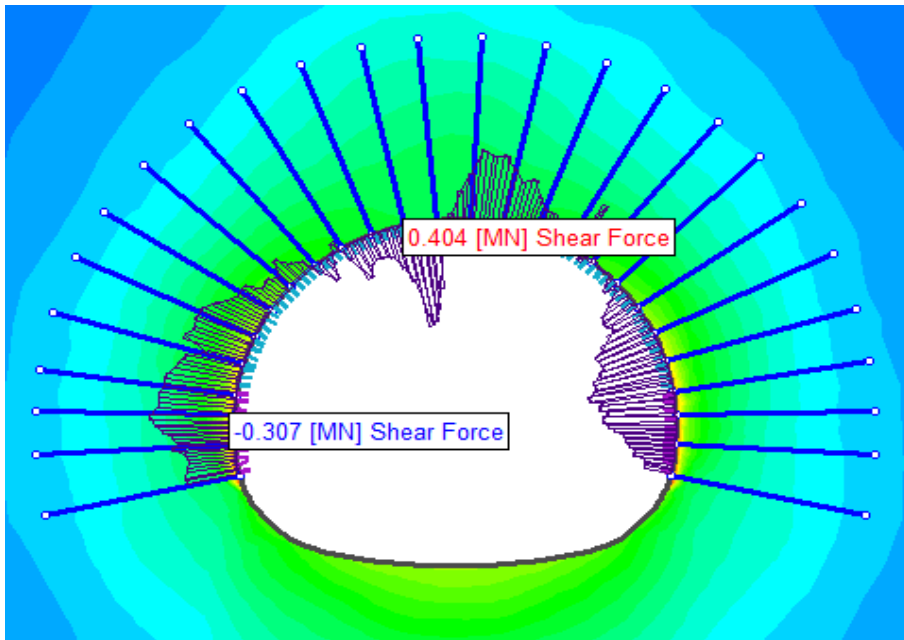
Figure 5.7 Shear forces after the strength reduction for Case I, Alternative A
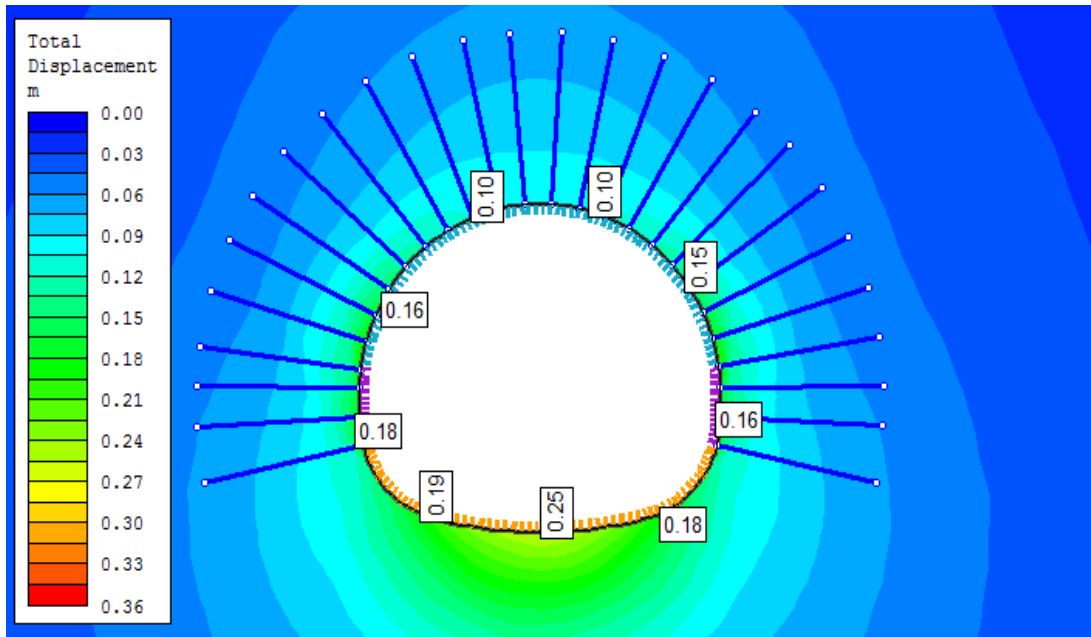
Figure 5.8 Radial deformations after the completion of excavation for Case I, Alternative B
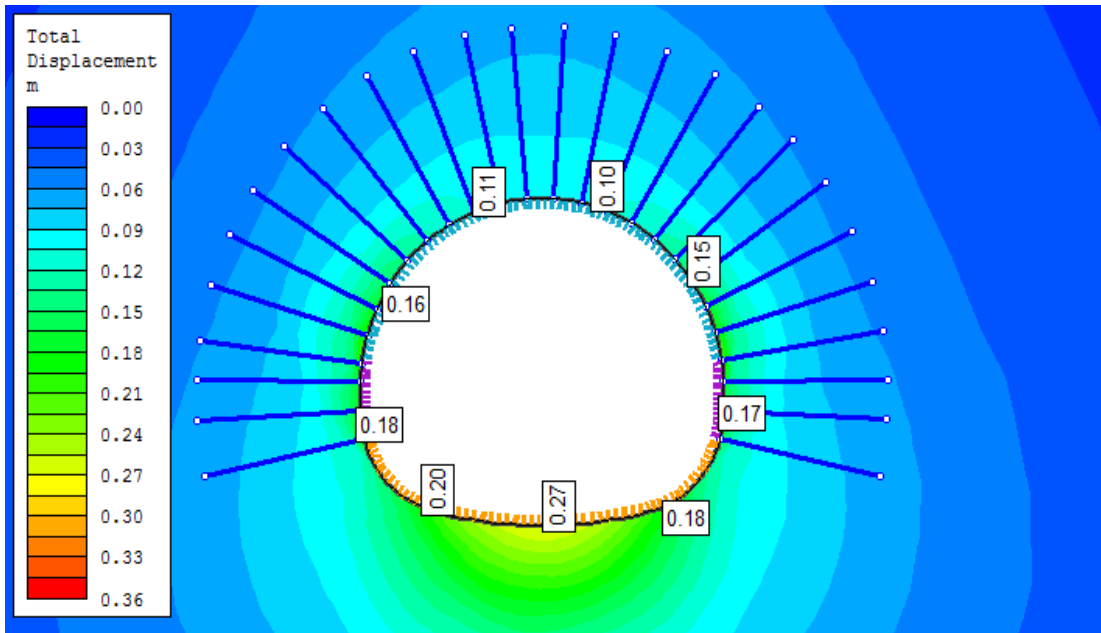
Figure 5.9 Radial deformations after strength reduction for Case I, Alternative B
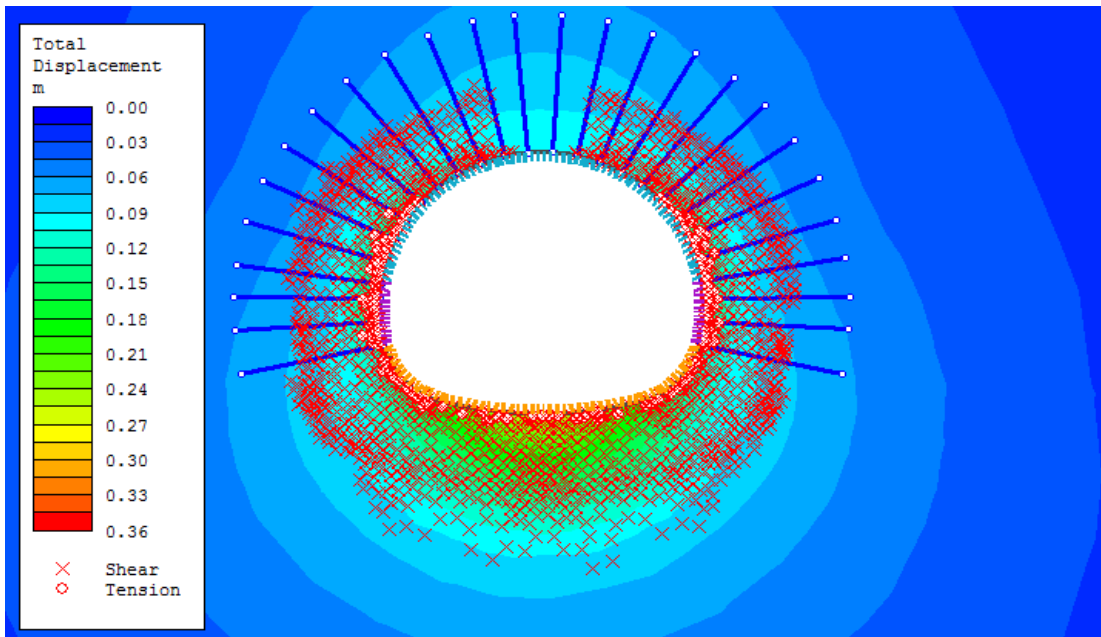
Figure 5.10 Plastic zone radius after the completion of excavation for Case I, Alternative B
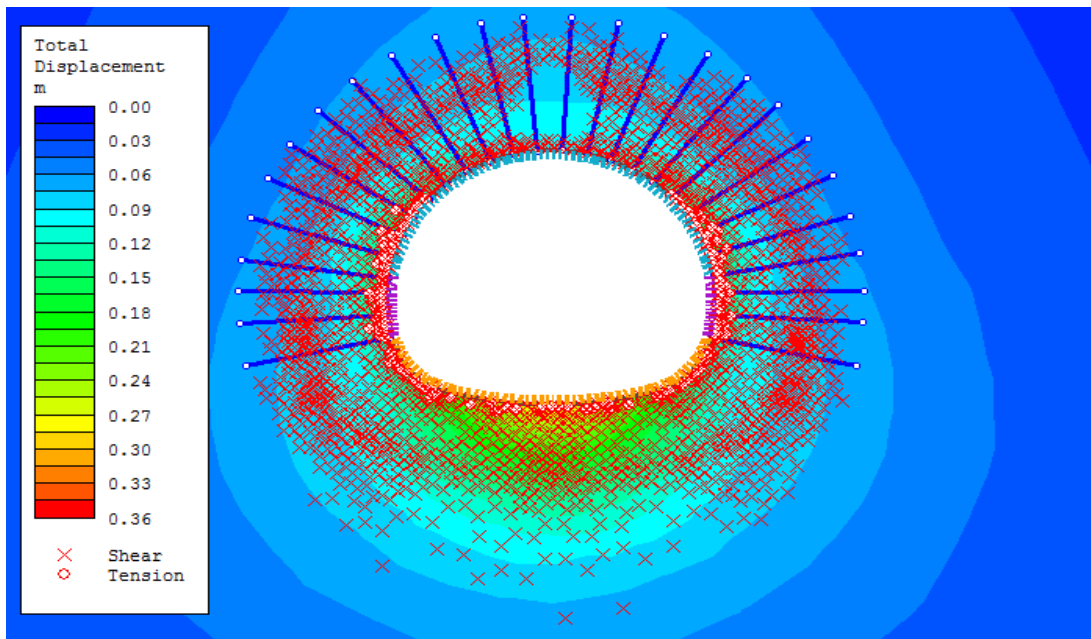
Figure 5.11 Plastic zone radius after the strength reduction for Case I, Alternative B
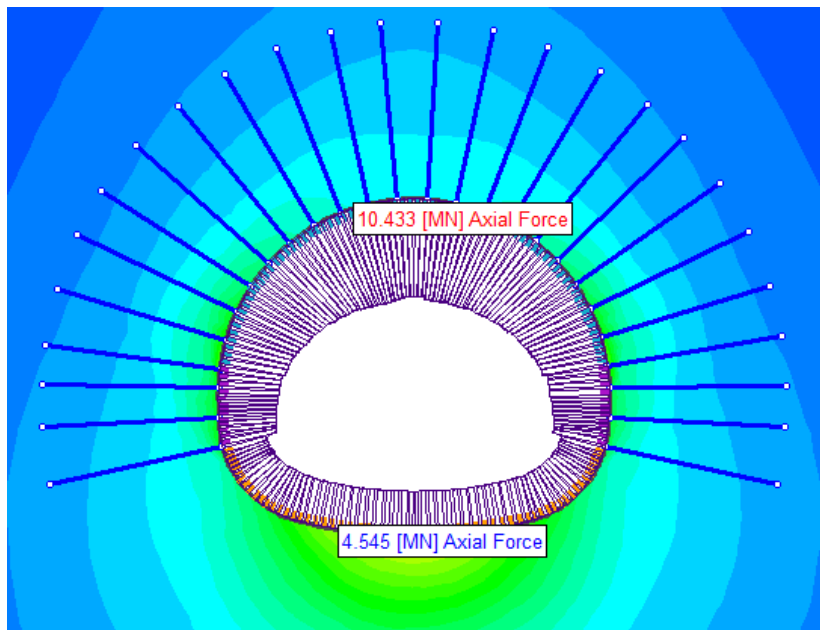
Figure 5.12 Axial forces after the strength reduction for Case I, Alternative B

Figure 5.13 Bending moments after the strength reduction for Case I, Alternative B

Figure 5.14 Shear forces after the strength reduction for Case I, Alternative B

CHAPTER 6

CONCLUSIONS AND RECOMMENDATIONS

6.1   Conclusions

Performance of the BT24 Tunnel is investigated with and without ring closure, and each for five different cases involving fault scenarios as well as considering the effects of possible creep of the rock mass on a comparative basis in order to understand the reason behind the collapse of the tunnel. According to the results of the analyses, the most significant observation is that the existence of fault zones and creep behavior of the rock mass can result in excessive deformations, particularly when the ring closure of the lining is not provided in the invert. This finding is in accord with the observations made and the measurements taken previous to the occurrence of the collapse of the tunnel section, at which no ring closure was provided, and excessive deformations took place in time particularly at the invert.

Accordingly, it can be argued that the ring closure plays a key role for the rock mass that is characterized by the large, continued deformations which could only be stopped or at least considerably reduced with the ring closure. Another noteworthy unfavorable factor appears to be the extreme variability of the ground conditions including fault zones with different orientations as revealed by the face maps throughout the tunnel route within the collapsed section. Therefore, one can state that the rock mass strength could have been overestimated for the collapsed section in the design phase, leading to the selection of an insufficient primary support system.

In usual NATM applications the final (inner) liner is not considered to be a load bearing element, but provides extra structural safety. In the case of BT24 Tunnel, however, if the inner lining, which provided ring closure and consisted of reinforcements as well, could have been constructed timely, it appears that the collapse could have likely been prevented.

6.2   Recommendations for Further Study

The standard practice for analyzing the behavior of tunnel is through the use of 2D plane-strain finite element computations. Three-dimensional (3D) models are not commonly used since they are rather sophisticated, costly and time consuming regarding model construction and input preparation. Besides, improved precision in modeling may not be compatible with the available level of information on the ground conditions. Still, however, excavation of a tunnel is uniquely a 3D phenomenon and 3D modeling provides a more realistic implementation of the tunnel construction. Accordingly, as a further study, the validity of 2D plane-strain idealization of the collapsed section of the BT24 Tunnel can be investigated using 3D models. Also in the numerical models, the value of K_0 may be taken greater than 1.0 considering the fault zones along the tunnel route, to account for the effect of different K_0 values on the analysis results. In addition, the influence of the Simav Earthquake which occurred on May 19, 2011 can be implemented in the numerical models. Finally, long term creep behavior can be simulated with more realistic material models.

REFERENCES

Barton, N. et al. 1974. Engineering classification of rock masses for the design of tunnel support. Rock Mechanics, v.6, no.2, p. 189-236

Bieniawski, Z.T. (1974). Geomechanics classification of rock masses and its application in tunneling. 3rd International Congress on Rock Mechanics, ISRM, Denver, Vol. IIA, 27-32.

Bieniawski, Z.T. (1979). Geomechanics classification of rock engineering applications. 4th International Congress on Rock Mechanics, Montreux (Suisse), Vol. 2, p. 41-48.

Brown, E.T., 1981. Putting the NATM into perspective Tunnels Tunnel., 1981, pp. 13–17

Chopman, D., Metje, N. and Stark, A., 2010, Introduction to Tunnel Construction, Spon Press, pp. 1-417.

Deere, D. U. (1964). Technical Description of Rock Cores for Engineering Purpose, Rock Mechanics and Engineering Geology, Vol. 1, No. 1, p. 17-22.

Gnilsen R., Underground Structures Design and Instrumentation (ed. Sinha R.S.), 1989, Elsevier, Amsterdam, pp. 84-128

Hoek, E. and Brown, E.T., 1980, Underground excavation in rock: The Institution of Mining and Metallurgy, London, England.

ISRM, 1981 Rock Characterisation, Testing and Monitoring ISRM Suggested Methods Pergamon, Oxford

Kontogianni, V.A. and Stiros, S.C. 2003. Tunnel Monitoring during the excavation phase: 3-D Kinematic Analysis Based on Geodetic Data. Proceedings from 11th FIG Symposium on Deformation Measurements, Santorini, Greece, 2003.

Kripakov, N.P., 1983, Finite element method of design: U.S. Department of Interior, Bureau of Mines, Denver, Colorado, 17 p.

Ladanyi, B., 1974. Use of the log-term strength concept in the determination of ground pressure on tunnel lining: Proc. 3rd Cong. On Rock Mech., ISRM, v.11, Part B, Denver, Coloroda.

Müller L. 1978. The reasons for unsuccessful applications of the New Austrian Tunnelling Method, Tunnelling Under Difficult Conditions, Proceedings of the International Tunnel Symposium, Tokyo, Pergamon Press, 67-72.

Peck R.B. (1969). 'Advantages and limitations of the Observational Method in applied soil mechanics'. Géotechnique, 19(2): 171–87.

Phase[2] (2012), Reference Manual. Rock Engineering Group, University of Toronto.

Rabcewicz L. 1964. The New Austrian Tunnelling Method, Part one, Water Power, November 1964, 453-457, Part two, Water Power, December 1964, 511-515

Rabcewicz, L., Golser, J. 1973. Principal of dimensioning the supporting system for the New Austrian Tunneling Method. Water Power, March, 88–93.

Roclab, 2007. http://www.rocscience.com/products/Roclab.asp

Sial, (2010). Ankara-İstanbul Hızlı Tren Projesi (2.Etap) Eskişehir-Köseköy Demiryolu Tünel İksa Destek Sistemleri Hesap Raporu (Report No: EKD-BT0-STR-002-U0)

Sial, (2011). Ankara-İstanbul Hızlı Tren Projesi Vezirhan-İnönü (Kesim 2) Tünel 24: KM-215+370 ile KM: 215+500 Arası Tarama ve Göçük Kazı Projesi Raporu (Report No: EKD-T26R-BT24-STR-U0)

Singh, B. and Goel, R.K. 2006, Tunneling in weak rocks: Elsevier Geo-engineering Book Series, 489 p.

Sinha, R.S., and Schoeman, K.D., 1983, Rock tunnels and rock reinforcement: U.S. Department of Interior, Bureau of Reclamation, Denver, Colorado.

Sinha, R.S. (1989). Underground Structures, Design and Instrumentation. Elsevier, pp. 1-546.

Swoboda, G., 1979. Finite element analysis of the New Austrian Tunnelling Method (NATM). In: Proceedings of the 3rd International Conference on Numerical Methods in Geomechanics, Aachen, 2: 581–586.

Swoboda, G., Marence, M., Mader, I., 1994. Finite element modelling of tunnel excavation. International Journal of Engineering Modelling 6: 51–63.

Terzaghi, K. (1946), "Rock Defects and Loads on Tunnel Support", Rock Tunneling with Steel Supports, eds. R. V. Proctor and T. White, Commercial Shearing Co., Youngstown, Ohio, USA, pp. 15–99

Yüksel Project, (2008). Eskişehir-Köseköy Demiryolu Jeolojik-Jeoteknik Etüt Raporu (Report No: EKD-000-JER-001-U-0

APPENDIX A
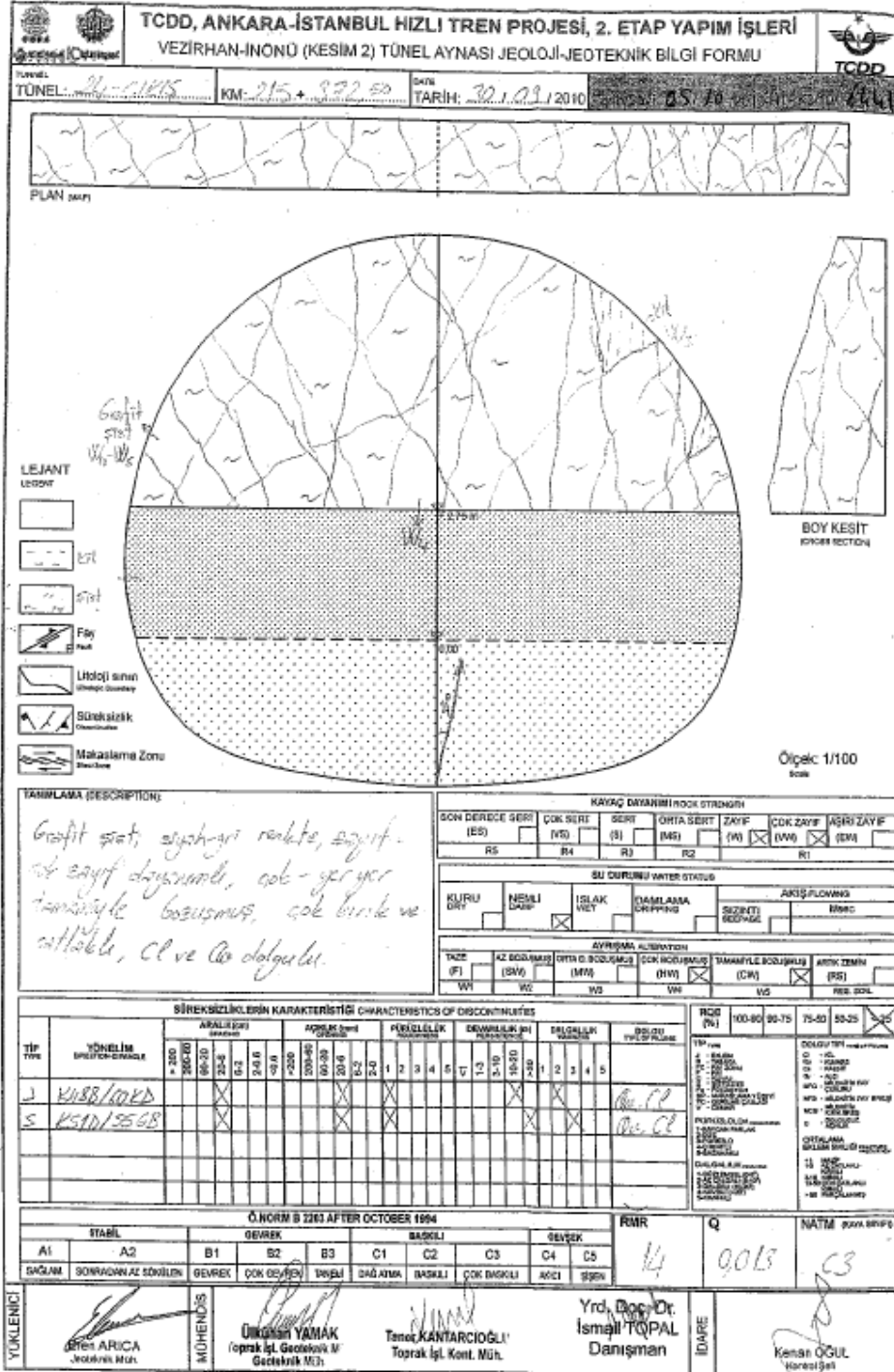
Figure A.1 Tunnel face map at Km: 215+372.5 of the tunnel
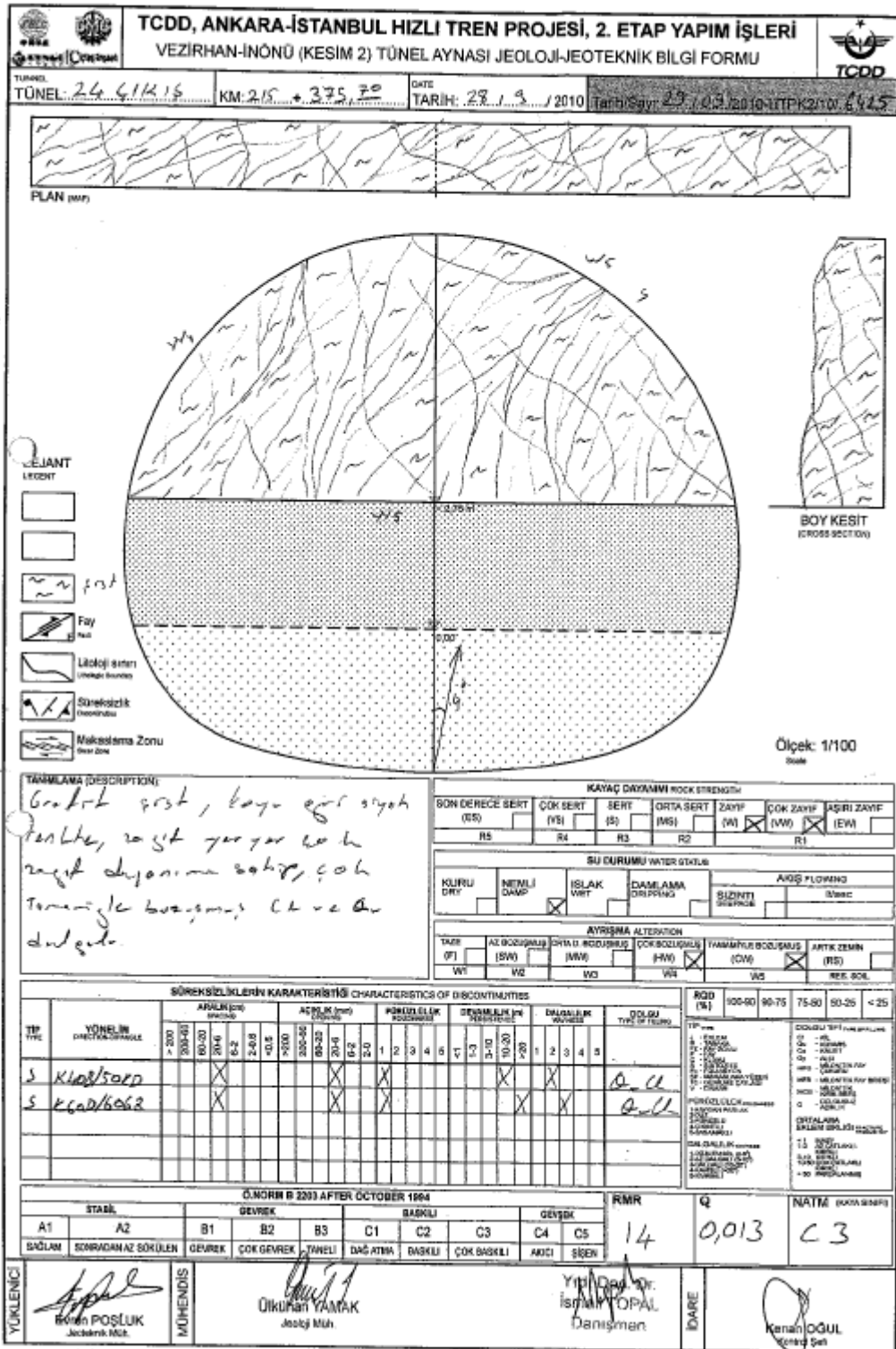
Figure A.2 Tunnel face map at Km: 215+375.7 of the tunnel

TCDD, ANKARA-İSTANBUL HIZLI TREN PROJESİ, 2. ETAP YAPIM İŞLERİ

VEZİRHAN-İNÖNÜ (KESİM 2) TÜNEL AYNASI JEOLOJİ-JEOTEKNİK BİLGİ FORMU

TCDD

TÜNEL: 24 ÇIKIŞ   KM: 215 + 382 85   TARİH: 24 / 3 / 2010   Tarih/Say: 28 / 04 (2010) (TPK2/10) 6301

PLAN (MAP)

LEJANT
LEGEND

~~ Çrt
/ Fay
Fault
Litoloji sınırı
Süreksizlik
Makaslama Zonu
Shear Zone

BOY KESİT
(CROSS SECTION)

Ölçek: 1/100
Scale

TANIMLAMA (DESCRIPTION):

Grafit şist/grimsi-yeşil renkte, zayıf dayanıma sahip, damarlı bozunmuş çok süreksiz. Süreksizlikler de az su sızıntılı.

KAYAÇ DAYANIMI ROCK STRENGTH

SON DERECE SERT (ES)	ÇOK SERT (VS)	SERT (S)	ORTA SERT (MS)	ZAYIF (W)	ÇOK ZAYIF (VW)	AŞIRI ZAYIF (EW)
R6	R4	R3	R2	☒	☒	R1

SU DURUMU WATER STATUS

| KURU DRY | NEMLİ DAMP | ISLAK WET ☒ | DAMLAMA DRIPPING | SIZINTI SEEPAGE | AKIŞ FLOWING lt/sec |

AYRIŞMA ALTERATION

| TAZE (F) W1 | AZ BOZUŞMUŞ (SW) W2 | ORTA D. BOZUŞMUŞ (MW) W3 | ÇOK BOZUŞMUŞ (HW) ☒ W4 | TAMAMIYLE BOZUŞMUŞ (CW) ☒ W5 | ARTIK ZEMİN (RS) RES. SOIL |

SÜREKSİZLİKLERİN KARAKTERİSTİĞİ CHARACTERISTICS OF DISCONTINUITIES

ROD (%) 100-90 90-75 75-50 50-25 (<25)

ÖNORM B 2203 AFTER OCTOBER 1994

STABİL		GEVREK			BASKILI			GEVREK		RMR	Q	NATM (KAYA SINIFI)
A1	A2	B1	B2	B3	C1	C2	C3	C4	C5	14	0,013	C 3
SAĞLAM	SONRADAN AZ SÖKÜLEN	GEVREK	ÇOK GEVREK	TANELİ	DAĞ ATMA	BASKILI	ÇOK BASKILI	AKICI	ŞİŞEN			

YÜKLENİCİ
POSLUK
Jeoteknik Müh.

MÜHENDİS
Ülkühan YAMAK
Jeoloji Müh.

Dr.
İsmail TOPAL
Danışman

İDARE
Kenan OĞUL
Kontrol Şefi

Figure A.3 Tunnel face map at Km: 215+382.85 of the tunnel

Figure A.4 Tunnel face map at Km: 215+391.00 of the tunnel
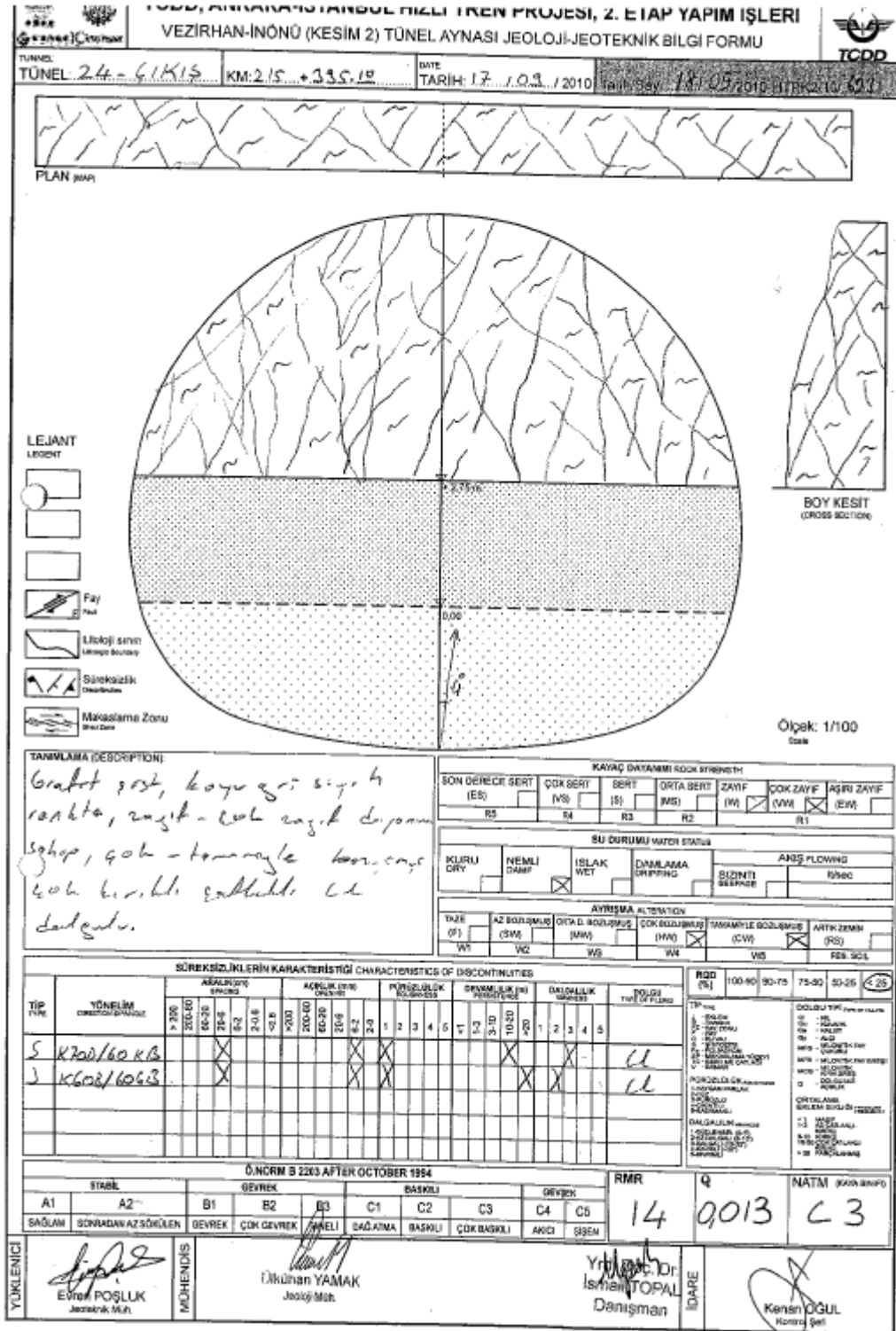
Figure A.5 Tunnel face map at Km: 215+395.10 of the tunnel
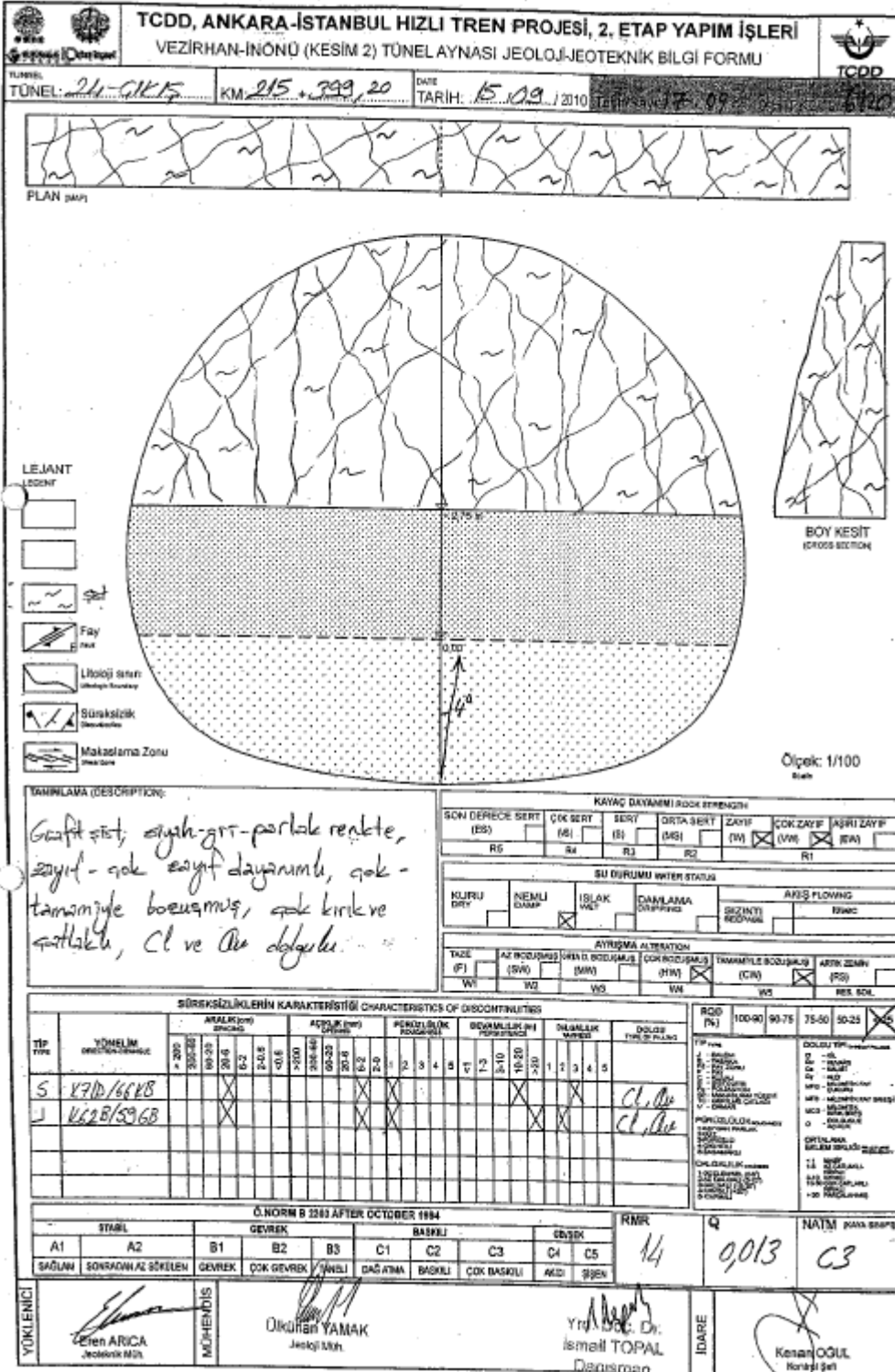
Figure A.6 Tunnel face map at Km: 215+399.20 of the tunnel
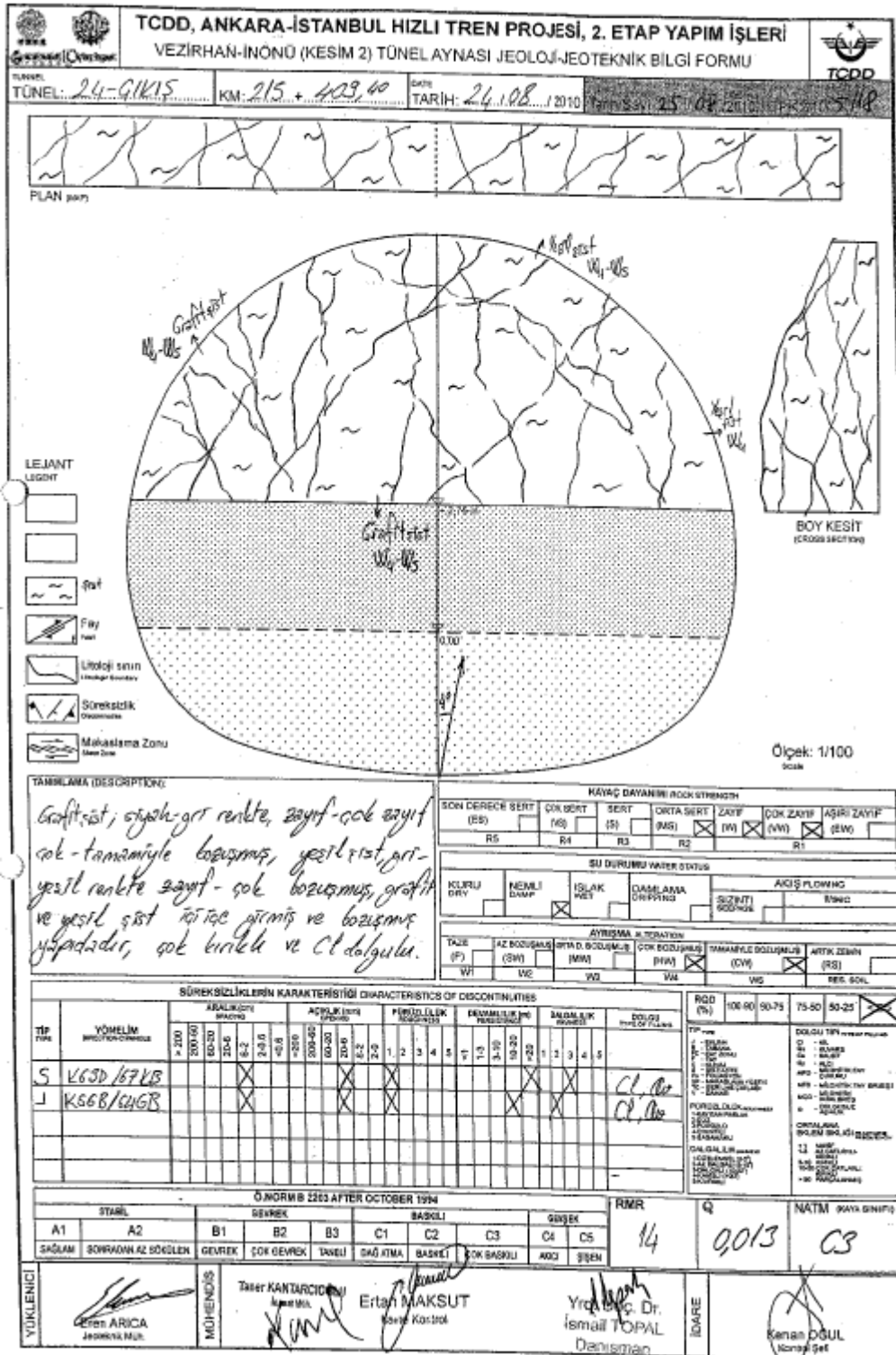
Figure A.7 Tunnel face map at Km: 215+409.40 of the tunnel

Figure A.8 Tunnel face map at Km: 215+423.65 of the tunnel

58

Figure A.9 Tunnel face map at Km: 215+430.90 of the tunnel
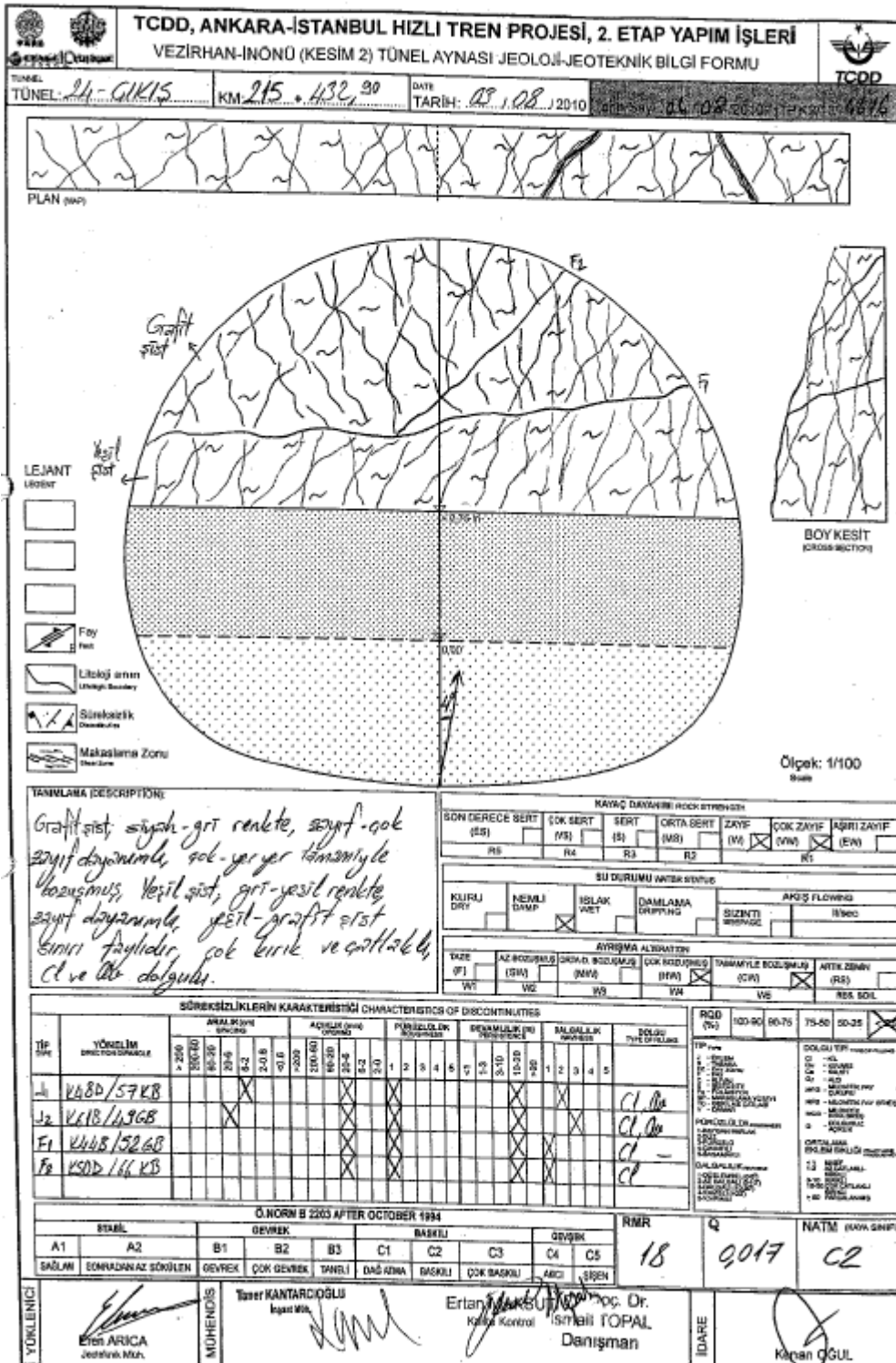
Figure A.10 Tunnel face map at Km: 215+432.90 of the tunnel
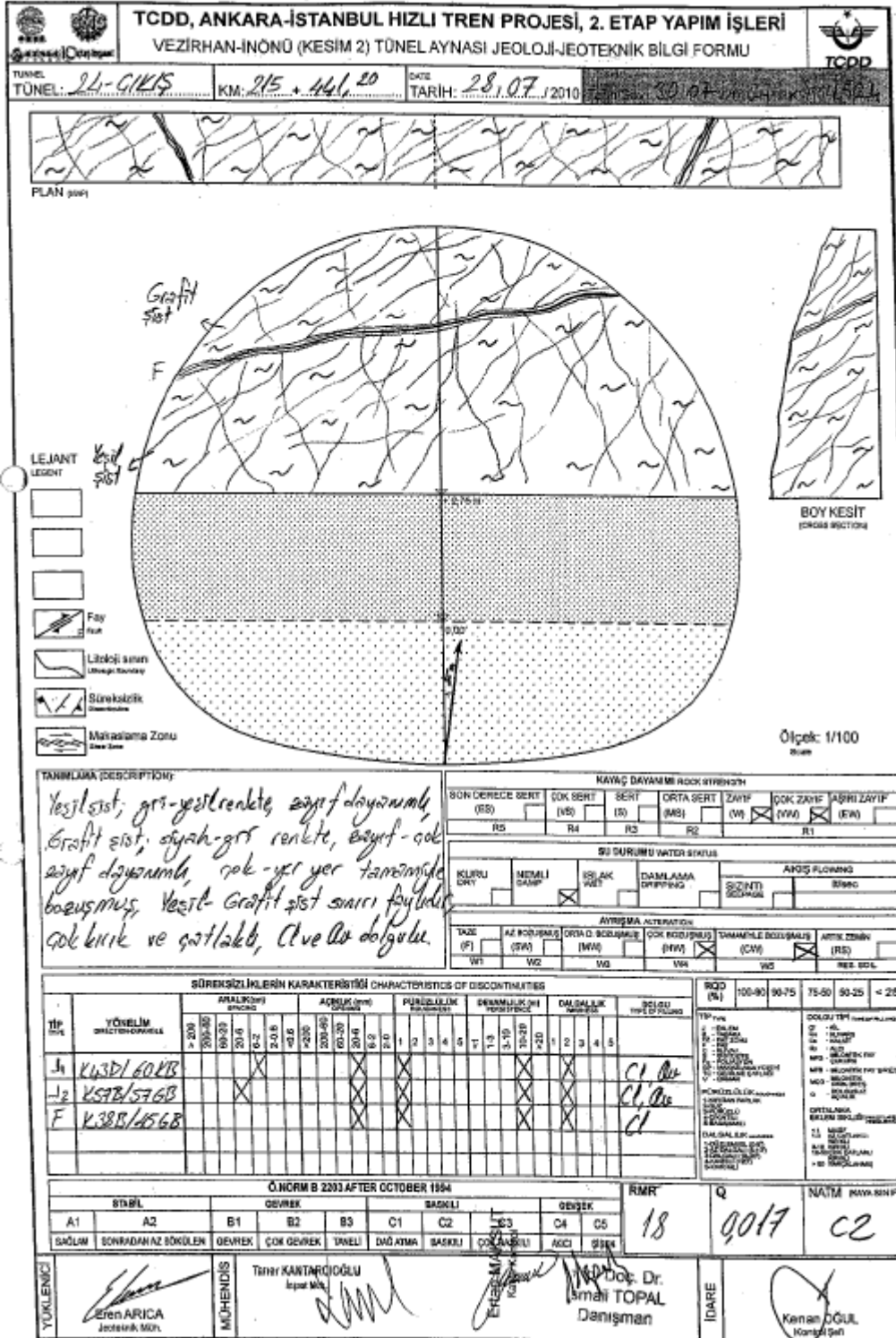
Figure A.11 Tunnel face map at Km: 215+441.20 of the tunnel
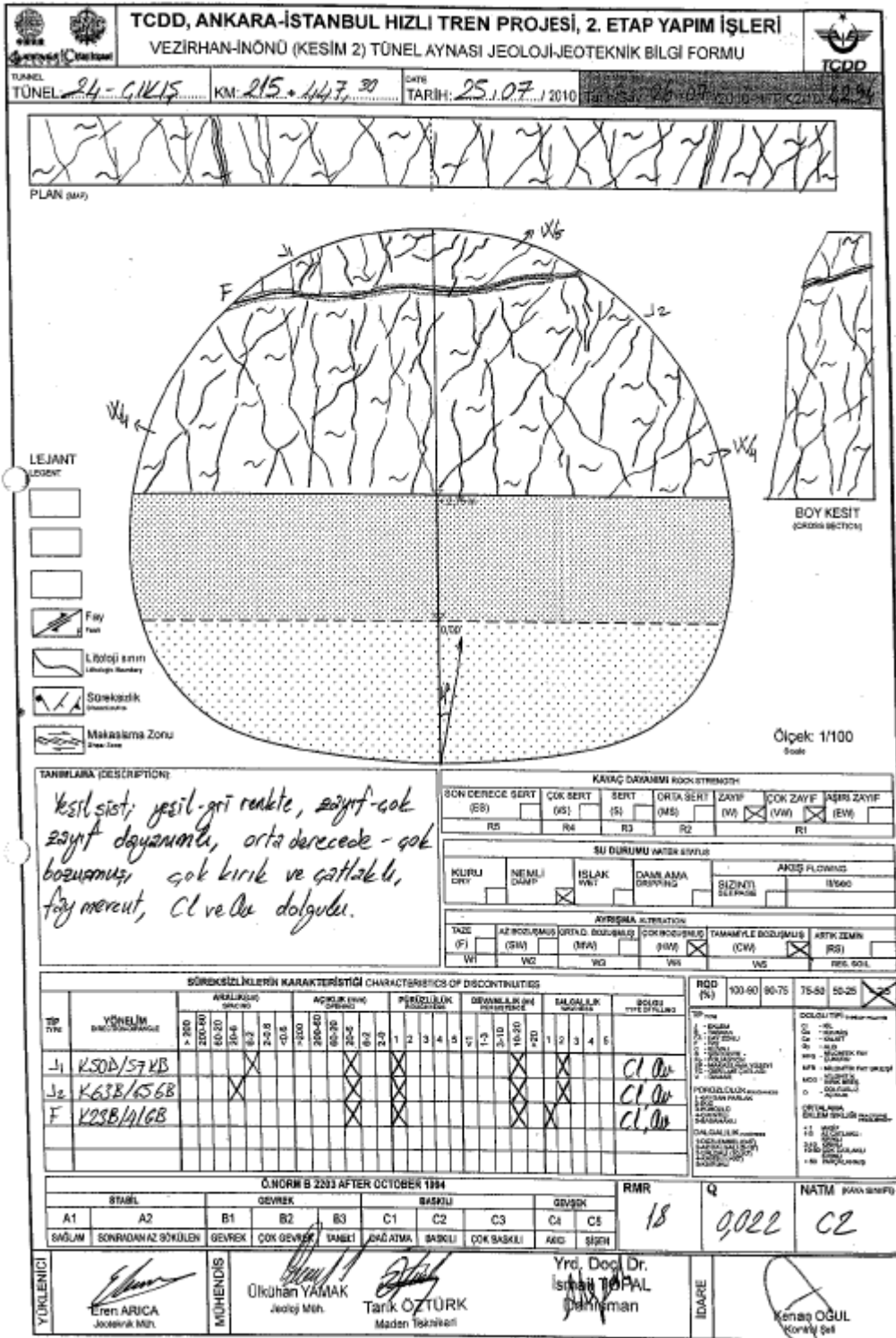
Figure A.12 Tunnel face map at Km: 215+447.30 of the tunnel

Figure A.13 Tunnel face map at Km: 215+459.50 of the tunnel

TÜNEL: 24. ÇIKIŞ   KM: 215 + 460,50   TARİH: 18 / 7 / 2010

PLAN (MAP)

LEJANT (LEGENT)

	Granit / Granite
	Şist / Schist
	Fay / Fault
	Litoloji sınırı / Lithology Boundary
	Süreksizlik / Discontinuities
	Makaslama Zonu / Shear Zone

BOY KESİT (CROSS SECTION)

Ölçek: 1/100 Scale

TANIMLAMA (DESCRIPTION)

KAYAÇ DAYANIMI ROCK STRENGTH

SON DERECE SERT (ES) R5	ÇOK SERT (VS) R4	SERT (S) R3	ORTA SERT (MS) R3 ☒	ZAYIF (W) R2 ☒	ÇOK ZAYIF (VW) R1	AŞIRI ZAYIF (EW)

SU DURUMU WATER STATUS

KURU DRY	NEMLİ DAMP	ISLAK WET ☒	DAMLAMA DRIPPING	SIZINTI SEEPAGE	AKIŞ FLOWING lt/sec

AYRIŞMA ALTERATION

TAZE (F) W1	AZ BOZUŞMUŞ (SW) W2	ORTA D. BOZUŞMUŞ (MW) W3 ☒	ÇOK BOZUŞMUŞ (HW) W4 ☒	TAMAMIYLE BOZUŞMUŞ (CW) W5 ☒	ARTIK ZEMİN (RS)

SÜREKSİZLİKLERİN KARAKTERİSTİĞİ CHARACTERISTICS OF DISCONTINUITIES

TİP TYPE	YÖNELİM DIRECTION/DIP ANGLE	DOLGU TYPE OF FILLING
J_1	K35D/55KB	D.cl
J_2	K45B/60GB	D.cl
F_1	K10B/30KD	cl
F_2	K60/63GD	MFB,cl

ROD (%): < 25

ÖNORM B 2203 AFTER OCTOBER 1994

STABİL		GEVREK			BASKILI			GEVŞEK	
A1	A2	B1	B2	B3	C1	C2	C3	C4	C5
SAĞLAM	SONRADAN AZ SÖKÜLEN	GEVREK	ÇOK GEVREK	TABELİ	DAĞ ATMA	BASKILI	ÇOK BASKILI	AKICI	ŞİŞEN

RMR	Q	NATM (KAYA SINIFI)
18	0,022	C2

YÜKLENİCİ: Evren POŞLUK, Jeoteknik Müh.

MÜHENDİS: Ülkühan YAMAK, Jeoloji Müh.

Tarık ÖZTÜRK, Maden Teknikeri

Yrd. Doç. Dr. İsmail TOPAL, Danışman

İDARE: Kenan OĞUL, Kontrol Şefi

Figure A.14 Tunnel face map at Km: 215+460.50 of the tunnel

Figure A.15 Tunnel face map at Km: 215+467.80 of the tunnel

Figure A.16 Tunnel face map at Km: 215+480.20 of the tunnel
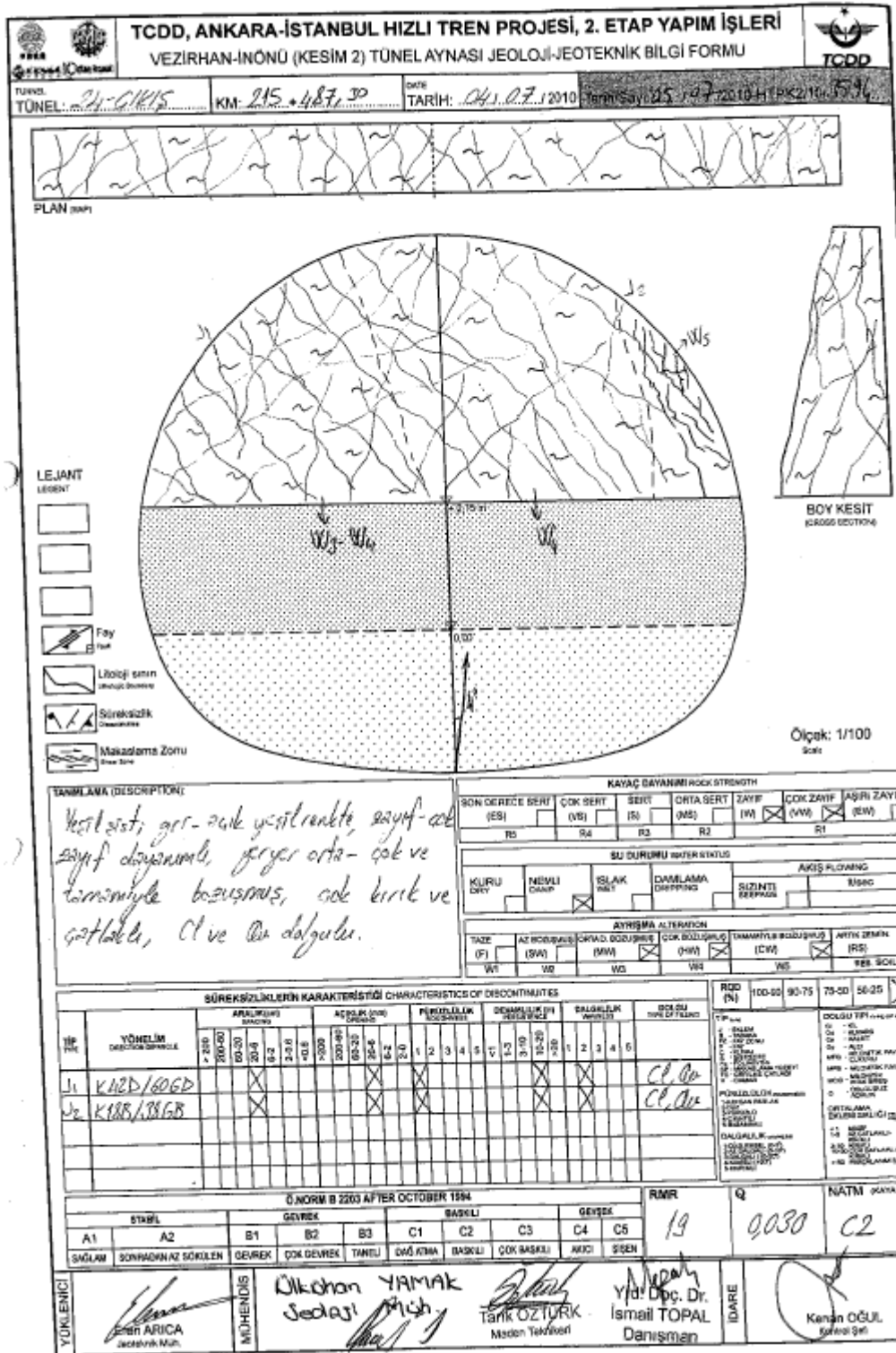
Figure A.17 Tunnel face map at Km: 215+487.30 of the tunnel
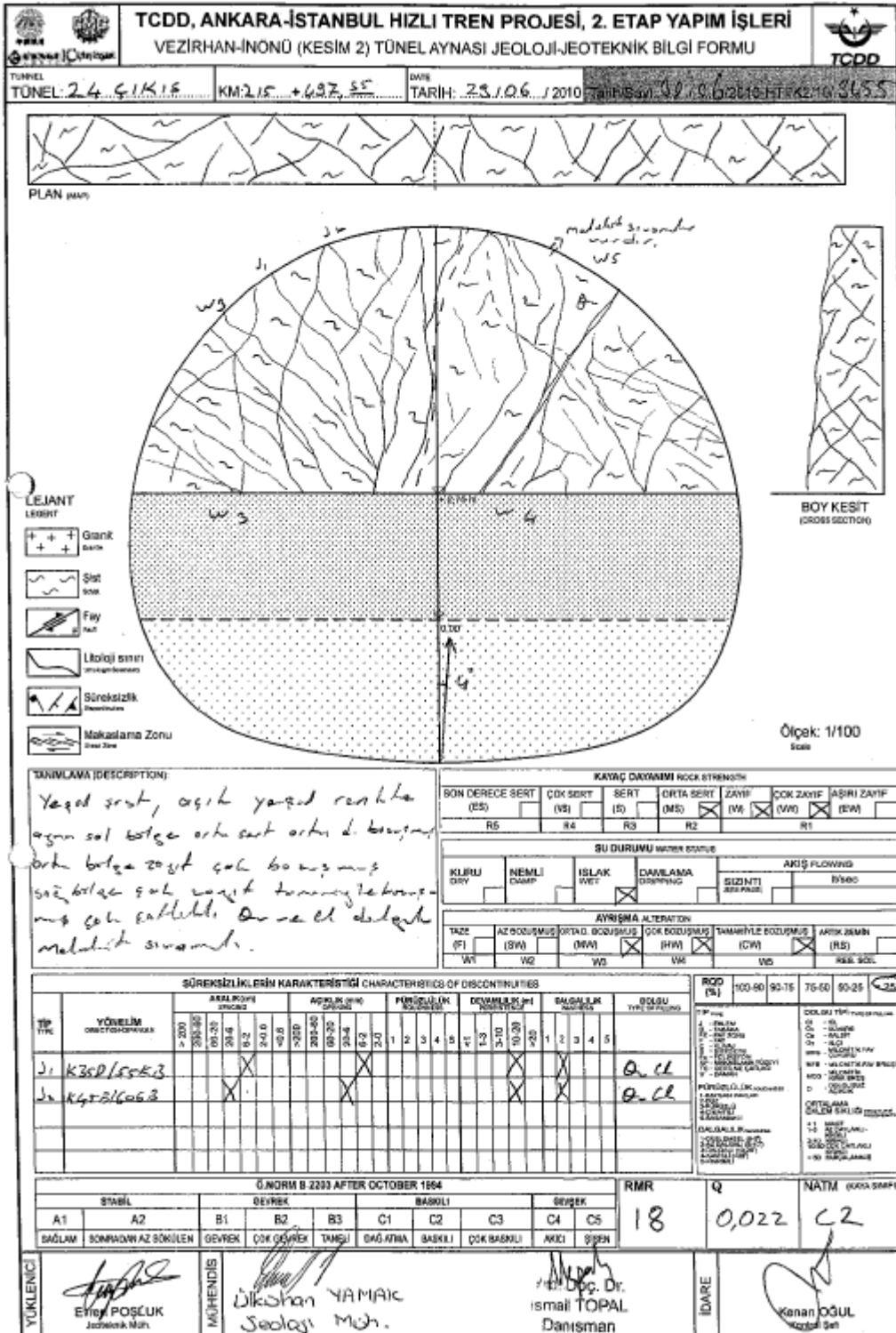
Figure A.18 Tunnel face map at Km: 215+497.55 of the tunnel

68

Figure A.19 Tunnel face map at Km: 215+501.55 of the tunnel

Figure A.20 Tunnel face map at Km: 215+504.55 of the tunnel

APPENDIX B
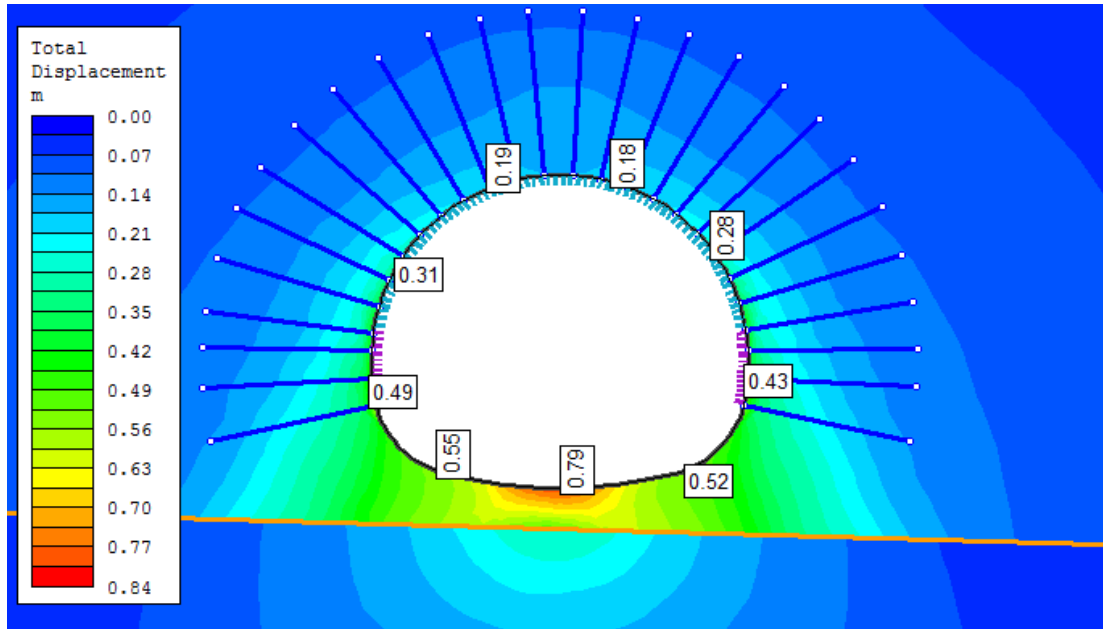
Figure B.1 Radial deformations after the completion of excavation for Case 2, Alternative A
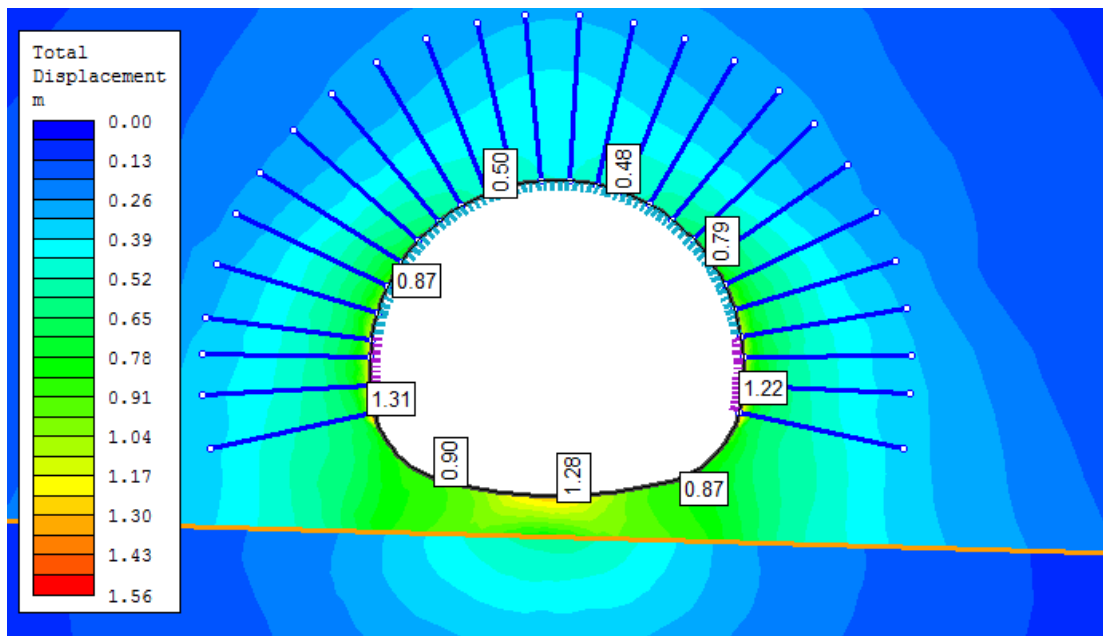
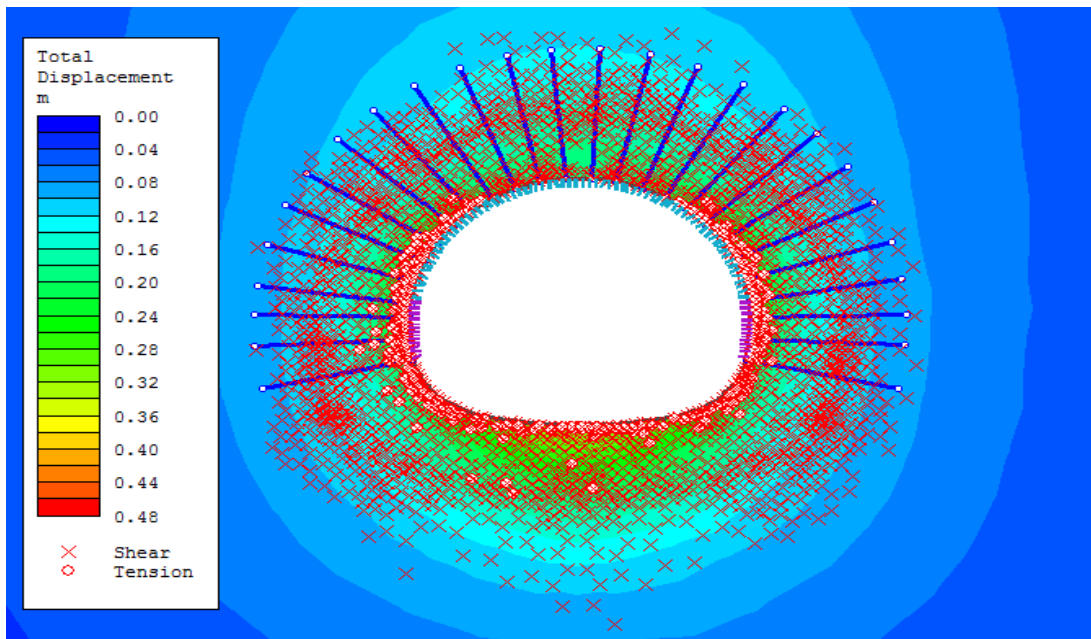Figure B.2 Radial deformations after strength reduction for Case 2, Alternative A
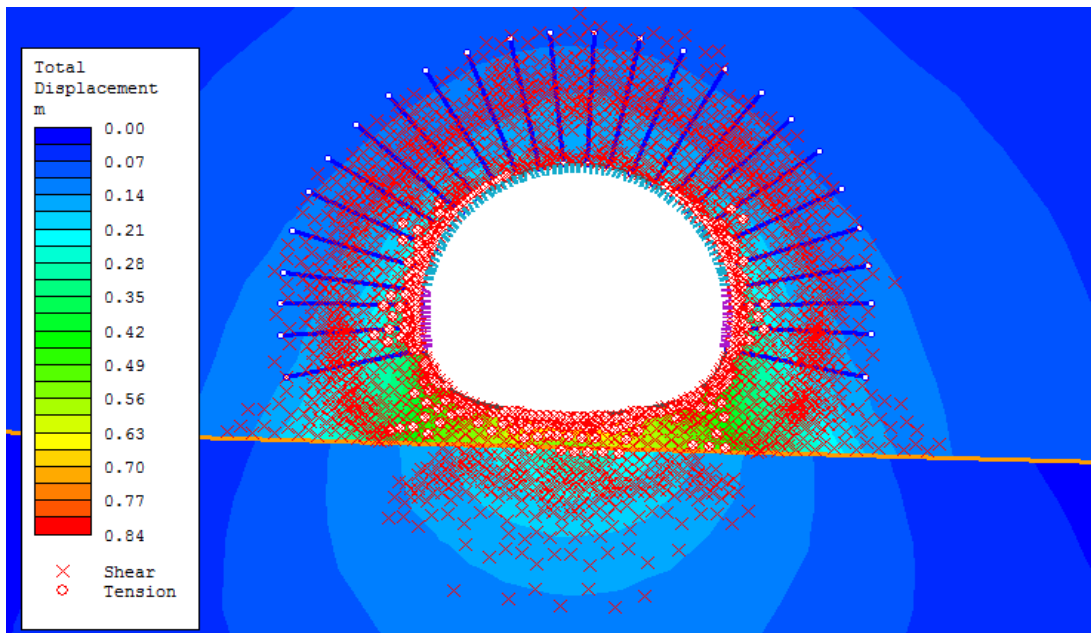
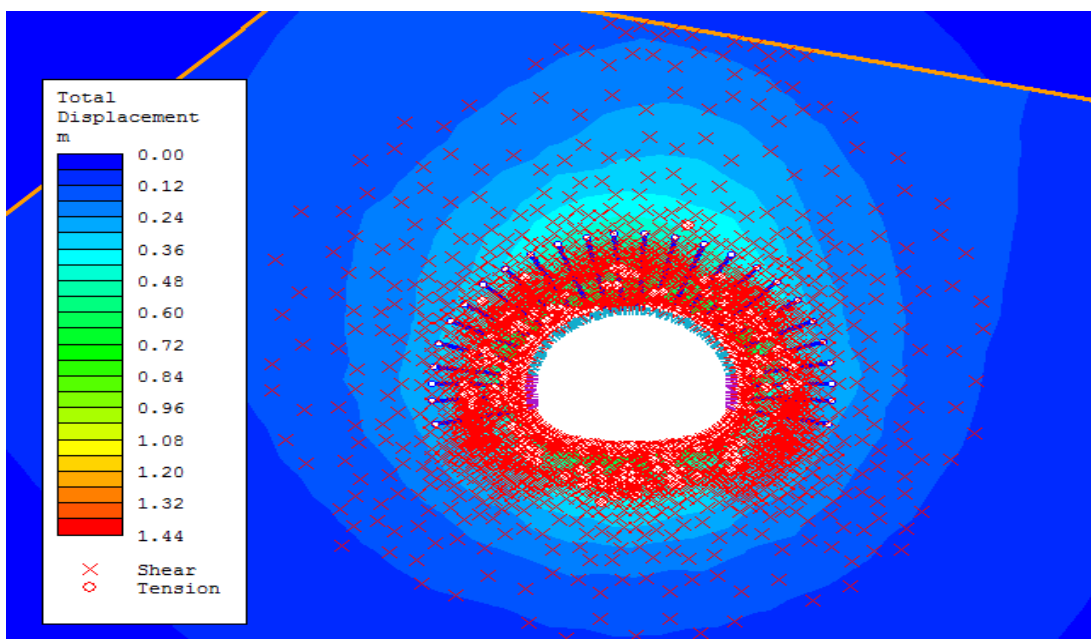Figure B.3 Plastic zone radius after the completion of excavation for Case 2, Alternative A
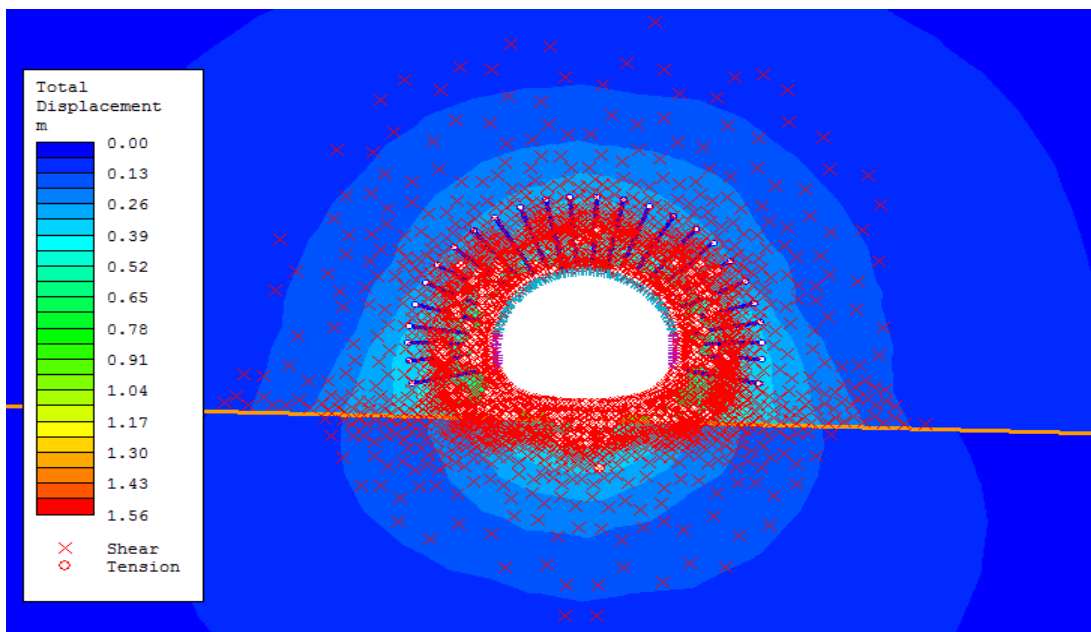
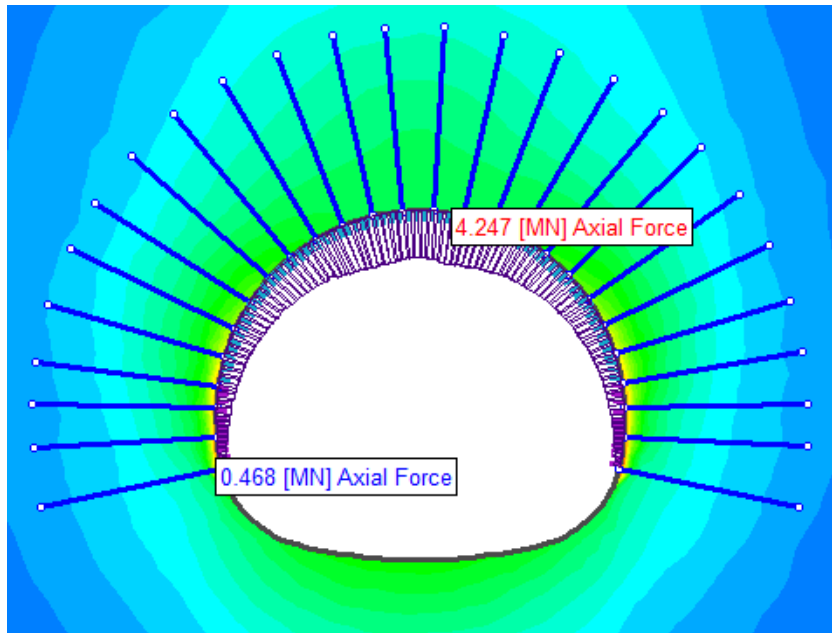Figure B.4 Plastic zone radius after the strength reduction for Case 2, Alternative A
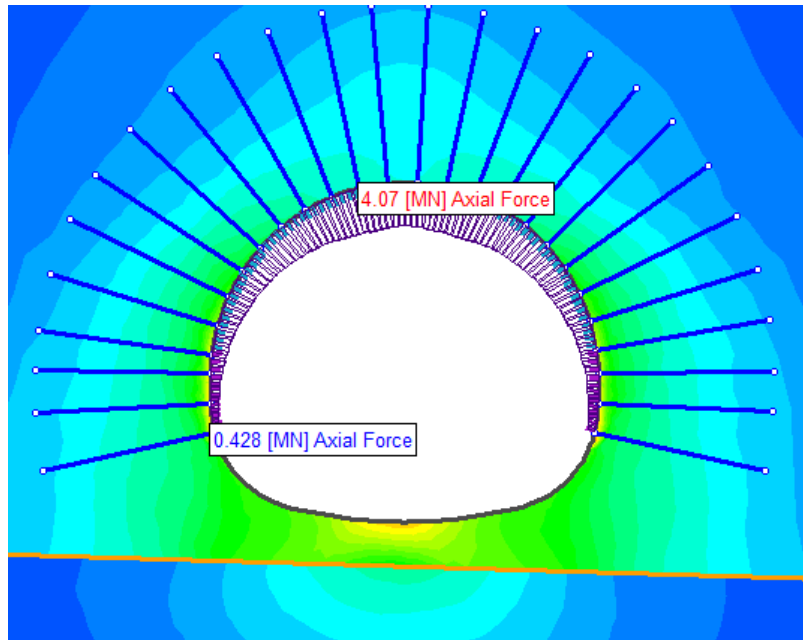
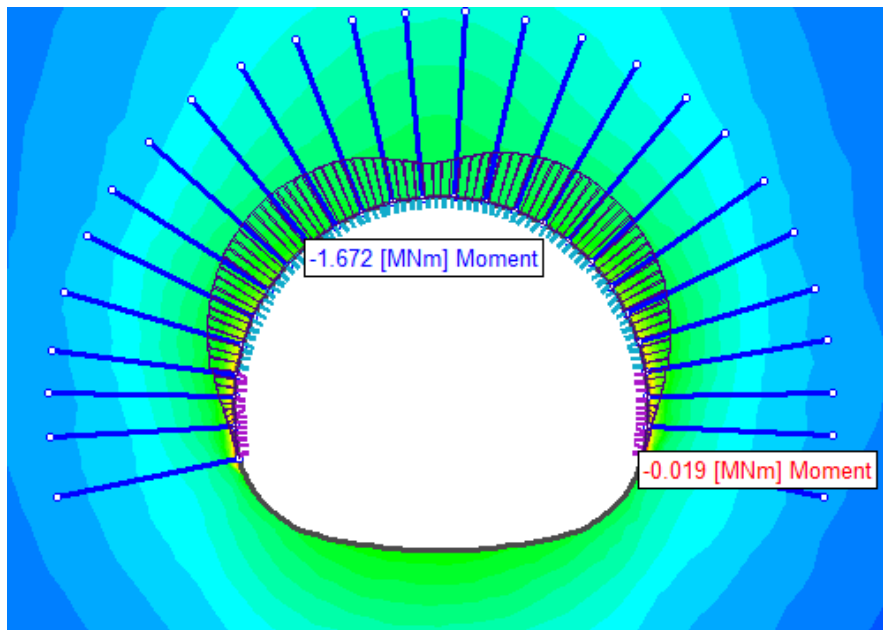Figure B.5 Axial forces after the strength reduction for Case 2, Alternative A
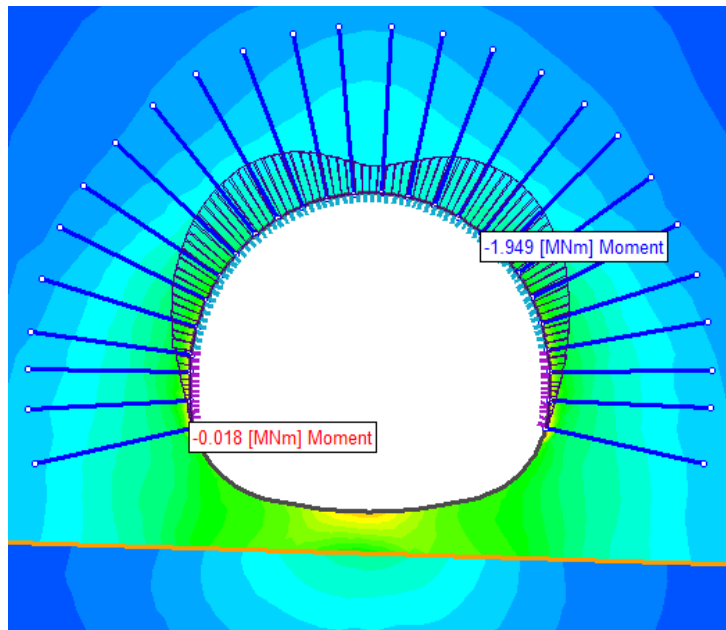
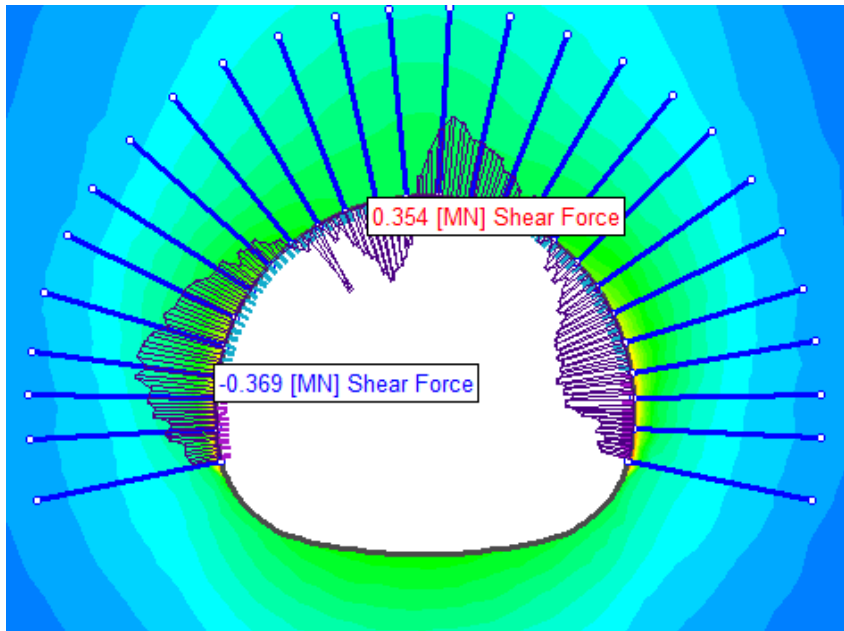Figure B.6 Bending moments after the strength reduction for Case 2, Alternative A
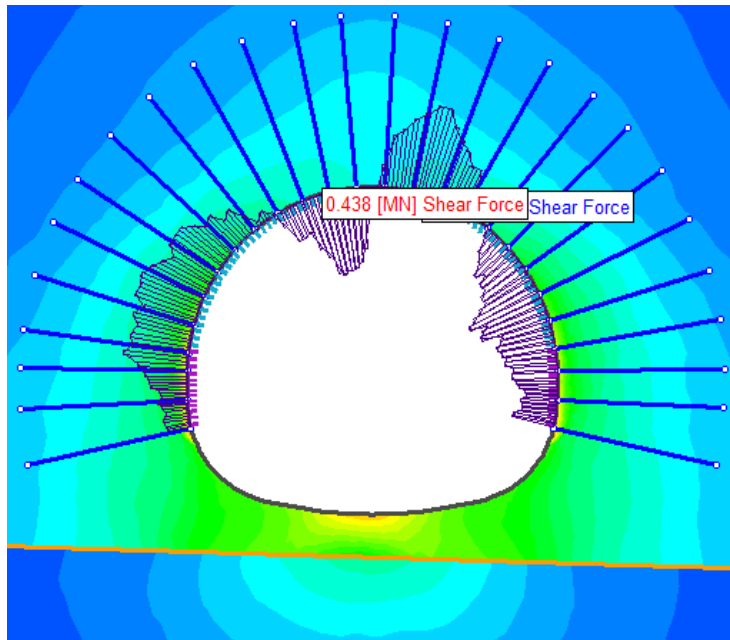
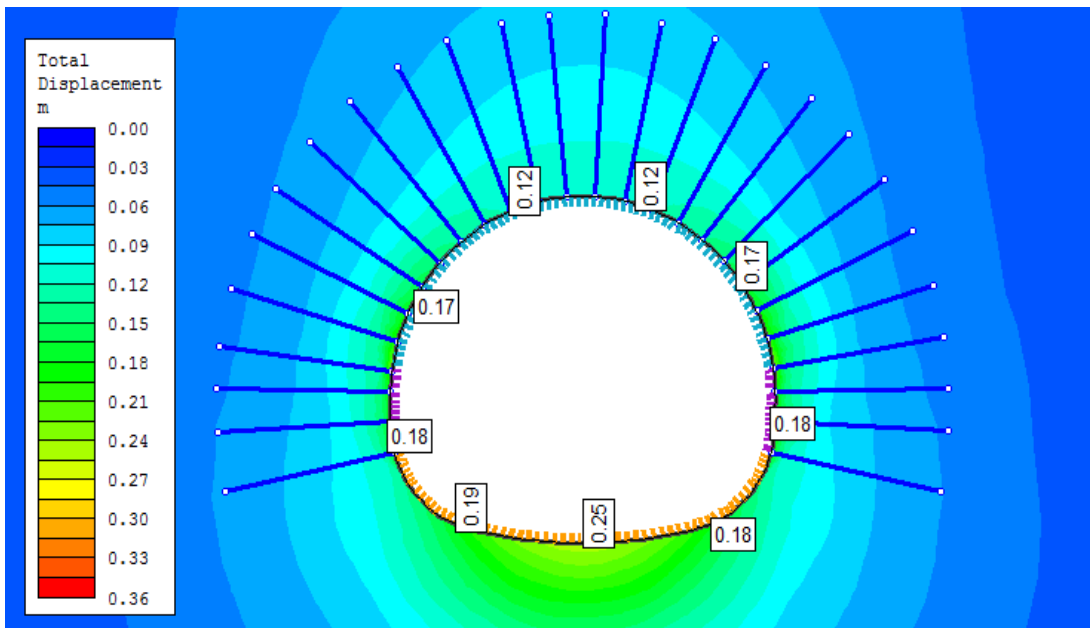Figure B.7 Shear forces after the strength reduction for Case 2, Alternative A
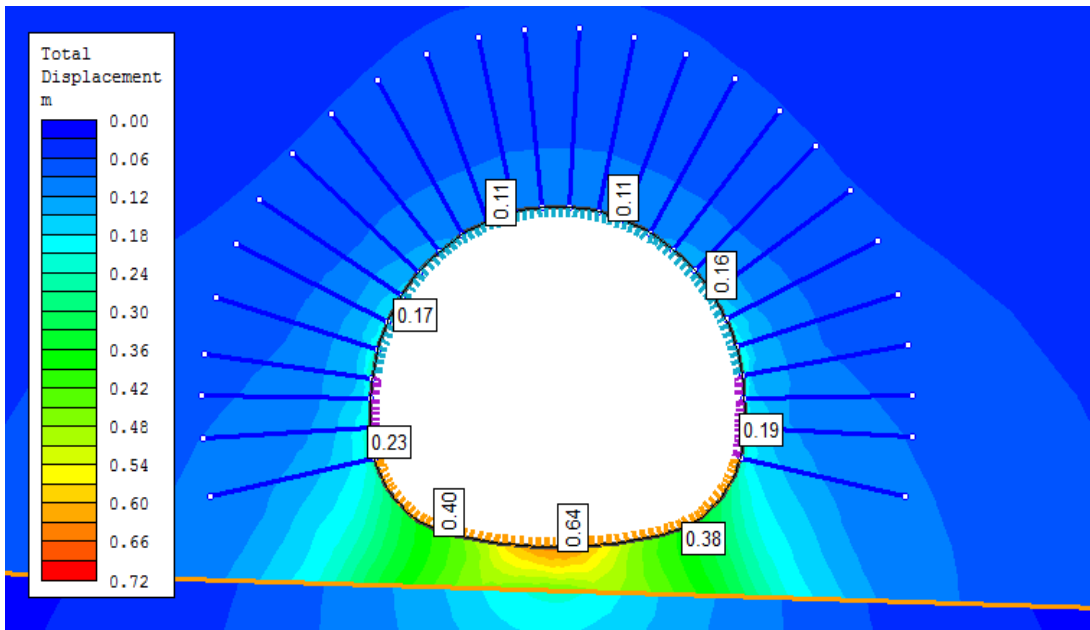
Figure B.8 Radial deformations after the completion of excavation for Case 2, Alternative B
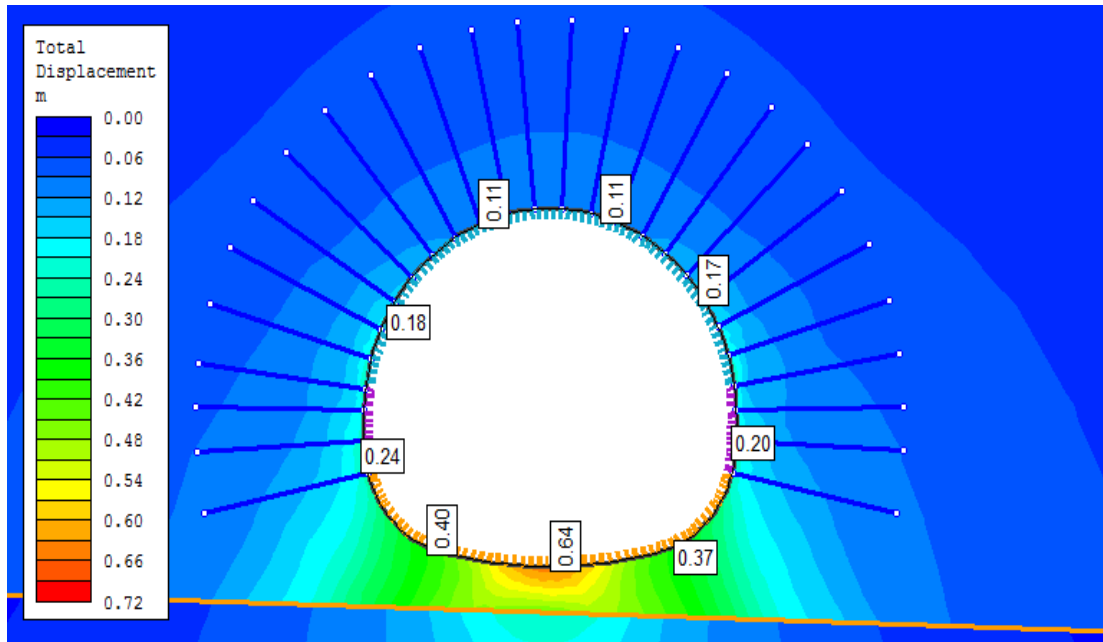
Figure B.9 Radial deformations after strength reduction for Case 2, Alternative B
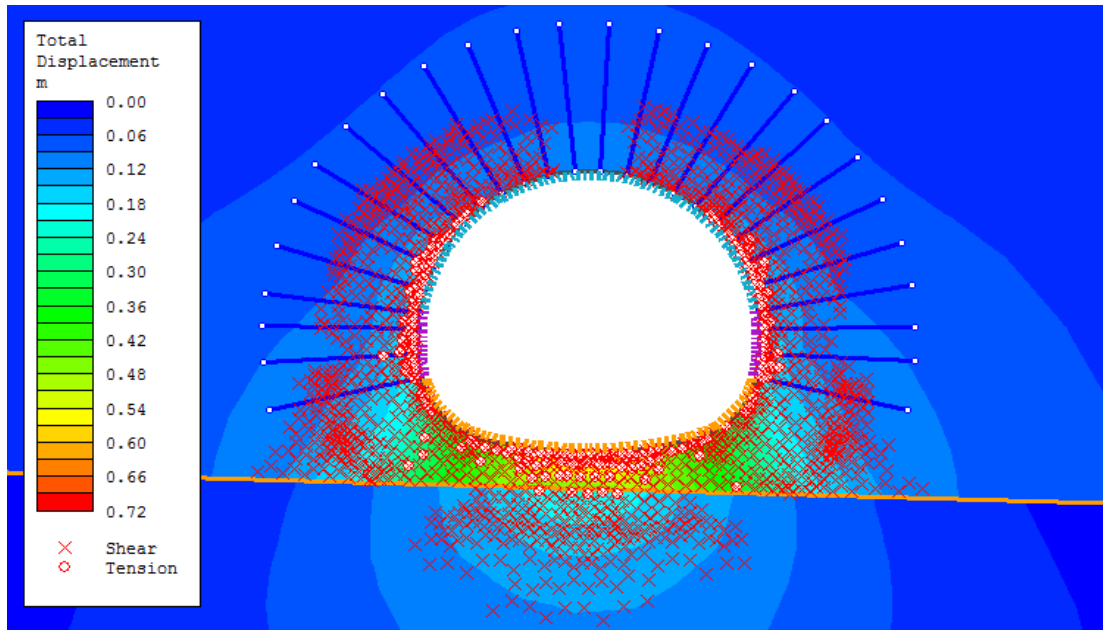
Figure B.10 Plastic zone radius after the completion of excavation for Case 2, Alternative B
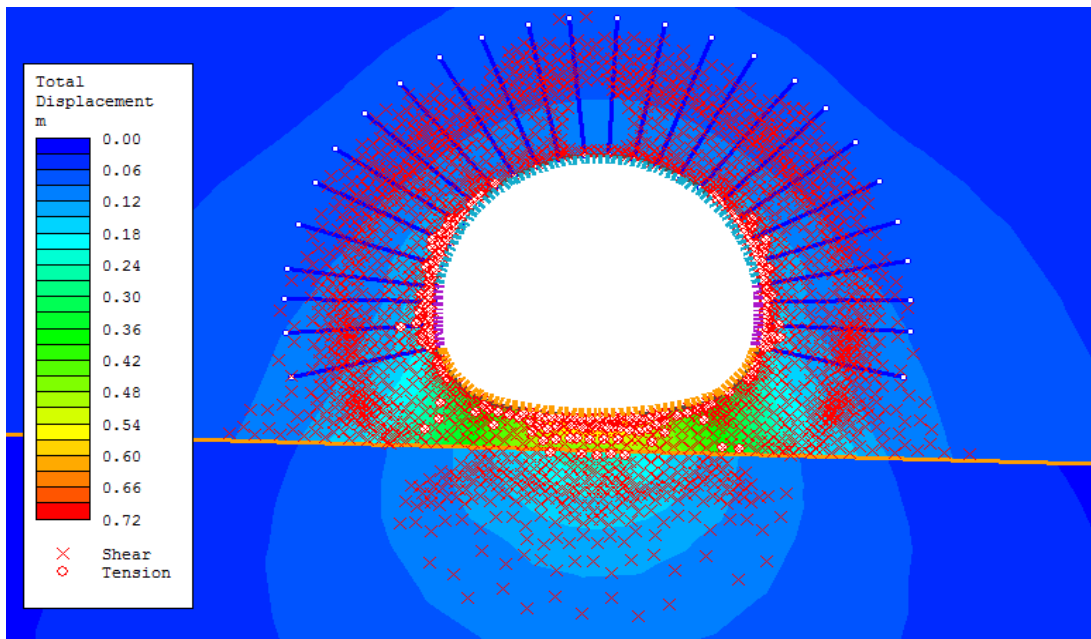
Figure B.11 Plastic zone radius after the strength reduction for Case 2, Alternative B
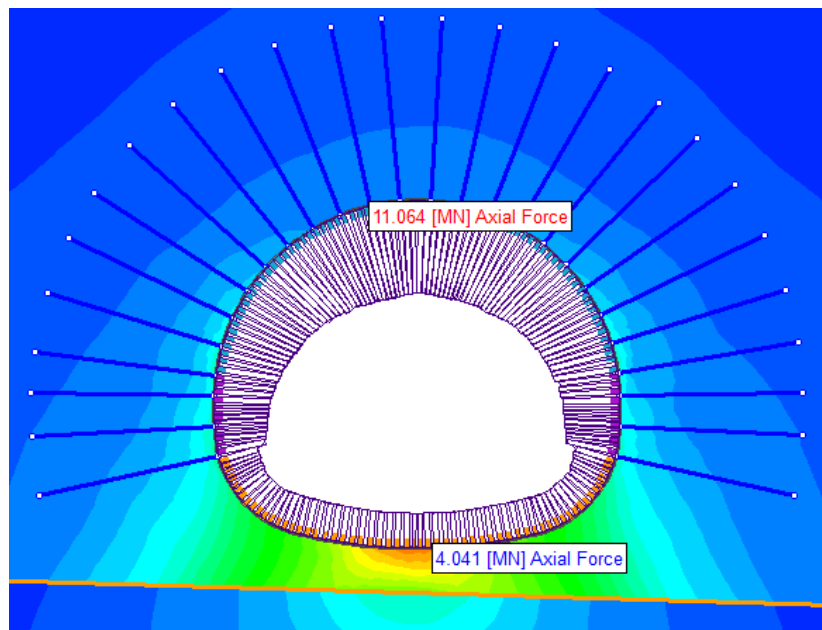
Figure B.12 Axial forces after the strength reduction for Case 2, Alternative B
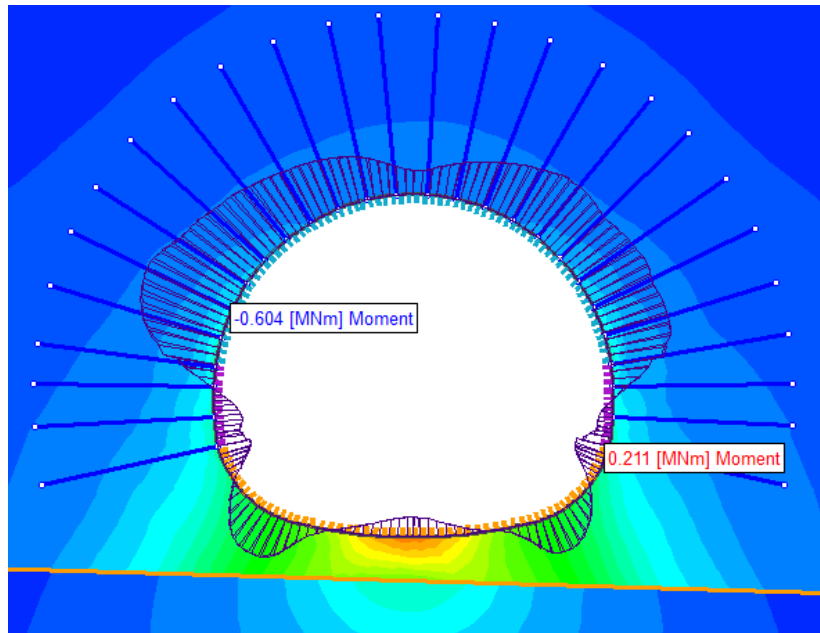
Figure B.13 Bending moments after the strength reduction for Case 2, Alternative B
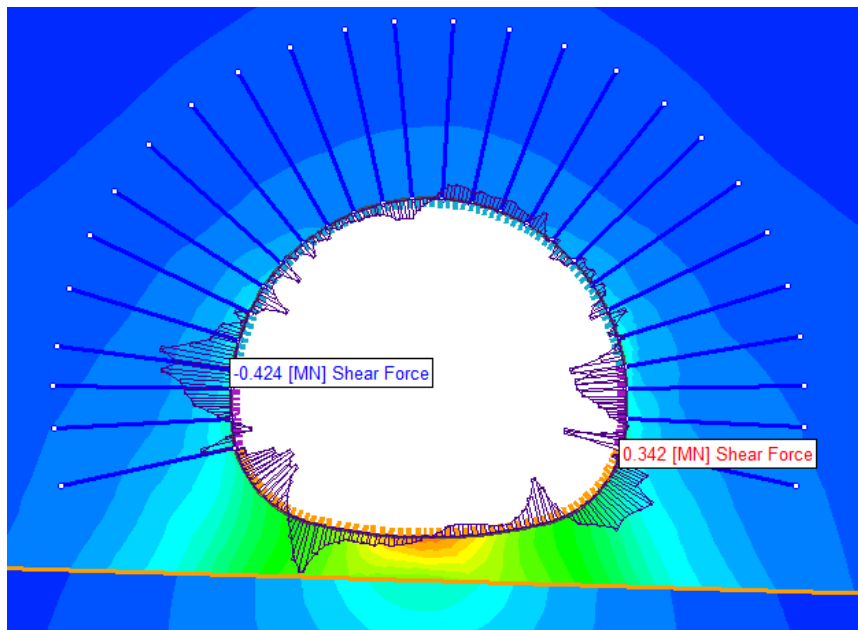
Figure B.14 Shear forces after the strength reduction for Case 2, Alternative B

77
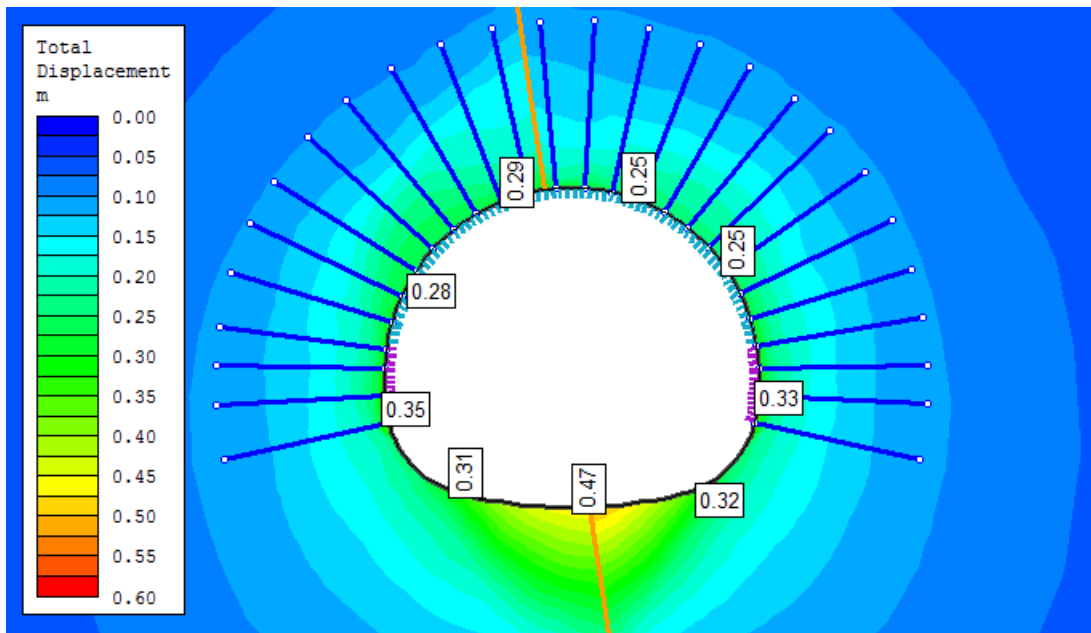
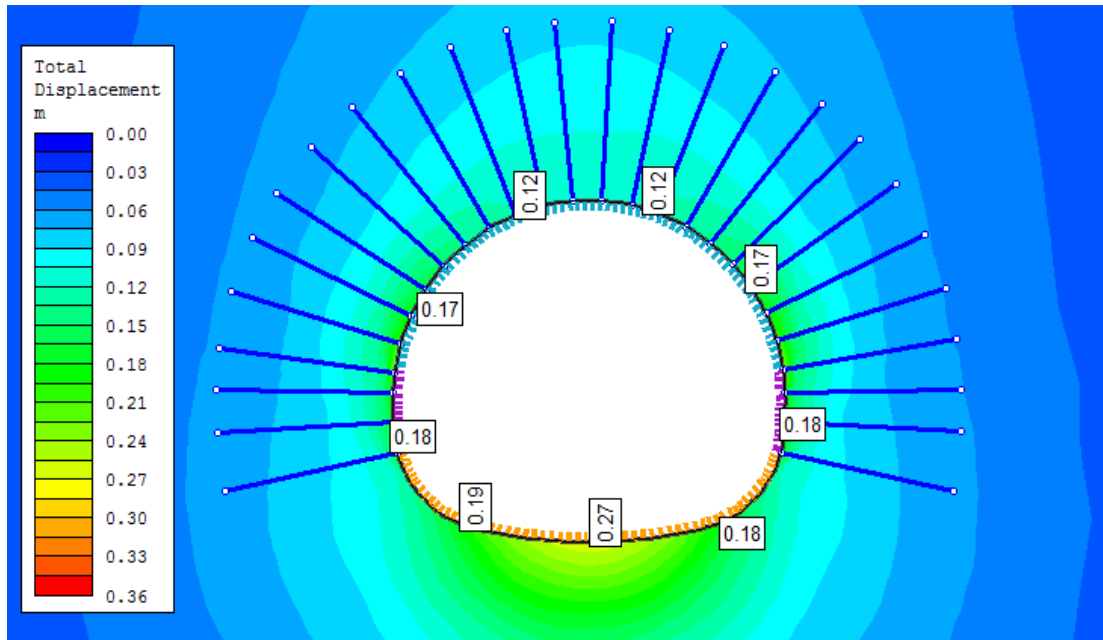Figure B.15 Radial deformations after the completion of excavation for Case 3, Alternative A
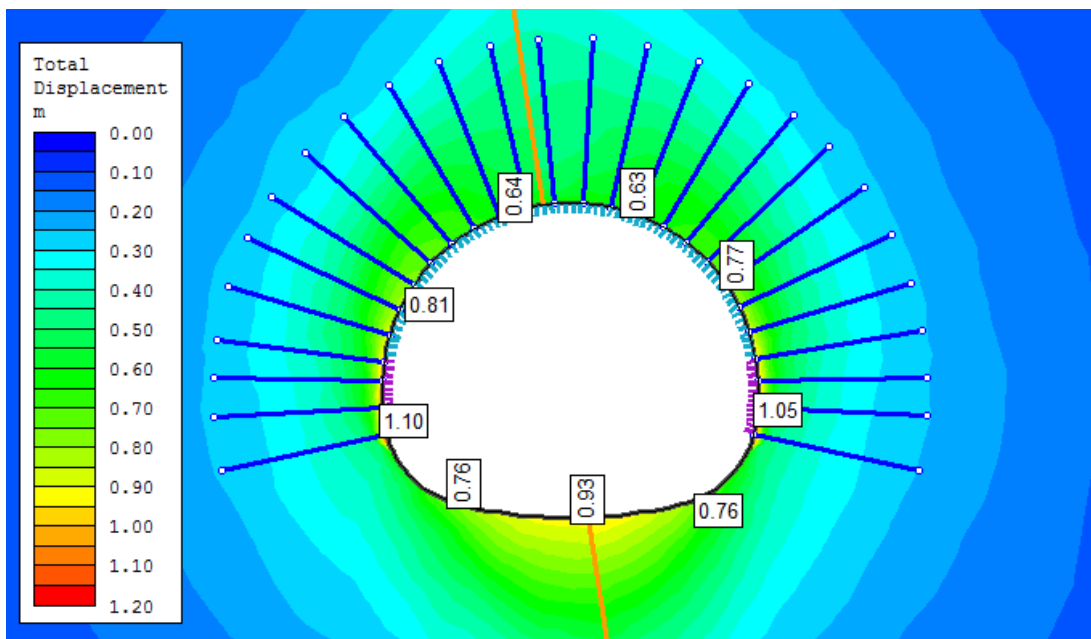
Figure B.16 Radial deformations after strength reduction for Case 3, Alternative A
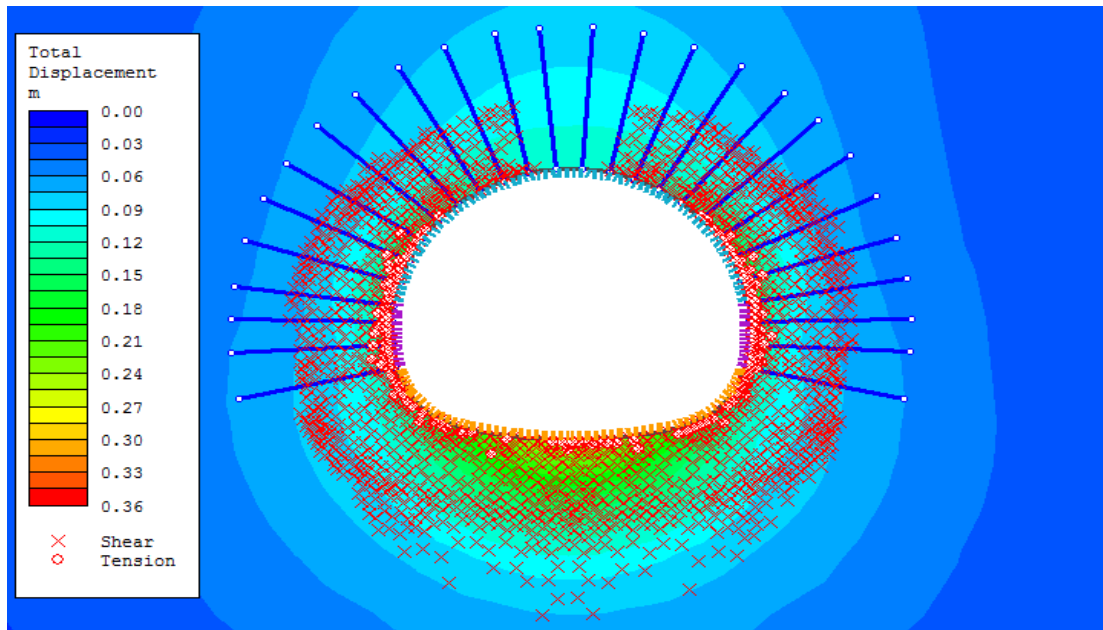
78
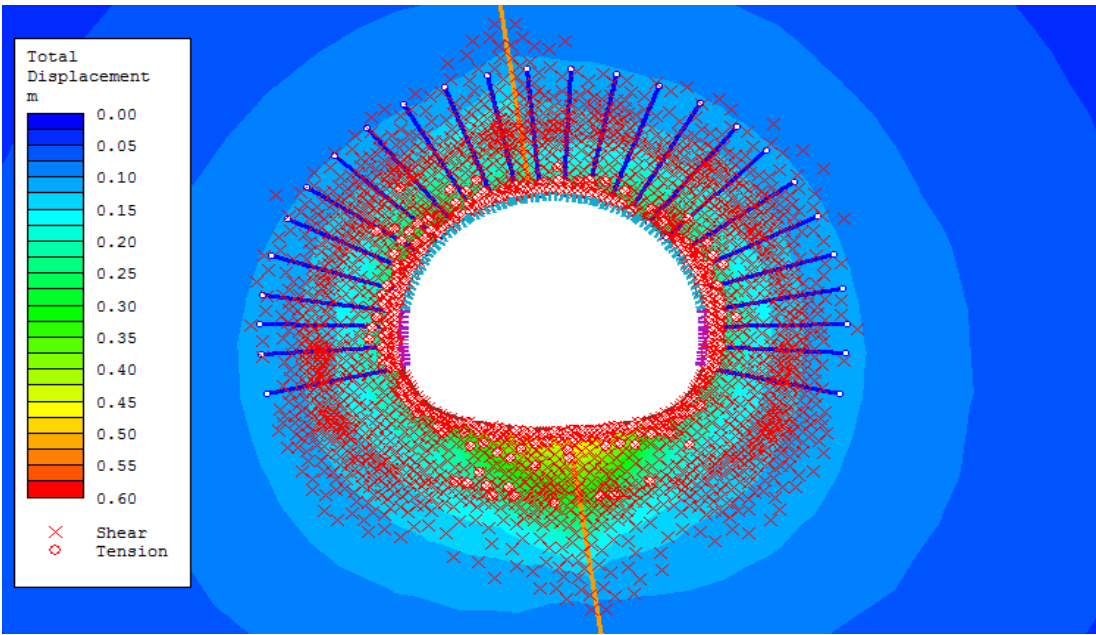
Figure B.17 Plastic zone radius after the completion of excavation for Case 3, Alternative A
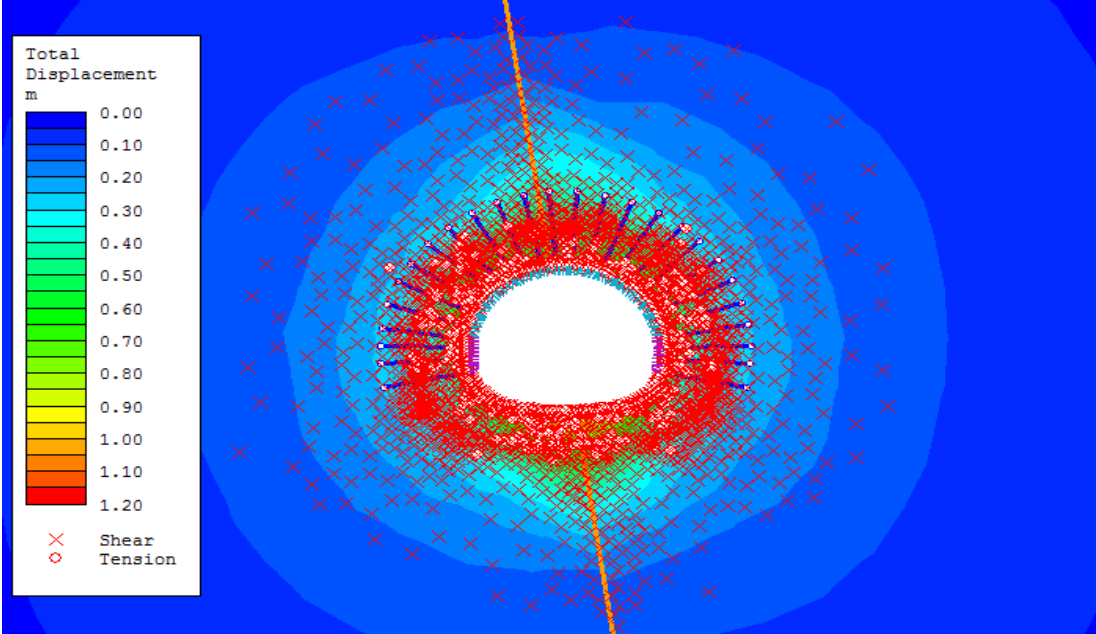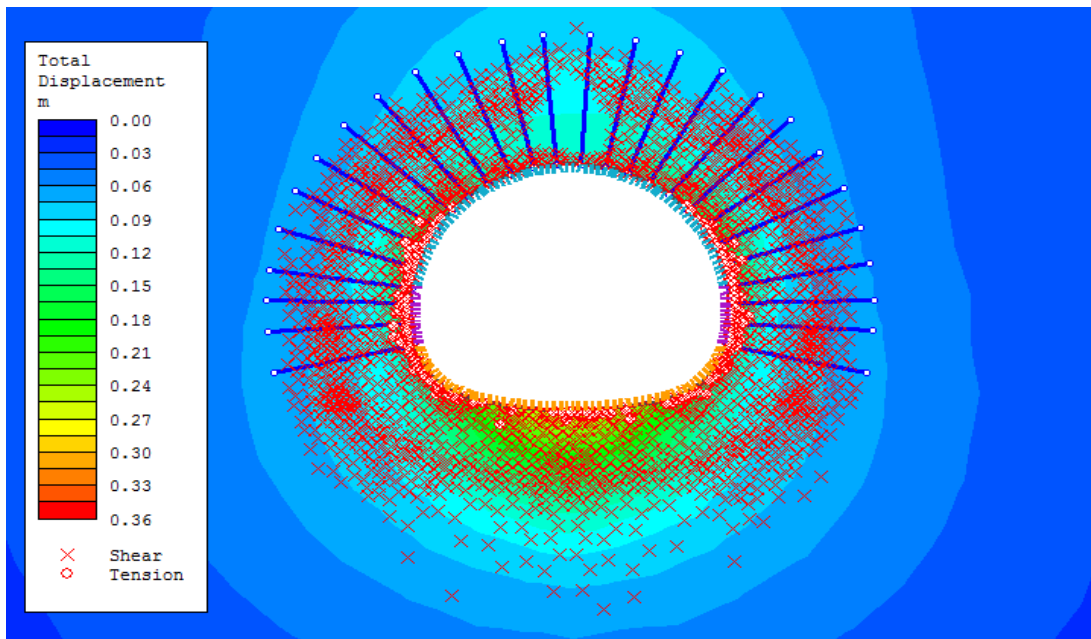

Figure B.18 Plastic zone radius after the strength reduction for Case 3, Alternative A
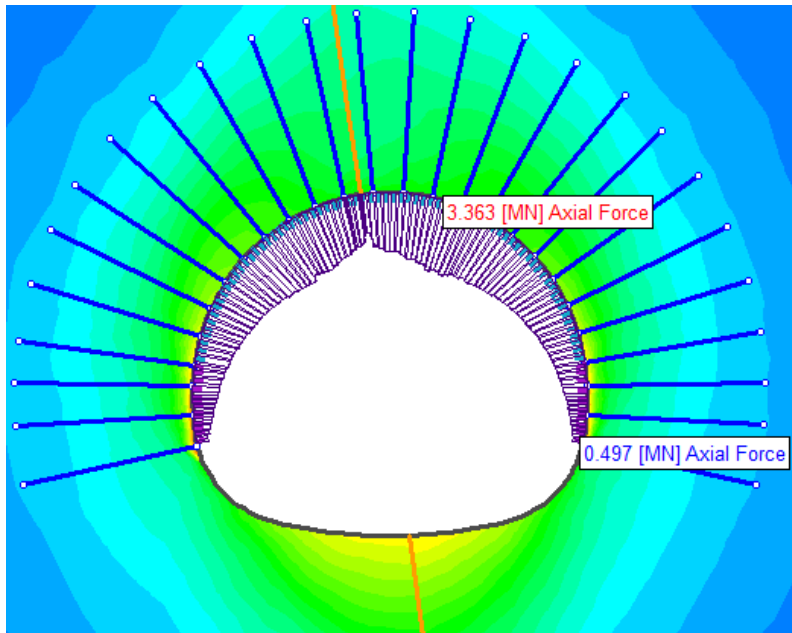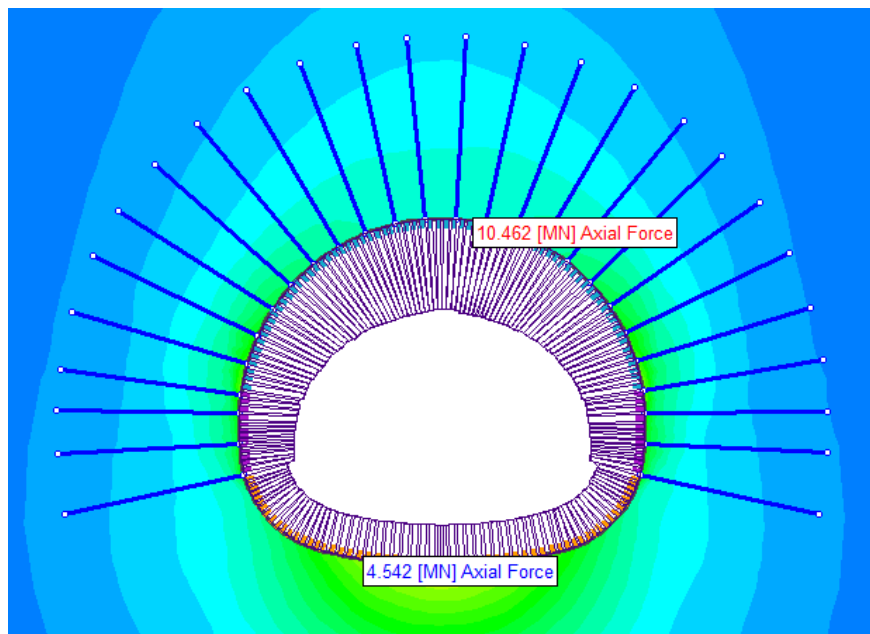
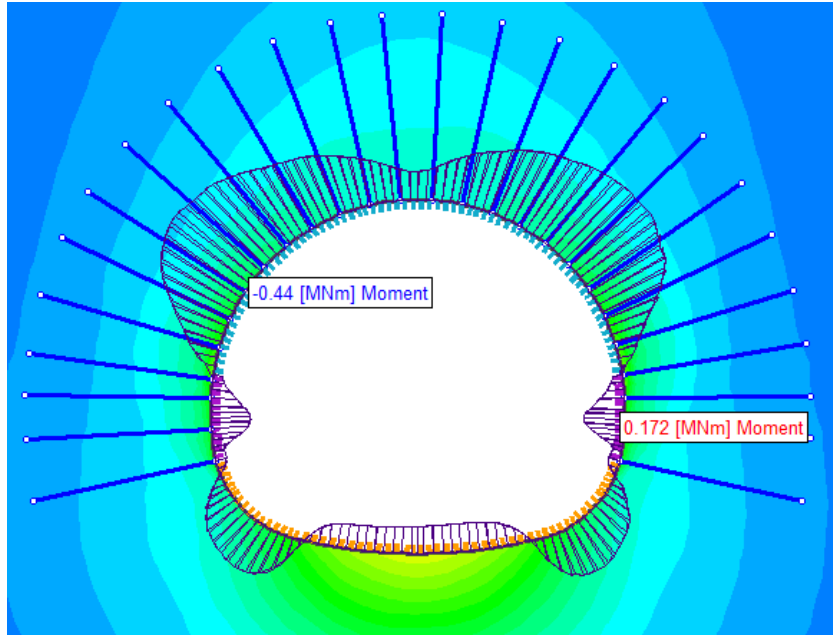Figure B.19 Axial forces after the strength reduction for Case 3, Alternative A
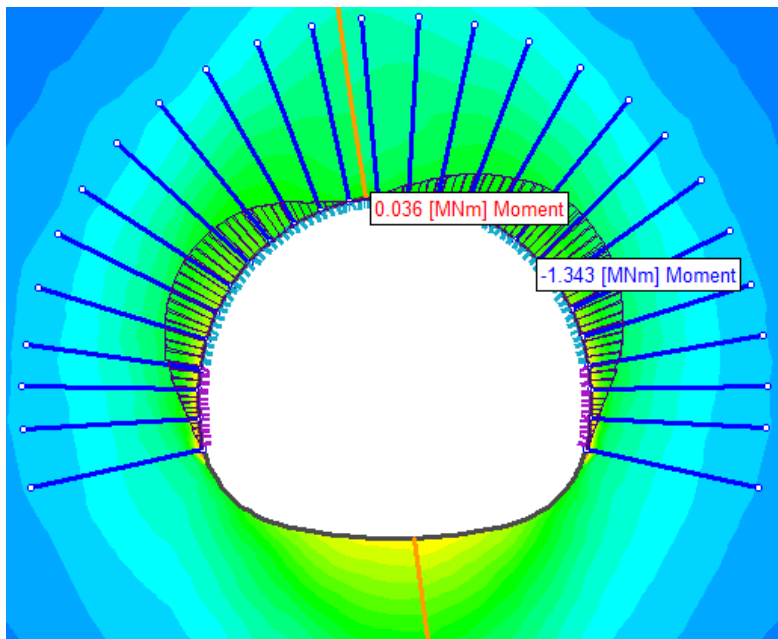
Figure B.20 Bending moments after the strength reduction for Case 3, Alternative A
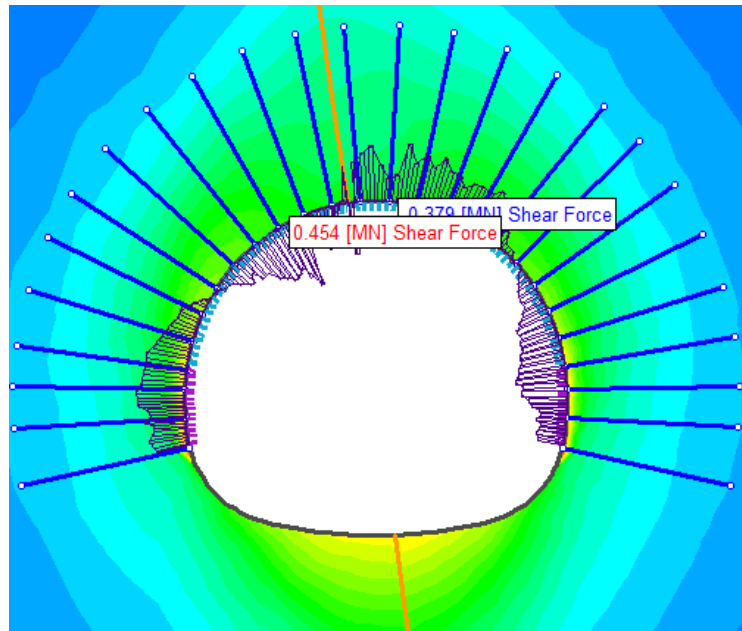
Figure B.21 Shear forces after the strength reduction for Case 3, Alternative A
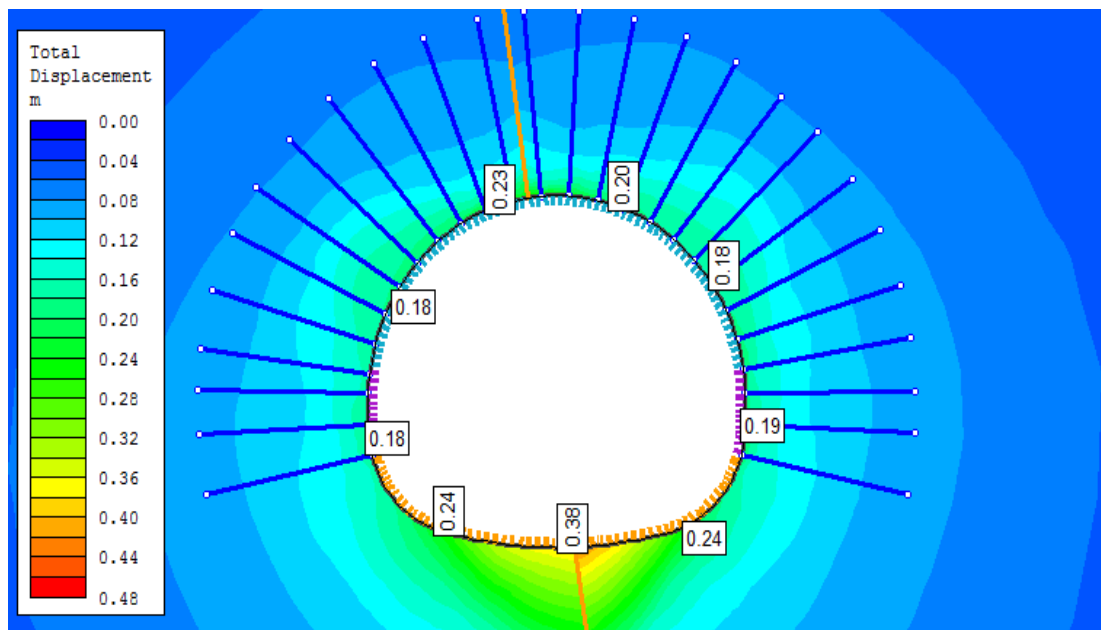
Figure B.22 Radial deformations after the completion of excavation for Case 3, Alternative B
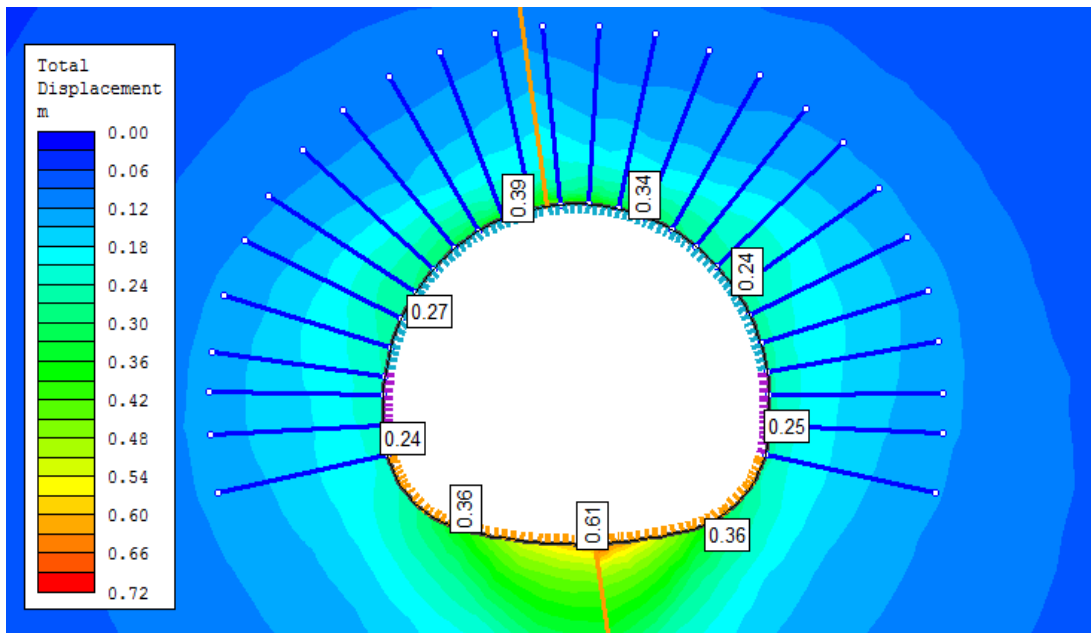
Figure B.23 Radial deformations after strength reduction for Case 3, Alternative B
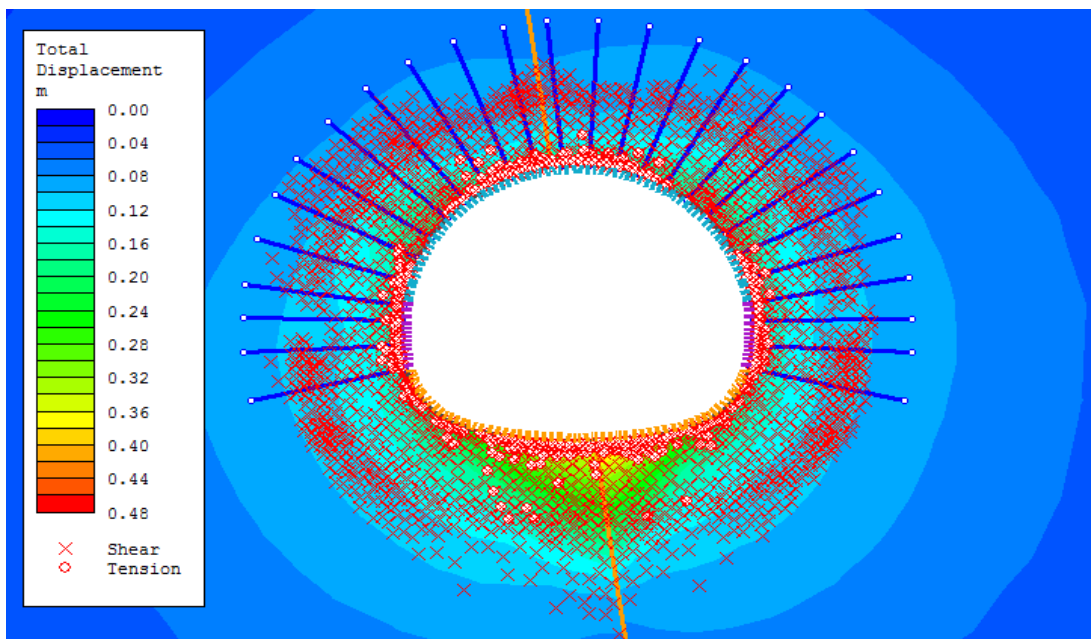
Figure B.24 Plastic zone radius after the completion of excavation for Case 3, Alternative B
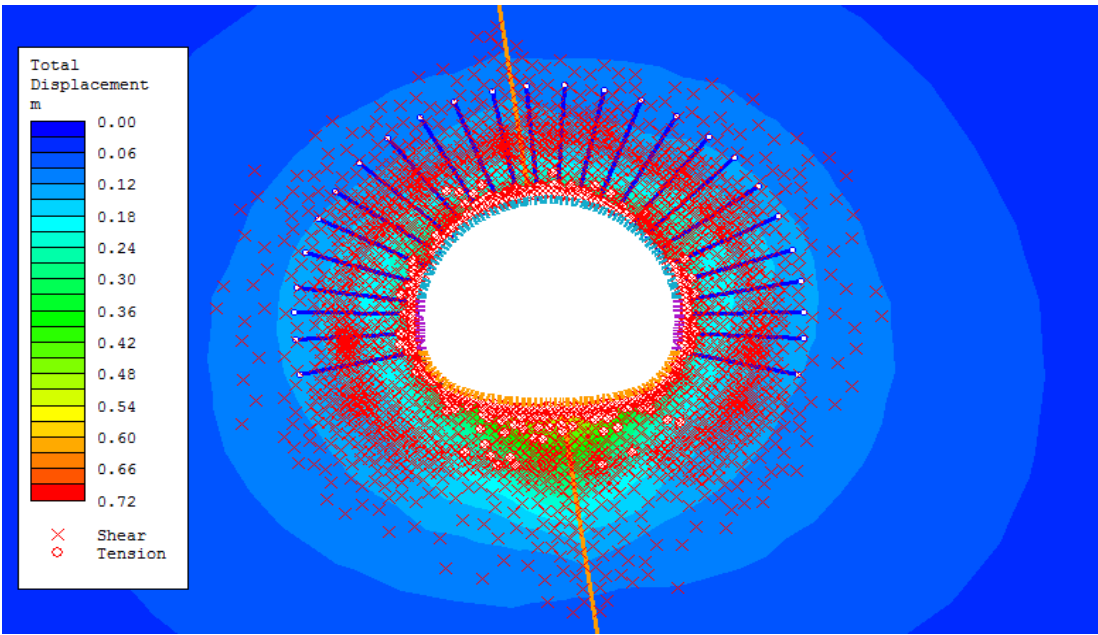
Figure B.25 Plastic zone radius after the strength reduction for Case 3, Alternative B
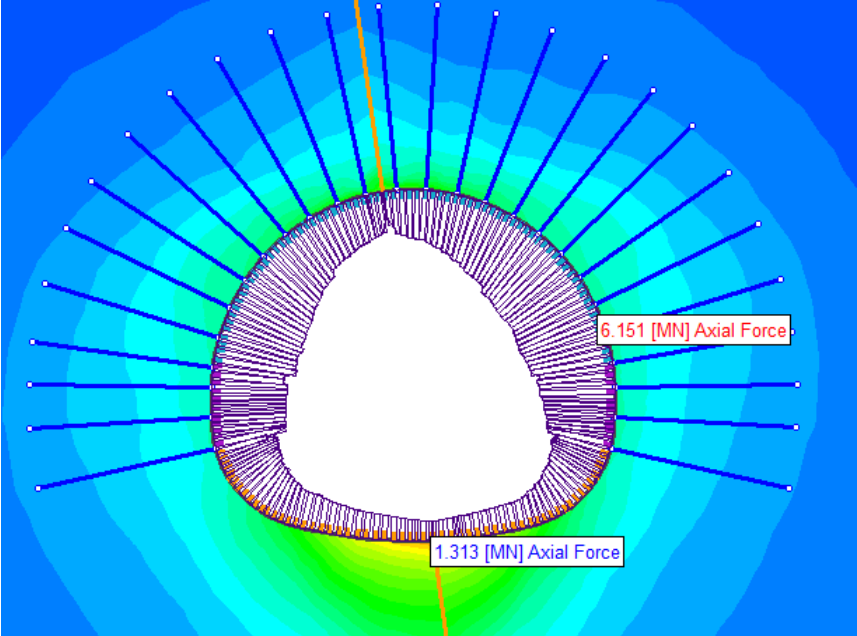
Figure B.26 Axial forces after the strength reduction for Case 3, Alternative B
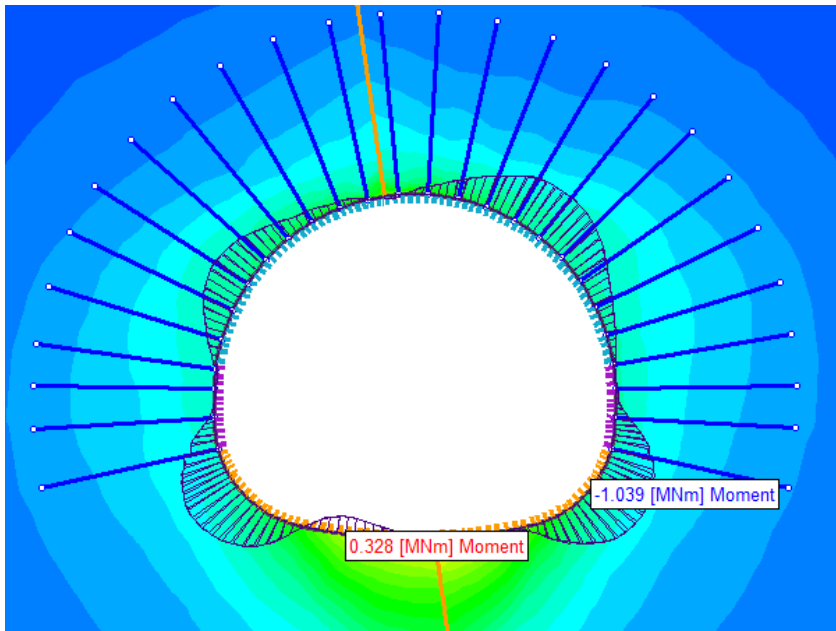
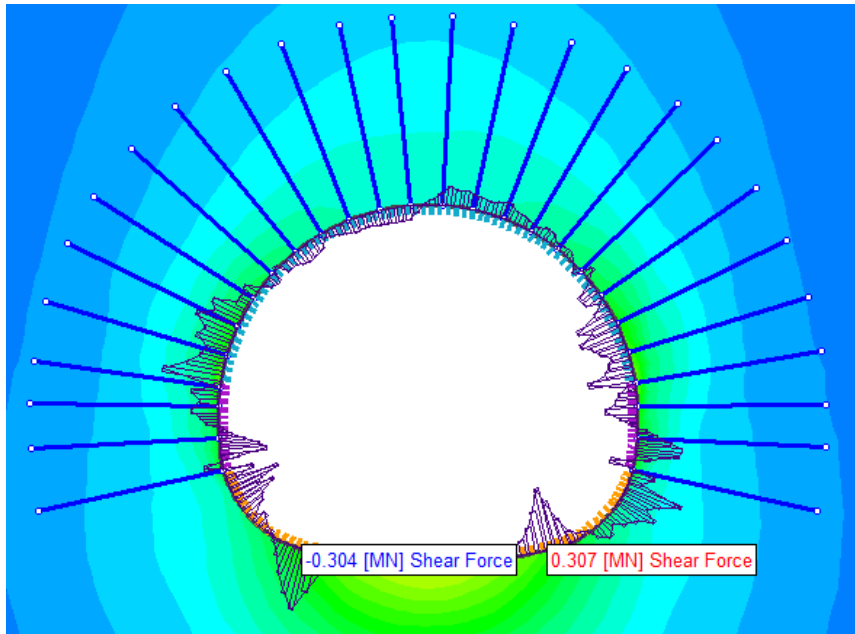Figure B.27 Bending moments after the strength reduction for Case 3, Alternative B
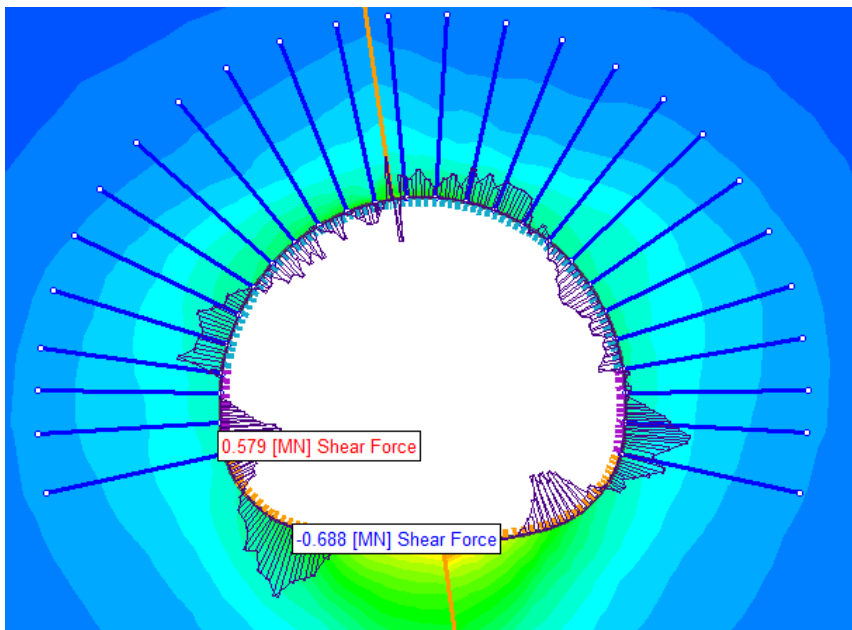
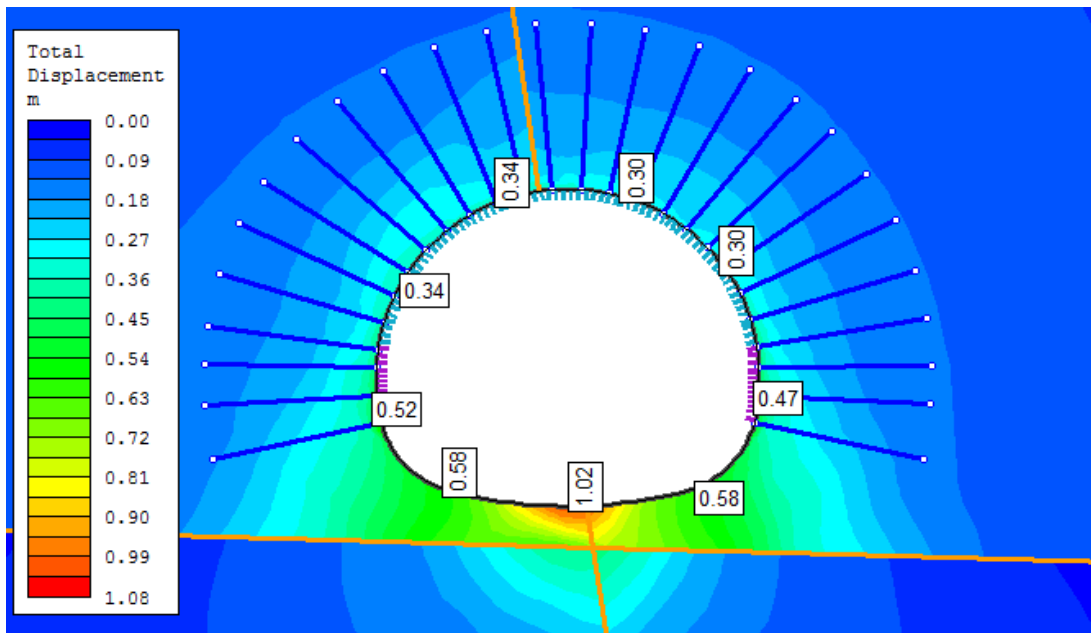Figure B.28 Shear forces after the strength reduction for Case 3, Alternative B
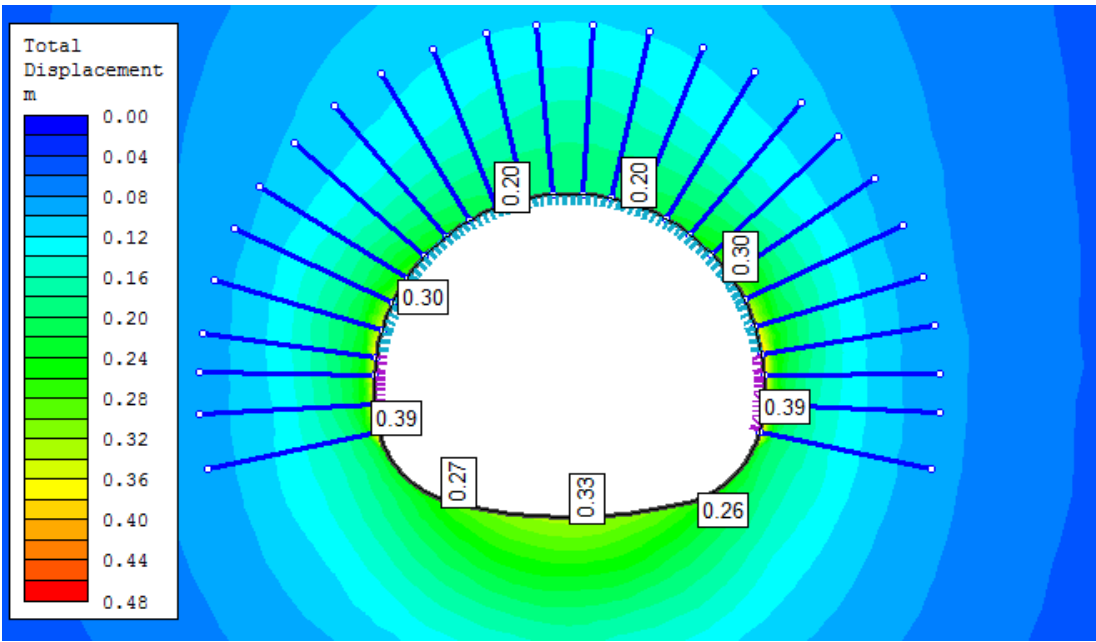
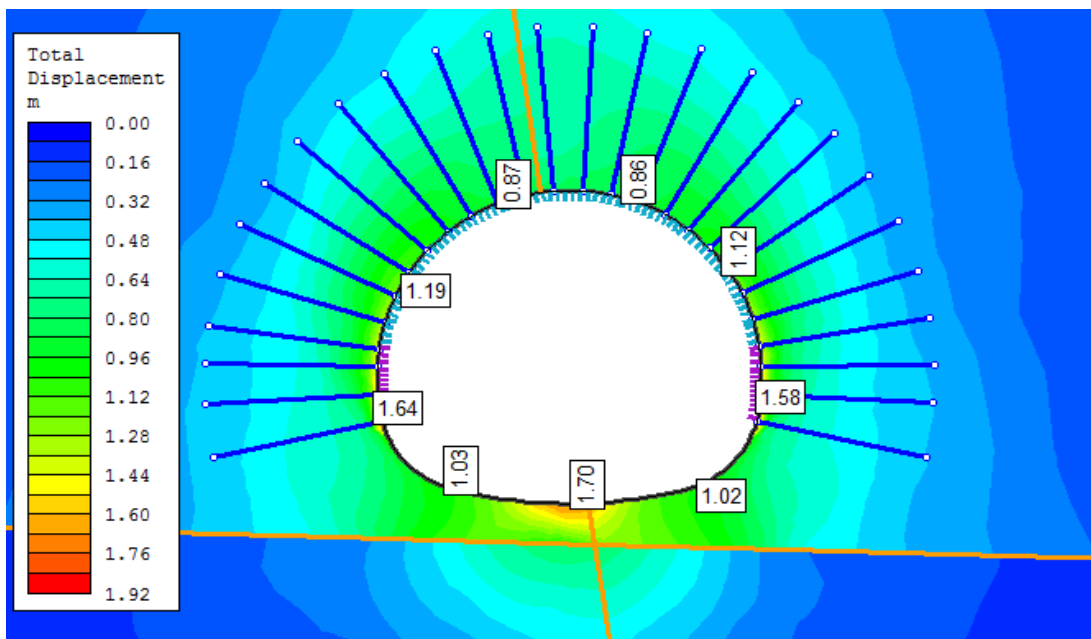Figure B.29 Radial deformations after the completion of excavation for Case 4, Alternative A
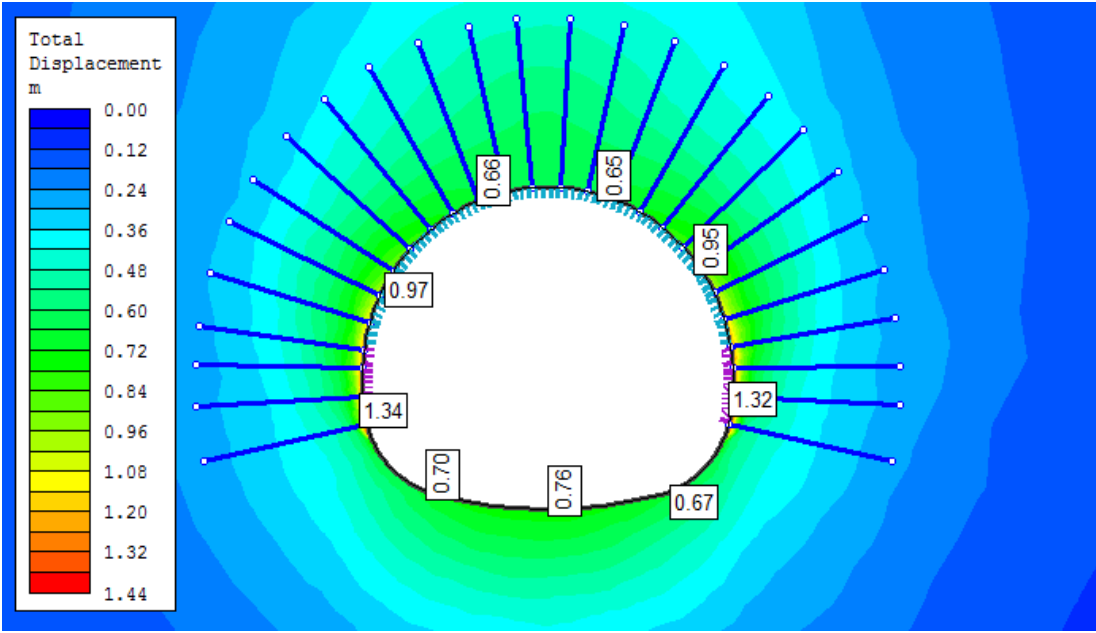
Figure B.30 Radial deformations after strength reduction for Case 4, Alternative A
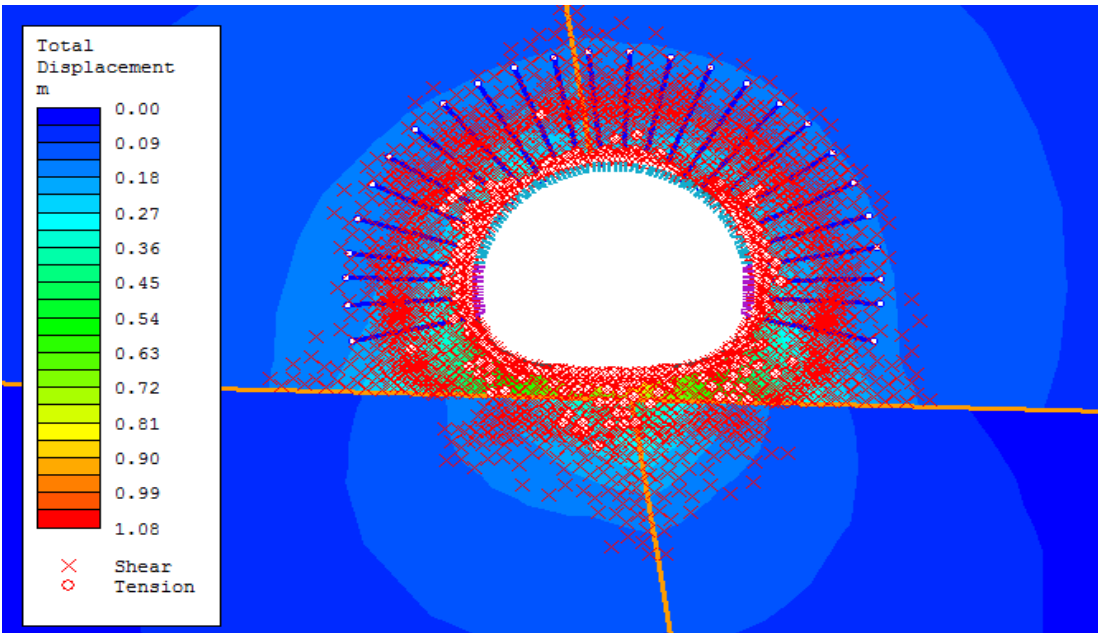
Figure B.31 Plastic zone radius after the completion of excavation for Case 4, Alternative A
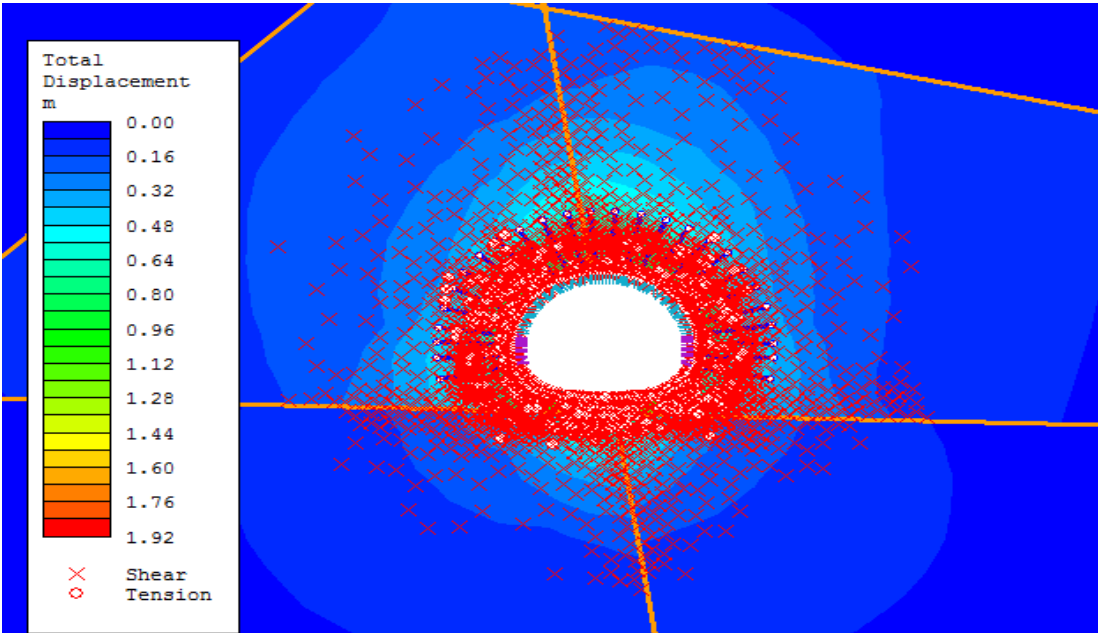

Figure B.32 Plastic zone radius after the strength reduction for Case 4, Alternative A
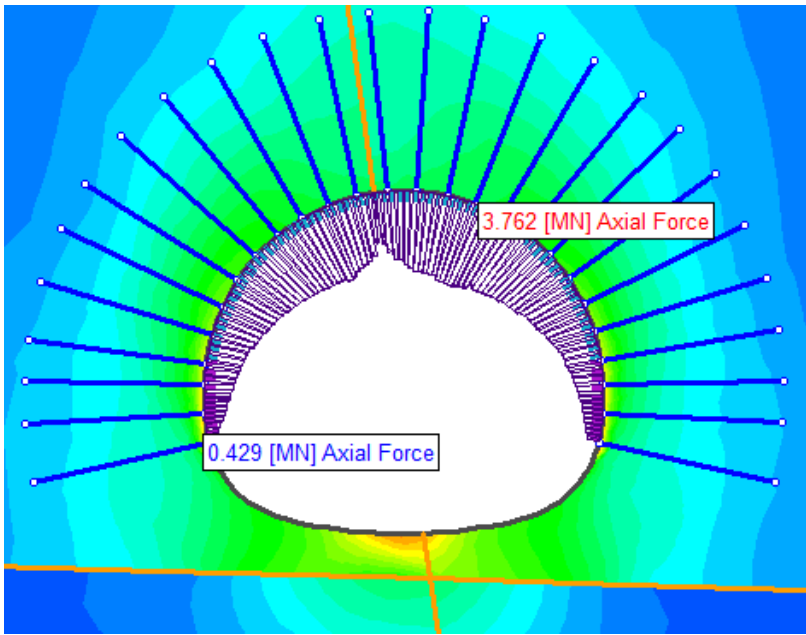
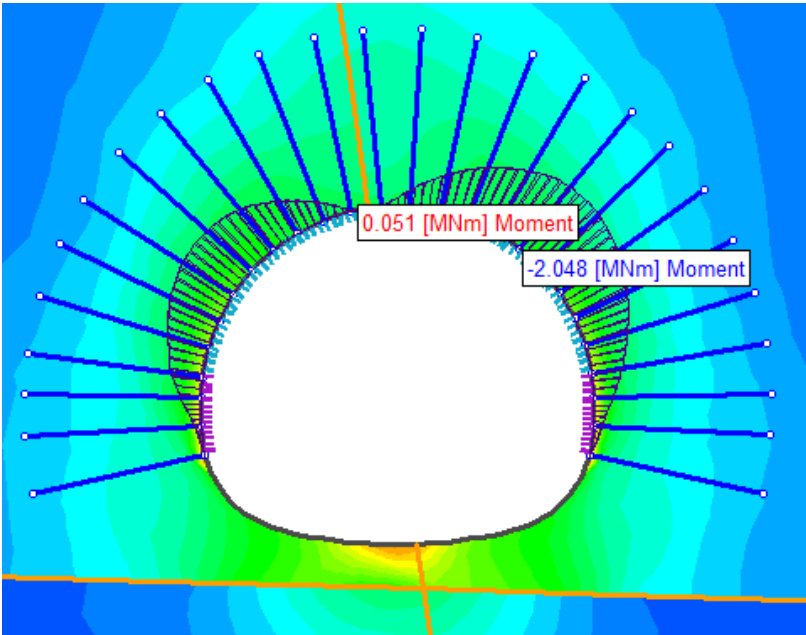Figure B.33 Axial forces after the strength reduction for Case 4, Alternative A

Figure B.34 Bending moments after the strength reduction for Case 4, Alternative A

Figure B.35 Shear forces after the strength reduction for Case 4, Alternative A

Figure B.36 Radial deformations after the completion of excavation for Case 4, Alternative B

Figure B.37 Radial deformations after strength reduction for Case 4, Alternative B

Figure B.38 Plastic zone radius after the completion of excavation for Case 4, Alternative B

Figure B.39 Plastic zone radius after the strength reduction for Case 4, Alternative B

10.462 [MN] Axial Force

4.542 [MN] Axial Force

Figure B.40 Axial forces after the strength reduction for Case 4, Alternative B

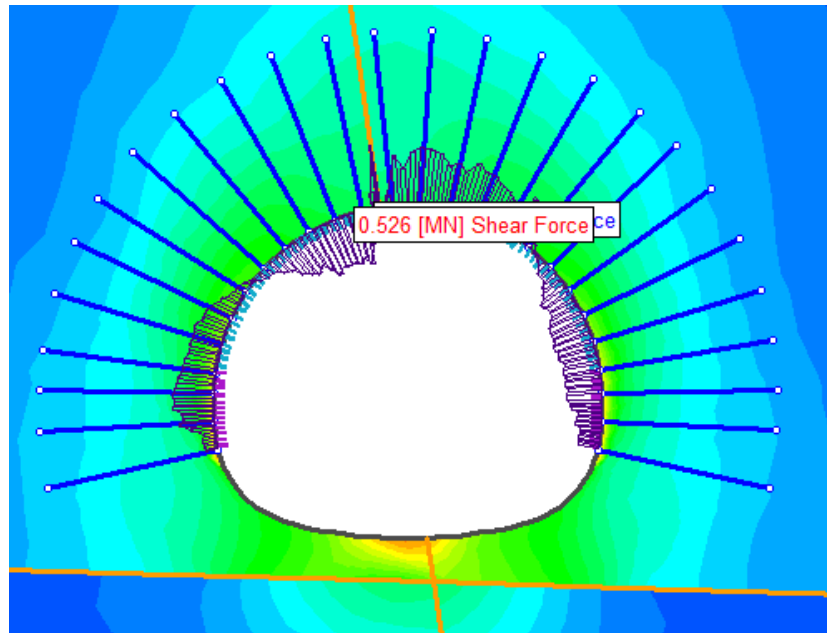Figure B.41 Bending moments after the strength reduction for Case 4, Alternative B

Figure B.42 Shear forces after the strength reduction for Case 4, Alternative B
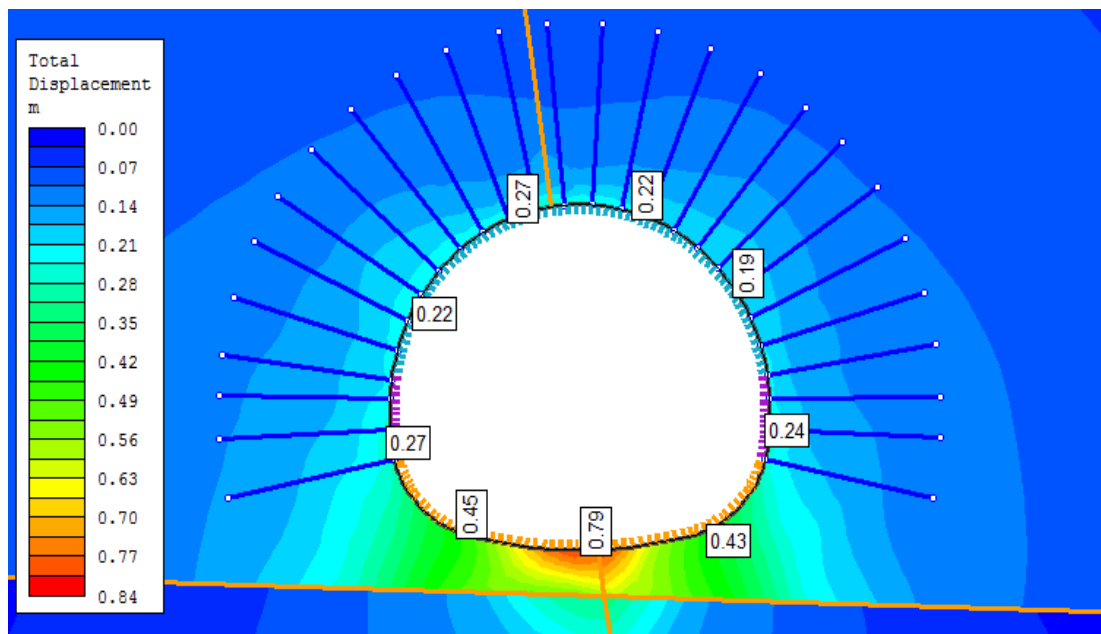
Figure B.43 Radial deformations after the completion of excavation for Case 5, Alternative A
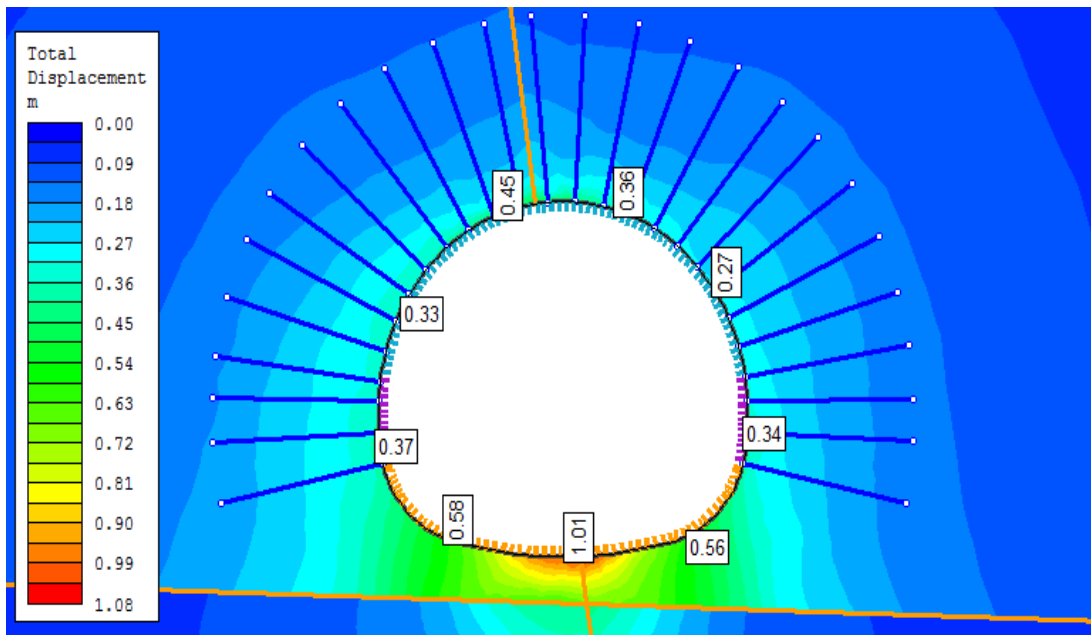

Figure B.44 Radial deformations after strength reduction for Case 5, Alternative A
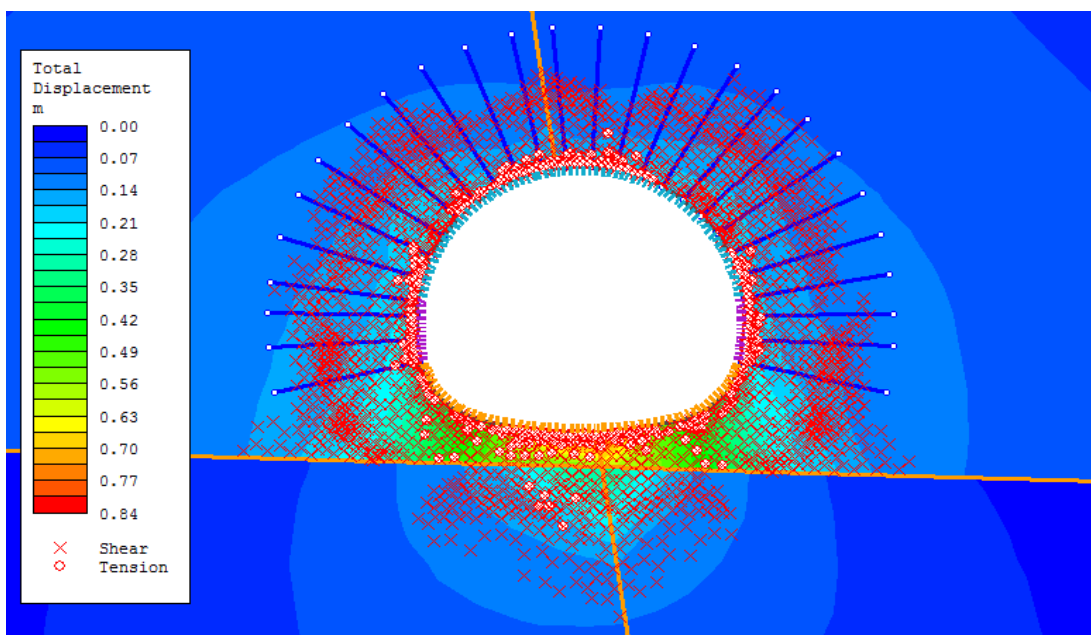
Figure B.45 Plastic zone radius after the completion of excavation for Case 5, Alternative A

Figure B.46 Plastic zone radius after the strength reduction for Case 5, Alternative A

Figure B.47 Axial forces after the strength reduction for Case 5, Alternative A

Figure B.48 Bending moments after the strength reduction for Case 5, Alternative A

Figure B.49 Shear forces after the strength reduction for Case 5, Alternative A

Figure B.50 Radial deformations after the completion of excavation for Case 5, Alternative B

Figure B.51 Radial deformations after strength reduction for Case 5, Alternative B

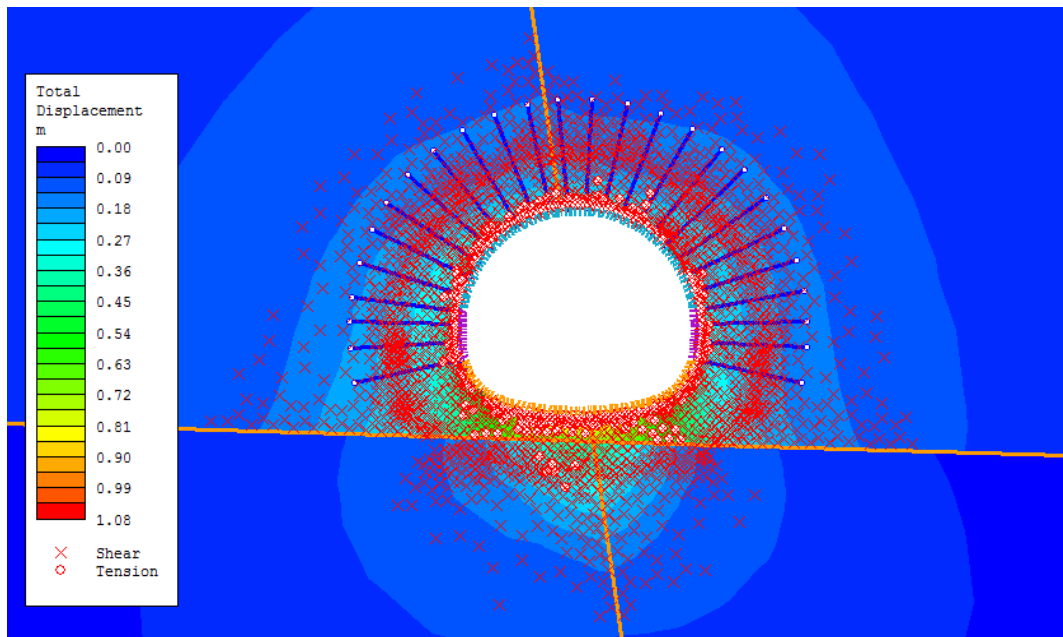Figure B.52 Plastic zone radius after the completion of excavation for Case 5, Alternative B

Figure B.53 Plastic zone radius after the strength reduction for Case 5, Alternative B
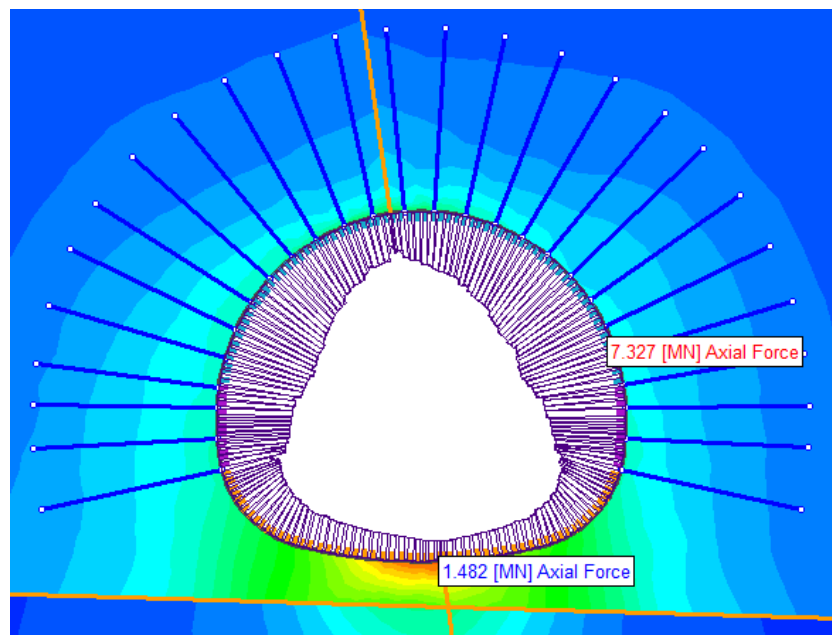

Figure B.54 Axial forces after the strength reduction for Case 5, Alternative B
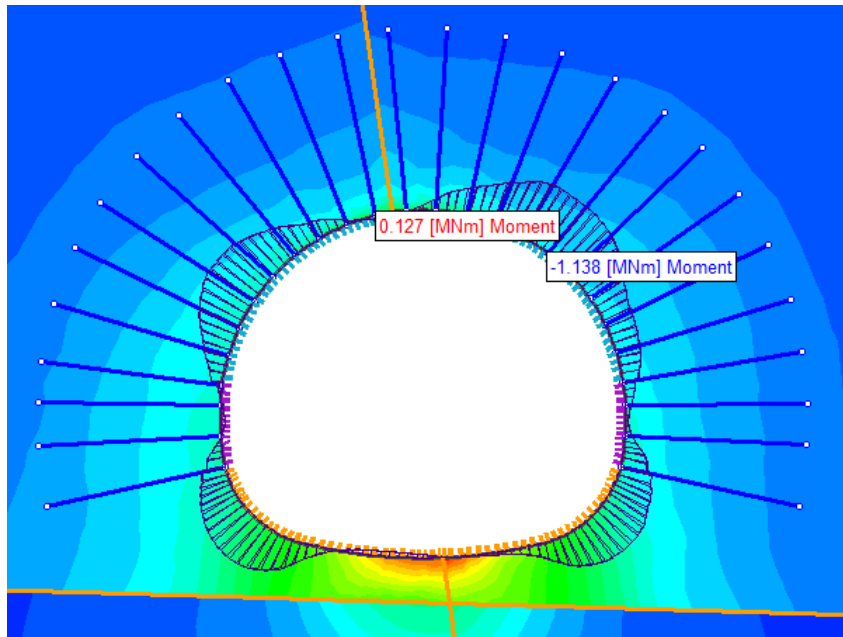
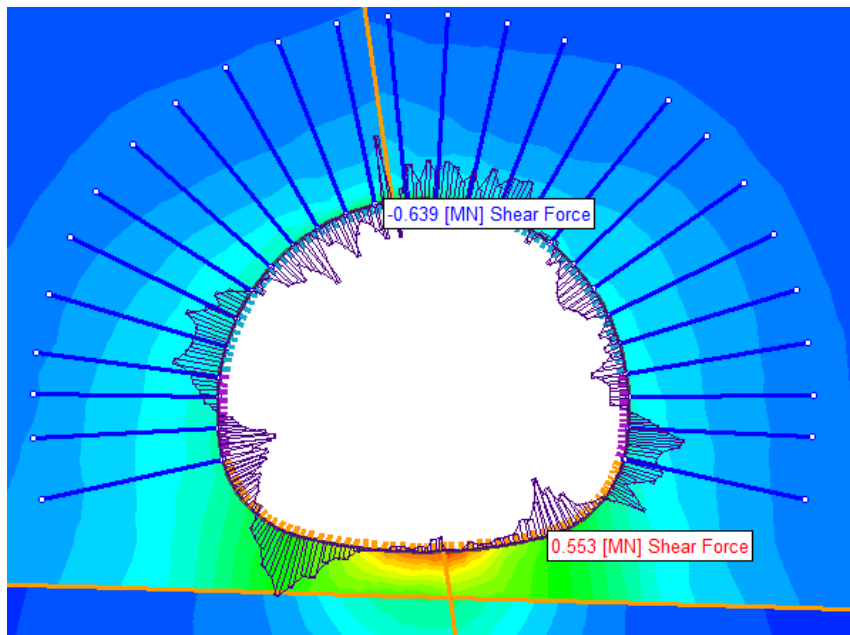Figure B.55 Bending moments after the strength reduction for Case 5, Alternative B

Figure B.56 Shear forces after the strength reduction for Case 5, Alternative B